

Aus dem Fachbereich Medizin
der Johann Wolfgang Goethe-Universität
Frankfurt am Main

betreut am
Gustav Embden-Zentrum der Biochemie
Institut für Biochemie I - Pathobiochemie
Direktor: Prof. Dr. Bernhard Brüne

**The PGE₂/cAMP signaling axis in macrophages
during inflammation**

Dissertation
zur Erlangung des Doktorgrades der Medizin
des Fachbereichs Medizin
der Johann Wolfgang Goethe-Universität
Frankfurt am Main

vorgelegt von
Bernd Patrick Maul

aus Frankfurt am Main

Frankfurt am Main, 2019

Dekan:	Prof. Dr. Josef Pfeilschifter
Referent:	Prof. Dr. Bernhard Brüne
Korreferentin:	Prof. Dr. Ellen Niederberger
Tag der mündlichen Prüfung:	10. März 2020

„Geheimnisvoll am lichten Tag
Läßt sich Natur des Schleiers nicht berauben,
Und was sie deinem Geist nicht offenbaren mag,
Das zwingst du ihr nicht ab mit Hebeln und mit Schrauben.“

Johann Wolfgang von Goethe.

Faust I, 1808.

Index

I. Abbreviations, symbols and units.....	VII
II. List of tables.....	XII
III. List of figures.....	XIII
1 Summary.....	1
2 Zusammenfassung	3
3 Introduction	5
3.1 Inflammation	5
3.2 Macrophages	8
3.3 Prostaglandins	11
3.4 Aims of this thesis.....	15
4 Animals, materials and methods	16
4.1 Animals	16
4.2 Materials.....	16
4.2.1 Cells.....	16
4.2.2 Chemicals and reagents.....	16
4.2.3 Media and reagents for cell culture	18
4.2.4 Buffers and solutions	19
4.2.5 Stimuli and inhibitors.....	22
4.2.6 Antibodies.....	23
4.2.7 Kits	23
4.2.8 Consumables and instruments	24
4.2.9 Quantitative PCR oligonucleotides	26
4.2.10 Software.....	27
4.3 Methods.....	28
4.3.1 Cell culture.....	28
4.3.1.1 Cell culture conditions	28
4.3.1.2 Isolation and culture of BMDMs.....	28

4.3.1.3	BMDM stimulation	29
4.3.2	Protein analytics	29
4.3.2.1	Cell lysis.....	29
4.3.2.2	Protein quantification.....	30
4.3.2.3	SDS-polyacrylamide gel electrophoresis (PAGE) and Western blotting.	30
4.3.3	RNA analytics	31
4.3.3.1	Isolation	31
4.3.3.2	Reverse transcription	31
4.3.3.3	Quantitative PCR (qPCR).....	32
4.3.4	Immunoprecipitation.....	33
4.3.5	pCREB-ChIP	34
4.3.6	Next-Generation-Sequencing (NGS).....	36
4.3.7	Genotyping	37
4.3.8	Prostanoid quantification	39
4.3.9	Statistical analysis.....	40
5	Results	41
5.1	Characterization of mPGES-1, pCREB and COX-2	41
5.2	Prostanoid profiles	46
5.3	Establishing of the ChIP-protocol	51
5.3.1	Validation of pCREB-Ab	51
5.3.2	Amplification of pCREB-ChIP	52
5.4	ChIP-seq.....	55
5.5	Validation of pCREB-ChIP-seq.....	59
6	Discussion	61
7	References	72
8	Danksagung.....	82
9	Lebenslauf.....	83
10	Schriftliche Erklärung	85

I. Abbreviations, symbols and units

Å	Ångström [10^{-10} meter]
A	Ampere
AA	Arachidonic acid
ABC	ATP-binding cassette
AC	Adenylyl cyclase
AP1	Activator protein 1
APS	Ammonium persulfate
Arg1	Arginase 1
BMDM	Bone marrow-derived macrophages
bp	Base pair
BSA	Bovine serum albumin
bZIP	Basic leucine zipper
°C	Centigrade
CaMK	Calcium/calmodulin-dependent protein kinase
cAMP	Cyclic adenosine monophosphate
CD	Cluster of differentiation
cDNA	Complementary DNA
cGCR	Cytosolic glucocorticoid receptor
ChIP	Chromatin immunoprecipitation
ChIP-seq	Chromatin immunoprecipitation followed by sequencing
chr	Chromosome
CIA	Collagen-induced arthritis
Compound III	Selective inhibitor of mPGES-1
COX	Cyclooxygenase
CpG	5'-cytosine-phosphate-guanine-3'
cPGES	Cytosolic prostaglandin E synthase
CRE	cAMP response element
CREB	cAMP response element-binding protein
CREM	cAMP response element modulator
CST	Cell Signaling Technology
DAMP	Damage-associated molecular pattern
ddH ₂ O	Double-distilled water
DMSO	Dimethylsulfoxide
DNA	Deoxyribonucleic acid

DTT	Dithiothreitol
EB	Elution buffer
EBV	Epstein-Barr virus
EDTA	Ethylenediaminetetraacetate
Elovl5	Elongation of very long chain fatty acids protein 5
EP	PG receptors for prostaglandin E ₂
ER	Endoplasmatic reticulum
ERAD	Endoplasmic reticulum-associated degradation
ERK	Extracellular signal-regulated kinase
Erlin1	Endoplasmic reticulum lipid raft-associated protein 1
FCS	Fetal calf serum
FDR	False Discovery Rate
Fos	FBJ osteosarcoma oncogene
FU	Fluorescence Units
G	Wire gauge
g	Gravity
GM-CSF	Granulocyte-macrophage colony-stimulating factor
GO	Gene Ontology
GPCR	G-protein-coupled receptor
GSH	Glutathion
h	Hour
³ H	Tritium
HAT	Histone acetyltransferase
HIV	Human immunodeficiency virus
HPLC	High performance liquid chromatography
IFNGR	Interferon-gamma receptor
IFN-γ	Interferon gamma
lg	Logarithm
IKK	Inhibitory κB kinase
IL	Interleukin
iNOS	Inducible NO synthase
InsP3	Inositol 1,4,5-trisphosphate
InsP3R	Inositol 1,4,5-trisphosphate receptor
IP	Immunoprecipitation
IP-10	Interferon gamma-induced protein 10
IRAK	IL-1 receptor-associated kinase

IRF	Interferon regulatory factor
I κ B	NF- κ B inhibitory protein
JNK	C-Jun N-terminal kinase
Jun	Jun proto-oncogene
kDa	Kilodalton
KID	Kinase-inducible domain
KIX	KID-interacting domain
KO	Knock-out
LBP	LPS-binding protein
LC-MS/MS	Liquid chromatography-mass spectrometry/mass spectrometry
LO	Lipoxygenase
LPS	Lipopolysaccharides
M	Molar
MAC	Membrane attack complex
MAP3K	Mitogen-activated protein kinase kinase kinase
MAPEG	Membrane-associated proteins involved in eicosanoid and glutathione metabolism
MAPK	Mitogen-activated protein kinase
MBL	Mannose-binding lectin
M-CSF	Macrophage colony-stimulating factor
MD-2	myeloid differentiation protein-2
mg	Milligram
MHC	Major histocompatibility complex
Milli	Merck Millipore
min	Minute
mL	Milliliter
mPGES-1	Microsomal prostaglandin E synthase-1
MPS	Mononuclear phagocyte system
MRP	Multidrug resistance protein
MSK-1	Mitogen- and stress-activated protein kinase 1
MyD88	Myeloid differentiation primary response 88
NEMO	NF- κ B essential modulator
NF- κ B	Nuclear factor ' κ -light-chain-enhancer' of activated B cells
ng	Nanogram
NGS	Next-Generation-Sequencing
nm	Nanometer

NO	Nitric oxide
NSAID	Nonsteroidal anti-inflammatory drug
NS-398	Selective inhibitor of COX-2
PAMP	Pathogen-associated molecular pattern
PBS	Phosphate buffered saline
PCR	Polymerase chain reaction
pCREB	Phosphorylated CREB
PDE	Phosphodiesterase
PG	Prostaglandin
pg	Picogram
PGES	Prostaglandin E synthase
PI	Protease inhibitor
PI3K	Phosphoinositide 3-kinase
PKA	Protein kinase A
PLA2	Phospholipase A2
pmol	Picomol
PMSF	Phenylmethylsulfonyl fluoride
PP1	Phosphoprotein phosphatase 1
p-p90RSK	Phospho-90 kDa ribosomal S6 kinase
PRR	Pattern recognition receptor
PTGS	Prostaglandin-endoperoxide synthase
qPCR	Quantitative PCR
RA	Rheumatoid arthritis
RNA	Ribonucleic acid
ROS	Reactive oxygen species
rpm	Revolutions per minute
RPMI	Rosewell Park Memorial Institute
RPS27a	40S ribosomal protein S27a
RT	Room temperature
s	Second
S1P	Sphingosine-1-phosphate
SDS	Sodium dodecyl sulfate
SDS-PAGE	SDS-polyacrylamide gel electrophoresis
SEM	Standard error of the mean
ser	Serine
SIRS	Systemic inflammatory response syndrome

Sp4	Trans-acting transcription factor 4
SPFH	Stomatin, prohibitin, flotillin, and HflK/C
SPM	Specialized pro-resolving mediators
SREBP	Sterol regulatory element binding protein
STAT1	signal transducer and activator of transcription 1
TAE	Tris-acetate-EDTA
TBS	Tris buffered saline
TBST	Tris buffered saline with Tween® 20
TE	Tris-EDTA
TEMED	Tetramethylethylenediamine
TGF-β	Transforming growth factor-β
Th1	T helper 1
TIR	Toll-interleukin 1 receptor
TLR	Toll-like receptor
TNF-α	Tumor necrosis factor-α
TRAF	TNF receptor-associated factor
TRAK	Transforming growth factor beta-activated kinase
TRIF	TIR-domain-containing adaptor-inducing interferon-β
TSS	Transcription start site
TX	Thromboxane
U	Unit
UPP	Ubiquitin-proteasome pathway
UV	Ultraviolet
V	Voltage
w/v	Mass/volume
WT	Wild-type
Z	Zymosan
α	Alpha
β	Beta
γ	Gamma
Δ	Difference
κ	Kappa
μg	Microgram
μL	Microliter

II. List of tables

Table 1. Chemicals and reagents.....	17
Table 2. Media and reagents for cell culture	18
Table 3. Stimuli and inhibitors.....	22
Table 4. Antibodies.....	23
Table 5. Kits	23
Table 6. Consumables.....	24
Table 7. Instruments	25
Table 8. Oligonucleotides for qPCR.....	26
Table 9. Software.....	27
Table 10. Reverse transcription reaction components per sample	31
Table 11. Reverse transcription program settings	32
Table 12. qPCR reaction components per sample	32
Table 13. qPCR program settings	33
Table 14. Program settings for sonication	35
Table 15. Oligonucleotides for genotyping-PCR	37
Table 16. Genotyping-PCR reaction components per sample	38
Table 17. PCR program settings for genotyping.....	38
Table 18. GO category analysis of pCREB-targeted genes	57

III. List of figures

Figure 1. Overview of macrophage differentiation and polarization.	9
Figure 2. Overview of the eicosanoids biosynthesis pathways.....	13
Figure 3. Representative size distribution of sequencing libraries.	37
Figure 4. Genotyping results of WT and mPGES-1 KO mice.....	39
Figure 5. Detection of COX-2, pCREB, and mPGES-1 upon stimulation with LPS+IFN- γ and zymosan in WT and mPGES-1 KO BMDMs.....	42
Figure 6. mPGES-1 protein expression in LPS+IFN- γ and zymosan-stimulated murine WT and mPGES-1 KO BMDMs.	43
Figure 7. pCREB protein expression in LPS+IFN- γ and zymosan-stimulated murine WT and mPGES-1 KO BMDMs.	44
Figure 8. COX-2 protein expression in LPS+IFN- γ and zymosan-stimulated murine WT and mPGES-1 KO BMDMs.	46
Figure 9. PGD ₂ levels in LPS+IFN- γ and zymosan-stimulated murine WT and mPGES-1 KO BMDMs.	47
Figure 10. TXB ₂ levels in LPS+IFN- γ and zymosan-stimulated murine WT and mPGES-1 KO BMDMs.....	48
Figure 11. PGF _{2α} levels in LPS+IFN- γ and zymosan-stimulated murine WT and mPGES-1 KO BMDMs.....	49
Figure 12. PGE ₂ levels in LPS+IFN- γ and zymosan-stimulated murine WT and mPGES-1 KO BMDMs.....	50
Figure 13. pCREB antibody validation by immunoprecipitation from NIH/3T3 fibroblast lysates.	52
Figure 14. PCR amplification of pCREB-ChIP in untreated samples for WT and mPGES-1 KO BMDMs.....	53

Figure 15. PCR amplification of pCREB-ChIP in LPS+IFN- γ and zymosan-treated murine WT and mPGES-1 KO BMDMs.....	54
Figure 16. Comparison of pCREB binding sites differentially bound in WT vs. mPGES-1 KO BMDMs upon LPS+IFN- γ stimulation.	56
Figure 17. pCREB-ChIP-seq peaks of Erlin1 and Elovl5.....	58
Figure 18. Erlin1 and Elovl5 ChIP-seq validation by qPCR.....	60
Figure 19. Schematic overview of the PGE ₂ /cAMP signaling axis in macrophages during inflammation.....	62
Figure 20. Enhancer and silencer of the transactivation potential of activated CREB. .	70

1 Summary

Acute and chronic inflammation play a pivotal role in various diseases, such as rheumatoid arthritis, atherosclerosis, bacterial as well as viral infections and therefore are an everyday-challenge in clinical practice. In this context, biologically active products of the cyclooxygenases and the prostanoid synthases, e.g. prostaglandins, critically contribute to various aspects of the inflammatory response in almost every tissue of the body. Emerging evidence over the past decades has demonstrated that these mediators are not only responsible for a pro-inflammatory response, but also show anti-inflammatory and pro-resolving properties. The relevance of biologically active lipids in this context is strengthened by the clinical efficacy of nonsteroidal anti-inflammatory drugs (NSAIDs), e.g. Aspirin[®], which block the biosynthesis of the mediators via the cyclooxygenase (COX) enzymes. Notably, microsomal prostaglandin E synthase-1 (mPGES-1)-derived prostaglandin E₂ (PGE₂) is a well-studied, functionally versatile PG, which promotes its effects via specific G protein-coupled receptors (GPCRs). Activation of these receptors elicits an internal signal transduction cascade, including activation of the adenylyl cyclase (AC). Active AC contributes to an elevated intracellular cyclic adenosine monophosphate (cAMP) level, which in turn activates the transcription factor cAMP response element-binding protein (CREB) via phosphorylation.

While the role of PGE₂ in the inflammatory context has been well-documented in previous literature, relatively little is known about CREB-dependent transcriptional changes in inflammation. Therefore, the aim of this study was to investigate the effect of mPGES-1-derived PGE₂ on CREB-mediated transcriptional changes specifically in murine wild-type (WT) and mPGES-1 knock-out (KO) macrophages in an inflammatory context. To address this issue, bone marrow-derived macrophages (BMDMs) were treated with either the bacterial cell wall component lipopolysaccharide (LPS) in combination with interferon- γ (IFN- γ) or the yeast extract zymosan. To analyze effects on CREB activation we determined protein expression profiles of relevant PGE₂-synthesizing enzymes, i.e. COX-2 and mPGES-1, as well as activity of the downstream transcription factor CREB. The activity of mPGES-1 was simultaneously determined by the analysis of the prostanoid kinetics. Under these experimental conditions we showed

that COX-2 is strongly induced, and we also observed elevated activated CREB levels in WT as well as in mPGES-1 KO macrophages. Further, both LPS+IFN- γ and zymosan increased expression of mPGES-1 in WT but not in mPGES-1-deficient macrophages. These findings go in hand with largely similar alterations in the PGD₂, TXB₂, PGF_{2 α} profiles in WT and mPGES-1 KO macrophages upon stimulation. Of note, an elevated PGE₂ production was also observed in mPGES-1-deficient macrophages at later stages upon inflammatory conditions. Subsequently, potential CREB-regulated targets were identified in macrophages upon inflammatory stimuli after 16 h by chromatin immunoprecipitation (ChIP) followed by Next-Generation-Sequencing (NGS). Surprisingly, despite equal levels of pCREB the characterization of CREB binding sites revealed different targetome profiles between WT and mPGES-1 KO macrophages. Specifically, the fatty acid metabolic processes-associated targets appeared to be selectively lost in mPGES-1-deficient vs. WT macrophages. We further validated one of those targets, i.e. the endoplasmic reticulum lipid raft-associated protein 1 (Erlin1), at the mRNA expression level, which indeed was differentially transcribed in response to different PGE₂ synthesizing conditions.

Mechanistically, CREB is a well-characterized phosphorylation-dependent transcription factor in cell survival, proliferation, differentiation, and immune responses. Yet, our understanding of the functions of CREB in inflammation, specifically with respect to its activation by PGE₂, is insufficient. Due to its biological relevance in inflammation it clearly requires additional studies to shed light on the details of CREB activation in macrophages to provide possibilities of therapeutic interventions.

2 Zusammenfassung

Entzündungen sind lebensnotwendige physiologische Immunreaktionen, aber auch Ursache einer Vielzahl von Krankheiten wie rheumatoider Arthritis, Atherosklerose, bakterieller sowie viraler Infektionen. Die Behandlung von chronischen und akuten Entzündungserkrankungen ist daher eine große Herausforderung im klinischen Alltag. In diesem Zusammenhang spielen biologisch-aktive Lipide, wie Prostaglandine, eine zentrale Rolle. Diese werden u. a. durch die Aktivität von Cyclooxygenasen und Prostanoidsynthasen gebildet und können sowohl als pro-entzündliche als auch als Entzündungs-auflösende Mediatoren agieren. Die Relevanz von Lipiden im Entzündungskontext zeigt sich insbesondere im breiten therapeutischen Einsatz von nicht-steroidalen Antirheumatika (NSAIDs), zu welchen Cyclooxygenase-Hemmer, wie Aspirin®, zählen. Diese können global die Bildung von Prostaglandinen hemmen. Hierbei ist u.a. die Reduktion von Prostaglandin E₂ (PGE₂) von großer Bedeutung. PGE₂ löst in Makrophagen nach Bindung an spezifische, G-Protein-gekoppelte Rezeptoren die Aktivierung der Adenylat-Zyklase aus, wodurch vermehrt cAMP gebildet wird, welches wiederum zur Aktivierung des Transkriptionsfaktors cAMP response element-binding protein (CREB) führt.

Während die Rolle von PGE₂ im Entzündungskontext gut beschrieben ist, sind über CREB-abhängige transkriptionelle Veränderungen im Entzündungsgeschehen vergleichsweise wenig bekannt. Um dabei den Einfluss von PGE₂ untersuchen zu können, wurden Makrophagen mit einem Knockout (KO) für die mikrosomale PGE-Synthase (mPGES-1) mit wildtypischen (WT) Makrophagen verglichen und Transkriptionsveränderungen als Antwort auf bakterielle Oberflächenbestandteile (Lipopolysaccharide) in Kombination mit Interferon-γ oder das in Hefezellwand vorkommende Homoglykan Zymosan untersucht. Um den Effekt auf die Aktivierung von CREB zu analysieren, schauten wir uns die Proteinexpression der relevanten PGE₂-synthetisierenden Enzyme COX-2 und mPGES-1, sowie die Aktivität des Transkriptionsfaktors CREB an. Außerdem wurden parallel zur Aktivität von mPGES-1, die Kinetiken von PGE₂ und weiteren Prostanoiden bestimmt. Unter diesen experimentellen Bedingungen konnten wir eine starke Induktion von COX-2 und erhöhte

pCREB Mengen sowohl in WT als auch in mPGES-1 KO Makrophagen nachweisen. Desweiteren zeigte sich unter Stimulation mit LPS+IFN- γ und Zymosan eine verstärkte Expression von mPGES-1 im WT, aber nicht im mPGES-1 KO. Ähnliche Veränderungen konnten wir auch in den Prostanoiden PGD₂, TXB₂, PGF_{2 α} in WT und mPGES-1 KO Makrophagen festhalten. Trotz des KO für die mikrosomale PGE-Synthase beobachteten wir in den späteren Phasen der Stimulation in mPGES-1 KO Makrophagen, entgegen unseren Erwartungen, ebenfalls eine erhöhte PGE₂ Produktion.

Um spezifisch CREB-vermittelte Transkriptionsveränderungen untersuchen zu können, wurden die Bindungsstellen von CREB auf der DNA mittels Chromatin-Immunopräzipitation und anschließender Hochdurchsatz-Sequenzierung bestimmt. Hierbei konnten wir im Entzündungskontext differentielle Bindungsmuster von CREB nachweisen. Wir konnten zeigen, dass insbesondere Targets, die dem Fettsäuremetabolismus angehören in mPGES-1 KO Makrophagen weniger gebunden wurden. Die Validierung eines der Targets aus diesem Prozess auf mRNA Expressionslevel zeigte ferner, dass dieses in Antwort auf verschiedene PGE₂-synthetisierenden Bedingungen unterschiedlich transkribiert wird.

Mechanistisch gesehen ist CREB ein gut charakterisierter Transkriptionsfaktor, der verschiedenste zelluläre Effekte wie Zellüberleben, Proliferation, Differenzierung und Immunantwort vermittelt. Dennoch sind die aktuellen Erkenntnisse über CREB im Entzündungsgeschehen, insbesondere die über PGE₂ vermittelten transkriptionellen Veränderungen, limitiert. Auf Grund seiner biologischen Relevanz im Entzündungsgeschehen sollte die CREB Aktivierung im Detail weiter charakterisiert werden, um neue Ansätze für therapeutische Interventionen zu schaffen.

3 Introduction

3.1 Inflammation

Inflammation has been found to be a fundamental component in many diseases. It describes a complex biological immune response against a diverse variety of interior or exterior stimuli.¹ The function of inflammation is to eliminate harmful stimuli to mediate the healing process, meanwhile it is also involved in the pathophysiology of many chronic diseases, such as atherosclerosis, inflammatory bowel disease, and rheumatoid arthritis (RA).^{2,3} In the 1st century AD, Roman doctor Celsus characterized major symptoms of inflammation known as “Celsus tetrad of inflammation”: *calor* (warmth), *dolor* (pain), *tumor* (swelling), and *rubor* (redness and hyperaemia).^{4,5} *Functio laesa* (disturbance of function) was added by Rudolph Virchow in 1858 in his book *Cellularpathologie*.⁴ Clinically, the five cardinal signs of inflammation still have relevance to describe and better diagnose a specific disease or syndrome. As inflammation occurs in various clinical contexts, there are several categories summarizing specific characteristics: e.g. the time course, inflammation can be acute or chronic; its distribution, local or systemic; macroscopic aspects, serous or fibrous.^{6,7} Generally, the innate immunity accomplishes a fast and nonspecific inflammatory response as the first line of defense, whereas the adaptive immune system is responsible for the second line of defense, which is characterized by a highly specialized response.⁸ Latest insights reveal adaptation of innate immunity and modulation of inflammatory response upon recurrent stimuli.⁹

Generally, acute inflammation through infection or injury occurs in two overlapping stages, the vascular and the cellular stage. It is initiated by sentinel innate immune cells, including tissue-resident macrophages (e.g. Kupffer cells and Langerhans cells), dendritic cells, and mast cells. As the immune systems first line of defense, pattern recognition receptors (PRR), such as Toll-like receptors (TLRs) – which are described in more detail in the next subchapter – on the surface of these innate immune cells are able to recognize pathogen-associated molecular patterns (PAMPs), carried by all microorganism, and damage-associated molecular patterns (DAMPs), i.e. compounds

that result upon tissue damage.^{10,11} Examples of PAMPs recognized by PRRs, which initiate phagocytosis by macrophages, include lipopolysaccharides (LPS), yeast zymosan, peptidoglycans, and lipoproteins. LPS, also known as endotoxins, are a specific class of glycolipids derived from the outer membrane of Gram-negative bacteria such as *E. coli* and find a wide range of usage in laboratory studies.¹² Initial recognition of these molecules induces the production of inflammatory mediators, such as cytokines, chemokines, vasoactive amines, and eicosanoids. Vasodilatation of microvessels near the site of lesion triggered by vasoactive mediators such as nitric oxide (NO) drive an increased blood flow, which is responsible for the clinical sign of increased local temperature and redness. Accompanying, the increase in capillary permeability leads to an extravascular accumulation of fluids (exudate) into the affected tissue, containing various antimicrobial mediators. This results in local edema, which again triggers pain receptors due to increased tissue pressure.¹³ In the cellular stage, the activated endothelium enables infiltration of neutrophils, followed by monocytes, which differentiate to macrophages. Both extravasate from the luminal site of venules towards the site of tissue lesion via chemotaxis. Extravasated neutrophils and macrophages become activated by direct contact with pathogens or by pro-inflammatory cytokines such as tumor necrosis factor- α (TNF- α) and interleukin-1 β (IL-1 β), derived from tissue-resident cells.¹⁴ Recruited leukocytes phagocytose pathogens and damaged cells, which leads to pus formation. Neutrophils eliminate intruders by releasing biocidal substances, e.g. reactive oxygen species (ROS).¹⁵ To further increase the phagocytotic efficiency, in case of persistent infestation, the complement system attacks the membrane integrity of the pathogen and complements the ability of the host defense. There are three pathways leading to the activation of the complement cascade: the alternative, the classical, and the mannose-binding lectin (MBL) complement pathway. Antigens such as endotoxins of Gram-negative bacteria and yeast cell wall components trigger the activation of the alternative pathway, which does not rely on pathogen-binding antibodies. In contrast, the formation of antigen-antibody complexes is crucial for initiating the classical and the MBL pathway. All cascades are followed by a final common pathway, leading to a terminal complement complex, also called membrane attack complex (MAC). The MAC forms transmembrane channels, which ensure the disruption of the bacterial cell wall and its lysis. The complement cascade is an important and

powerful mechanism of host defense. It is not only promoting cell lysis, but is also responsible to attract macrophages and neutrophils via chemotactic complement factors, such as C3a und C5a, to the area where the antigen is present.¹⁶ In addition, several complement factors have a direct effect on the activation of mast cells and basophils, which again secrete inflammatory mediators, e.g. histamine and serotonin, to potentiate the inflammatory immune response.¹⁷

Usually, an acute inflammatory response is self-limiting and results in the return to tissue homeostasis, once the triggering stimuli are eliminated and damaged tissue is repaired. Resolution of inflammation is an active process and involves the switch from pro-inflammatory to anti-inflammatory mediators like IL-10 and transforming growth factor- β (TGF- β) and further specialized pro-resolving mediators (SPMs), e.g. lipoxins and resolvins, secreted mainly by macrophages.¹⁸ If an acute inflammatory response is not able to eradicate irritants or persists for any other reasons, e.g. autoimmune genesis, it results in a chronic inflammation, characterized by fibrosis and tissue dysfunction.¹⁹ If a significant amount of tissue is inflamed or inflammatory stimuli are sufficiently strong, pathogens, inflammatory mediators, and cytokines are able to disseminate via the circulatory or lymphatic system, resulting in a systemic effect. Non-infectious stimuli, e.g. injuries, burns, or ischemia, result in a systemic inflammatory response syndrome (SIRS), meanwhile a detectable pathogen causes sepsis.²⁰ Symptomatically, fever is the clinical hallmark of a systemic inflammatory response. Circulating pyrogens like LPS and cytokines are mediators triggering heat-generating effects. In the thermoregulatory center of the hypothalamus, prostaglandin (PG) E₂ is a crucial mediator and activates PG receptors for PGE₂ (EP)-mediated cyclic adenosine monophosphate (cAMP) for temperature regulation.²¹

Inflammation, as a part of the innate and the adaptive immune system, is a complex physiological process to restore tissue integrity and homeostasis. If inflammation is not properly resolved, it may lead to a chronic course and the development of pathological remodeling. Due to their plastic phenotypes, macrophages play a crucial role in all stages of the inflammatory process, i.e. initiation, maintenance, and resolution. Their important role in inflammation make macrophages interesting for further investigations.

3.2 Macrophages

Monocytes are the undifferentiated precursors of macrophages. Bone marrow-located multipotent hematopoietic stem cells are able to develop to monoblasts upon presence of macrophage colony-stimulating factor (M-CSF) and granulocyte-macrophage colony-stimulating factor (GM-CSF) as seen in Figure 1. Monoblasts, in turn, differentiate to monocytes and are released from the bone marrow into the circulation, remaining for about 2 – 4 days.²² Monocytes compose about 1 – 12 % of all circulating leukocytes in the human body and share the phagocytic function of neutrophils, the most abundant leukocytes.²³ Together they form the mononuclear phagocyte system (MPS), consisting of all highly phagocytic mononuclear cells. As described in subchapter 3.1, circulating monocytes can be recruited to an affected tissue whereupon they differentiate into macrophages or dendritic cells. In addition to phagocytosis, they are able to express major histocompatibility complex (MHC) class II-proteins to present phagocytosed antigen fragments on the cell surface to helper T cells for the development of an adaptive immune response.²⁴

Since the 1990s, it has been recognized that macrophages show phenotypic heterogeneity and comply various functions in the inflammatory process.²⁵ Traditionally, macrophages were assumed to be either classically activated, leading to a pro-inflammatory M1 subtype, or by the alternative way, resulting in an anti-inflammatory M2 subtype (see Figure 1). Initiated by activation of the TLR via TLR ligands such as LPS or zymosan and upon presence of interferon gamma (IFN- γ) in the affected tissue, M1 macrophages normally respond by the secretion of pro-inflammatory cytokines, e.g. TNF- α , IL-1 β , IL-6, and IL-12.²⁶ Moreover, this pro-inflammatory cytotoxic setting leads to an upregulation of the inducible NO synthase (iNOS) as well as the cyclooxygenase (COX)-2. This inflammatory microenvironment forms a suitable basis for host defence. In contrast, M2 macrophages are characterized by the production of anti-inflammatory cytokines, like TGF- β , IL-4, IL-10, IL-13 and the upregulation of arginase 1 (Arg1), which promotes tissue regeneration and tissue fibrosis.^{27,28}

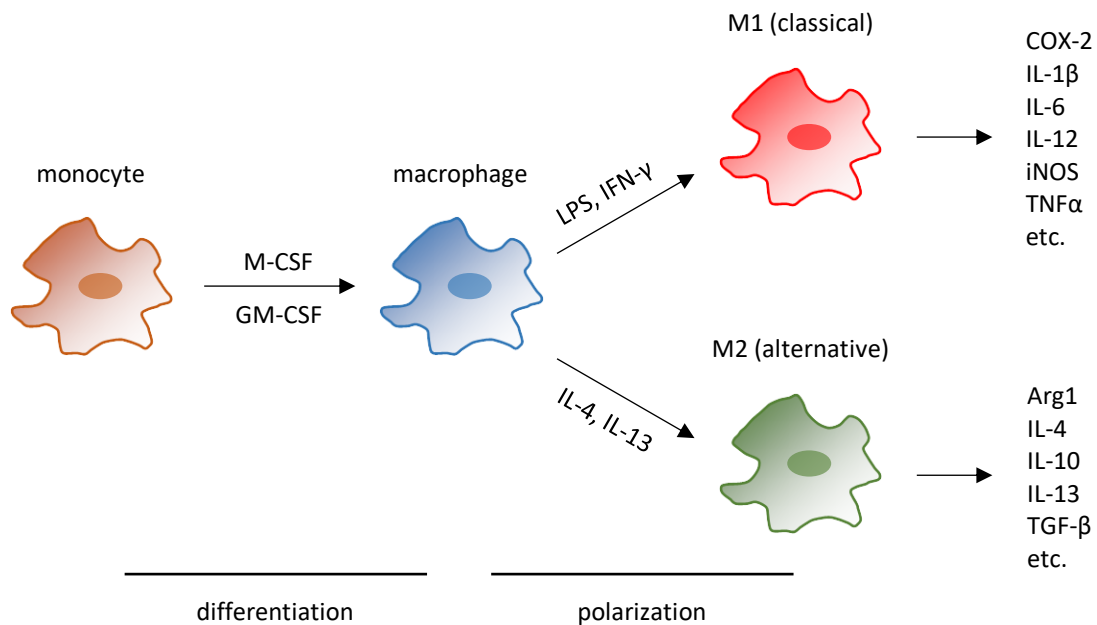


Figure 1. Overview of macrophage differentiation and polarization.

Monocyte-derived macrophages, differentiated in the presence of GM-CSF and M-CSF, can be subdivided into either a classically activated, pro-inflammatory M1 or an alternatively activated, anti-inflammatory M2 phenotype. They fulfill different roles and produce different mediators in the inflammatory process. *In vitro* the M1 subtype results from the treatment with e.g. lipopolysaccharides (LPS) and interferon gamma (IFN-γ), supporting T helper 1 (Th1) responses characterized by secreting cytokines, such as tumor necrosis factor-α (TNFα), interleukin (IL)-1β, IL-6, IL-12 as well as the inducible NO synthase (iNOS) and cyclooxygenase (COX)-2. Whereas the prototypical M2 subtype, induced by the treatment with IL-4 and IL-13, is characterized by the release of transforming growth factor-β (TGF-β), IL-4, IL-10, IL-13, and expression of high levels of Arginase 1 (Arg1).

Emerging evidence has now been found the conventional bipolar model as insufficient in fulfilling macrophages' astonishing functional plasticity. Macrophage characteristics become shaped through specific microenvironmental factors and can not be clearly classified into M1 or M2 polarization states.²⁹ Hence, this simple concept rather needs to be modified towards a model taking into account all different activation states as a spectrum of polarization, considering M1/M2 polarization as two extremes, ranging within this spectrum model. *In vitro*, macrophages are determined by the stimulus applied (e.g. LPS or zymosan) whereas, *in vivo*, macrophages are characterized by their combination of cell surface markers.³⁰ The M1 subpopulation, for instance, is characterized by a strong induction of MHC-II, cluster of differentiation (CD) 68, CD80,

and CD86. Concurrently, the M2 subpopulation is phenotypically defined, among others, by the expression of the CD200R membrane glycoprotein.³¹

As stated above, macrophages can be polarized towards a M1 type upon stimulation with LPS or zymosan via activation of TLRs. As a type of PRR, TLRs are primarily expressed on sentinel cells, such as macrophages and dendritic cells, but also on fibroblasts and epithelial cells. TLRs are the best characterized and most important receptors initiating an innate immune response. By now, the TLR family includes 10 members (TLR1-10) in human and 12 (TLR1-9, TLR11-13) in mouse, which are classified into cell surface TLRs, to detect extracellular pathogens, such as bacteria and fungi, and intracellular TLRs for the detection of intracellular pathogens like viruses.^{32,33} Both, cell surface and intracellular TLRs, share a common structure comprising a leucine-rich domain for PAMP recognition and binding, followed by a cysteine-rich domain, single transmembrane domain, and a Toll-interleukin 1 receptor (TIR) domain required for downstream signal transduction.³⁴ How do TLRs exactly get activated through bacterial surface membrane components like LPS? These components build a complex with the LPS-binding protein (LBP), which is recognized by the cell surface protein CD14. CD14, in turn, delivers the LPS-LBP complex to the TLR4-myeloid differentiation protein-2 (MD-2) complex, which initiates the canonical myeloid differentiation primary response 88 (MyD88)-dependent pathway.³³ The cytosolic adapter protein MyD88 binds to the activated TLR and recruits IL-1 receptor-associated kinases (IRAKs). IRAK activation results, in turn, in the recruitment of the E3 ubiquitin ligase TNF receptor-associated factor (TRAF)6. The subsequent polyubiquitination and activation of transforming growth factor beta-activated kinase (TAK)1, a member of the mitogen-activated protein kinase kinase kinase (MAP3K) family, leads to the activation of two downstream pathways. One is the mitogen-activated protein kinase (MAPK) cascade, comprising the extracellular signal-regulated kinase (ERK), the c-Jun N-terminal kinase (JNK), and the p38 MAPK, inducing activator protein (AP)-1-mediated gene expression.^{32,35} The other is the nuclear factor κ -light-chain-enhancer of activated B cells (NF- κ B) pathway. In the latter case, the inhibitory κ B kinase (IKK) complex, which is composed of three subunits IKK α , IKK β , and IKK γ (also called NEMO for NF- κ B essential modulator), phosphorylates the cytosolic NF- κ B inhibitory protein (I κ B). Phosphorylation of I κ B initiates its degradation by the

ubiquitin-proteasome pathway (UPP) and the release of NF- κ B. The dissociation from the complex allows NF- κ B to translocate into the nucleus. In addition, TLR4 also activates the noncanonical TIR-domain-containing adaptor-inducing interferon- β (TRIF)-dependent pathway, which promotes the production of pro-inflammatory type-I IFNs, such as IFN- α and IFN- β , as well as the activation of the NF- κ B signal transduction.³⁶ As a transcriptional regulator, NF- κ B is largely responsible for inducing genes within the innate as well as the adaptive immune response and especially plays a key role in pro-inflammatory gene expression. NF- κ B mediates the synthesis of inflammatory cytokines, chemokines, and adhesion molecules as well as the induction of enzymes, such as iNOS, phospholipase A2 (PLA2), and COX-2, which are essential for initiation and maintenance of acute and chronic inflammation.

3.3 Prostaglandins

The pivotal role of COX-1 and COX-2 and their products has been well known in inflammatory processes, nociception, and fever, emphasizing the importance of therapeutic interventions. Non-steroidal anti-inflammatory drugs (NSAIDs), such as acetylsalicylic acid (Aspirin[®]), have potent analgesic, antipyretic and, at higher doses, antiphlogistic effects.³⁷ Thus, they are the most abundant and commonly prescribed drugs in the world. Besides their contribution to inflammation, the innate as well as the adaptive immune response, cyclooxygenases and their products also contribute to a wide range of physiological processes, such as the regulation of the arterial blood pressure, the protection of the gastric mucosa, and platelet aggregation.³⁸ Hence, the inhibition of these enzymes are also responsible for a number of gastrointestinal and cardiovascular side effects.³⁹

At the molecular level, NSAIDs inhibit the biosynthesis of PGs through an irreversible acetylation of a serine residue in the active site of the COX enzymes.⁴⁰ Arachidonic acid (AA), a 20-carbon unsaturated fatty acid derived from membrane glycerophospholipids by PLA2, is the major precursor of the eicosanoid signal molecules. AA is further metabolized within the COX or the lipoxygenase (LO) pathway (see Figure 2). The enzymes 5-LO and 15-LO transform AA to various leukotrienes and lipoxins. In contrast, PGs and thromboxanes (TX), collectively termed prostanoids, are generated by both

COX-1 or COX-2 via the intermediate product PGH₂. COX-1 is constitutively expressed and fulfills housekeeping functions, notably in thrombocytes, the stomach, and the kidneys. Whereas, the COX-2 coding gene prostaglandin-endoperoxide synthase (PTGS)2, is an immediate-early gene, which gets induced by inflammatory stimuli.^{41,42} PG terminal-synthases isomerize the unstable intermediate PGH₂ to the biologically active PGs (i.e. PGE₂, PGD₂, PGF_{2α} and PGI₂) or TXs. PGE₂ is the physiologically most abundant eicosanoid in tissue homeostasis in humans and its various key functions have been described in the previous paragraphs.⁴³ Three different PGE synthase (PGES) isoforms have been identified, contributing to the production of PGE₂, including a cytosolic PGES (cPGES) (23 kDa) and two membrane-associated PGESs, the microsomal PGES-1 (mPGES)-1 (17 kDa) and mPGES-2 (33 kDa). The cytosolic isoform of PGES is ubiquitously expressed in the cytosol of various tissues and remains largely unaffected by pro-inflammatory stimuli.⁴⁴ Both, mPGES-1 and mPGES-2, are members of the membrane-associated proteins involved in eicosanoid and glutathione metabolism (MAPEG) superfamily and isomerize the glutathion (GSH)-dependent conversion of PGH₂ to PGE₂, in a strict substrate specific manner.⁴⁵ While mPGES-2 is constitutively expressed, mPGES-1 is markedly induced in a pro-inflammatory setting. In line, mPGES-1 is functionally coupled to the inducible isozyme COX-2 within the perinuclear membrane, facilitating an efficient and rapid transfer of the unstable PGH₂ between both.⁴⁵ The usually concomitant upregulation of COX-2 and mPGES-1 are followed by a strong increase in PGE₂ synthesis, which can be downregulated by glucocorticoids.⁴⁶ Glucocorticoids are a class of steroid hormones, which can easily diffuse through plasma membranes and bind to cytosolic glucocorticoid receptors (cGCRs). The glucocorticoid–cGCR complex translocates into the nucleus and induces the expression of anti-inflammatory proteins, such as IL-10 and IκB.⁴⁷ In the last two decades, new evidence has emerged about the essential role of mPGES-1-derived PGE₂ in the inflammatory context. Indeed, mPGES-1 is abundantly expressed in synovial cells in RA as well as in the collagen-induced arthritis (CIA) model in mice, a well-established model to study RA. One of the numerous studies, focusing on CIA revealed that the disease activity of RA in mPGES-1-deficient mice is strongly reduced.⁴⁸ Intracellularly generated PGE₂ is secreted by the multidrug resistance protein (MRP) 4, a member of the ATP-binding cassette (ABC) transporter superfamily and acts in an autocrine or paracrine manner.⁴⁹

Secreted PGE₂ exerts its biological effects via interaction with four G-protein-coupled receptors (GPCR), present on the target cells: E-prostanoid receptors (EP) 1, EP2, EP3, and EP4. These receptors target a series of intracellular signaling pathways that may even give rise to opposite effects on cellular response, depending on the receptor subtype.⁵⁰ EP1 is associated to the modulating G protein G_qα and EP3 is coupled to the inhibitory G_iα, both leading to a decrease in cAMP by direct inhibition of the adenylyl cyclase (AC).⁵¹ EP2 and EP4, on the other hand, activate the AC via the stimulating G_sα subunit, thereby increasing the intracellular cAMP level.⁵²

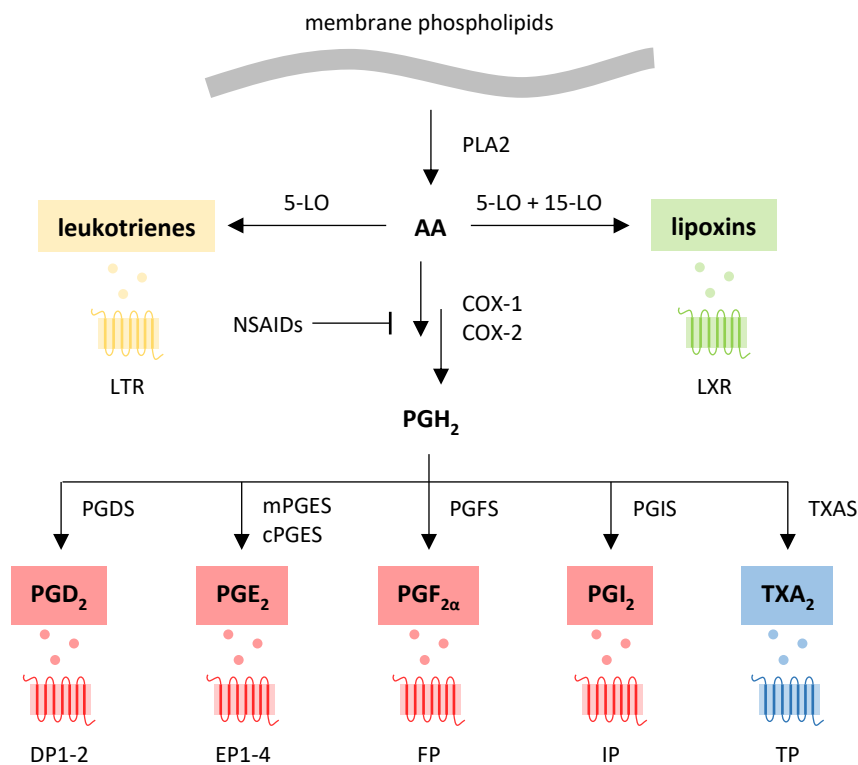


Figure 2. Overview of the eicosanoids biosynthesis pathways.

Arachidonic acid (AA) is a polyunsaturated fatty acid and the major precursor of the eicosanoids. It is released from a phospholipid molecule by the enzyme phospholipase A2 (PLA2) and is processed either in the lipoxygenase (LO) or in the cyclooxygenase (COX) pathway. The LO pathway generates metabolites, such as leukotrienes and lipoxins via the enzymes 5/15-LO. In a two-step reaction, COX enzymes catalyze the transformation of AA to the unstable intermediate prostaglandin (PG)H₂, which is transferred to the terminal synthases, creating prostaglandins and thromboxanes. Active lipid mediators are secreted and recognized by tissue-specific G-protein-coupled receptors (GPCR), respectively. The activity of the COX isoforms can be inhibited by nonsteroidal anti-inflammatory drugs (NSAIDs). Leukotriene receptor (LTR), lipoxin receptor (LXR), prostaglandin D, E, F, I synthase (PGDS, PGES, PGFS, PGIS), PG receptors for prostaglandin D₂, E₂, F_{2α}, I₂ (DP, EP, FP, IP), thromboxane A₂ (TXA₂), thromboxane receptors for thromboxane A₂ (TP).

cAMP is considered to be the most important second messenger of the mPGES-1/PGE₂ signaling axis in macrophages and other cells, especially in shaping a distinct immune response. Phosphodiesterase (PDE)-mediated cAMP degradation counterbalances the intracellular cAMP level by breaking its phosphodiester bond.⁵³ The binding of cAMP to the regulatory subunit of the cAMP-dependent protein kinase A (PKA) liberates the catalytically active subunit, which translocates into the cell nucleus. In the nuclear compartment the catalytic subunit of PKA induces gene expression changes by phosphorylating the cAMP response element-binding protein (CREB) at serine residue 133. The role of the cAMP-dependent CREB-activation was first characterized by the Nobel Prize winner Eric R. Kandel and colleagues at the end of the last century.⁵⁴⁻⁵⁶ CREB, a 43-kDa protein, contains a common transcription factor motif, i.e. the basic leucine zipper (bZIP), which mediates the DNA binding and is present in an entire superfamily of bZIP-containing transcription factors. CREB is also member of closely related transcription factors referred to as the CREB family, including cAMP response element modulator (CREM) and activating transcription factor 1 (ATF1). While CREB and ATF1 can be found ubiquitously, CREM is exclusively expressed in neuroendocrine tissues.⁵⁷

Phosphorylated, thus activated, CREB (pCREB) is capable of binding DNA sequences called cAMP response element (CRE). These comprise highly conserved eight-base-pair palindromic sequences (5'-TGACGTCA-3') recognized with strong affinity by pCREB.⁵⁸ CREs are classically located upstream of the targeted gene, within the promoter region. Upon activation, CREB forms a functionally active dimer, which is kept together by the bZIP domain. Subsequently, dimerized pCREB recruits other transcriptional coactivators, like CREB-binding protein (CBP). One domain of the CBP binds to the pCREB dimer, while another domain activates components of the basal transcriptional machinery. The interaction of CREB with DNA is achieved by the CREB bZIP domain bound to the palindromic CRE site.⁵⁹ Furthermore, the intrinsic histone acetyltransferase (HAT) activity in the CBP facilitates chromatin remodeling. Therefore, acetylation of histones opens the chromatin and promotes the transcriptional activation. The transcriptional signal is terminated by phosphoprotein phosphatase 1 (PP1), which is also phosphorylated via PKA. When the intracellular cAMP levels drop, PP1 promotes the dephosphorylation and thus the inactivation of CREB.⁶⁰

Importantly, while the role of the cAMP-responsive transcription through CREB and the mechanism of CREB-DNA binding is well studied, very little has been reported about the functions and targets specifically bound by activated CREB and, thus differentially regulated within the PGE₂/cAMP axis in WT and mPGES-1 KO macrophages.

3.4 Aims of this thesis

It is well known, that the PGE₂ synthesis is a prominent therapeutic target in the treatment of inflammation-associated diseases. Our understanding in the effects of PGE₂ in this context are well defined. However, a lack of knowledge exists about the specific impact of PGE₂ on CREB-dependent transcriptional changes. Therefore, the aims of this thesis were to characterize the effect of mPGES-1-derived PGE₂ on CREB-mediated transcriptional changes, specifically in murine macrophages in an inflammatory context.

To investigate the role of mPGES-1-derived PGE₂ on inflammation, I stimulated bone marrow-derived macrophages from WT and mPGES-1 KO mice. Initially, prostanoid kinetics were determined, followed by the characterization of the activation, i.e. phosphorylation, of the cAMP-response element binding (CREB) transcription factor. After I successfully established the pCREB-ChIP protocol, a pCREB-ChIP-seq analysis was performed to identify novel pCREB targets that differentially respond to the presence of mPGES-1 in macrophages. Finally, the transcriptional regulation of selected pCREB targets was validated on the mRNA expression level.

4 Animals, materials and methods

4.1 Animals

The mouse substrain used for this research project, C57Bl6/J, was obtained from the mfd Diagnostics GmbH in Wendelsheim, Germany and originally was procured from The Jackson Laboratory in Bar Harbor, Maine, USA. mPGES-1 KO mice were originally procured from Prof. Dr. Akira (Dep. of Host Defense, Osaka University, Osaka, Japan).⁶¹ As controls, Cre-recombinase negative mice with different floxed alleles were used.

Male and female C57Bl6/J were bred in individual cages and maintained in a 12 h/12 h light/dark cycle in a temperature-controlled environment ($22 \pm 1^\circ\text{C}$). Food and tap water in drinking bottles were given *ad libitum*.

4.2 Materials

4.2.1 Cells

Bone marrow-derived macrophages (BMDMs):

Primary murine BMDMs were isolated from bone marrows of male and female C57Bl6/J mPGES-1 KO mice. For comparison reasons, BMDMs were isolated from male and female C57Bl6/J with different floxed alleles, but Cre-recombinase negative WT mice and used as controls.

NIH/3T3:

NIH/3T3 is a mouse embryonic fibroblast cell line established in 1962 at the Department of Pathology in the New York University School of Medicine. Originally the cells were obtained from disaggregated NIH Swiss mouse embryonic fibroblasts.⁶² The cells were purchased from ATCC – LGC Standards GmbH (Wesel, Germany).

4.2.2 Chemicals and reagents

All chemicals and reagents were of highest grade of purity and are listed in Table 1.

Table 1. Chemicals and reagents

Substance	Supplier
Agarose	Sigma-Aldrich (St. Louis, MO, USA)
Ammonium persulfate (APS)	Sigma-Aldrich (St. Louis, MO, USA)
Bovine serum albumin (BSA)	Sigma-Aldrich (St. Louis, MO, USA)
Chloroform	Sigma-Aldrich (St. Louis, MO, USA)
cOmplete ULTRA Protease Inhibitor Tablets (PI)	Sigma-Aldrich (St. Louis, MO, USA)
Dimethyl sulfoxide (DMSO)	Carl Roth GmbH (Karlsruhe)
Dithiothreitol (DTT)	AppliChem GmbH (Darmstadt)
Dynabeads™ Protein G	Thermo Fisher Scientific Inc. (Waltham, MA, USA)
Ethanol	Carl Roth GmbH (Karlsruhe)
Ethidium bromide	Carl Roth GmbH (Karlsruhe)
Ethylenediaminetetraacetic acid (EDTA)	AppliChem GmbH (Darmstadt)
Formaldehyde solution 37%	AppliChem GmbH (Darmstadt)
Glycine	Sigma-Aldrich (St. Louis, MO, USA)
Hydrochloric acid (HCl)	Sigma-Aldrich (St. Louis, MO, USA)
Isopropanol	Merck Millipore (Burlington, MA, USA)
Lithium chloride (LiCl)	Carl Roth GmbH (Karlsruhe)
Methanol (MeOH)	Carl Roth GmbH (Karlsruhe)
Nonidet® P40 (NP-40)	AppliChem GmbH (Darmstadt)
NORMAPUR® Water (HPLC-water)	VWR International (Radnor, PA, USA)
PageRuler™ Prestained Protein Ladder	Thermo Fisher Scientific Inc. (Waltham, MA, USA)
PhosSTOP™	Sigma-Aldrich (St. Louis, MO, USA)
Phenylmethylsulfonyl fluoride (PMSF)	AppliChem GmbH (Darmstadt)
Potassium chloride (KCl)	Merck Millipore (Burlington, MA, USA)
Proteinase K	Thermo Fisher Scientific Inc. (Waltham, MA, USA)
RNase A	Thermo Fisher Scientific Inc. (Waltham, MA, USA)
Sepharose® CL-4B	Sigma-Aldrich (St. Louis, MO, USA)
Sheared salmon sperm DNA	Thermo Fisher Scientific Inc. (Waltham, MA, USA)

Skim milk powder	Merck Millipore (Burlington, MA, USA)
Sodium chloride (NaCl)	Merck Millipore (Burlington, MA, USA)
Sodium deoxycholate	AppliChem GmbH (Darmstadt)
Sodium dodecyl sulfate (SDS)	Merck Millipore (Burlington, MA, USA)
Sodium fluoride (NaF)	Merck Millipore (Burlington, MA, USA)
Sodium hydrogen carbonate	AppliChem GmbH (Darmstadt)
Sodium hydroxide (NaOH)	Merck Millipore (Burlington, MA, USA)
Sodium orthovanadate (Na ₃ VO ₄)	Sigma-Aldrich (St. Louis, MO, USA)
Tetramethylethylenediamine (TEMED)	Carl Roth GmbH (Karlsruhe)
Tris(hydroxymethyl)aminomethan hydrochlorid (Tris-HCl)	Carl Roth GmbH (Karlsruhe)
Triton™ X-100	Sigma-Aldrich (St. Louis, MO, USA)
Tween® 20	AppliChem GmbH (Darmstadt)

4.2.3 Media and reagents for cell culture

All media and reagents used for cell culture work are listed in Table 2.

Table 2. Media and reagents for cell culture

Substance	Supplier
Fetal calf serum (FCS)	Biochrom GmbH (Berlin)
Gibco™ RPMI 1640 Medium	Thermo Fisher Scientific Inc. (Waltham, MA, USA)
Granulocyte-macrophage colony-stimulating factor (GM-CSF)	Immunotools (Friesoythe)
Macrophage colony-stimulating factor (M-CSF)	Immunotools (Friesoythe)
Penicillin-Streptomycin	PAA Laboratories GmbH (Cölbe)
Phosphate buffered saline (PBS)	Biochrom GmbH (Berlin)
Trypsin/EDTA (3.5 U/mg, porcine)	PAA Laboratories GmbH (Cölbe)

4.2.4 Buffers and solutions

Except as noted otherwise, all buffers and solutions were prepared and diluted in double-distilled water (ddH₂O) using a Millipore Millipak 0.22 µM filter purification system. pH adjustment was performed with HCl or NaOH.

Buffers for cell culture

<u>Adherence and culture medium</u>		<u>Phosphate buffered saline (PBS)</u>	
Gibco™ RPMI 1640 Medium	500 mL	NaCl	137 mM
Penicillin	100 U/mL	KCl	2.7 mM
Streptomycin	100 µg/mL	Na ₂ HPO ₄	8.1 mM
heat-inactivated FCS	50 mL	KH ₂ PO ₄	1.5 mM
M-CSF	20 ng/mL	pH	7.4
GM-CSF	20 ng/mL		

Buffers for genotyping

<u>Lysis buffer</u>		<u>Neutralisation buffer</u>	
EDTA	10 mM	Tris-HCl	100 mM
NaOH	10 mM	BSA	1.5%
Tris-HCl	100 mM	pH	4
Proteinase K (50% glycerol)	20 mg/mL		
pH	9		

Buffers and solutions for Western blot analysis

<u>10x blotting buffer</u>		<u>1x blotting buffer</u>	
Tris-HCl	250 mM	10x blotting buffer	10% (v/v)
Glycine	1.9 M	Methanol	20%
pH	8.3		

SDS-running buffer	
Tris-HCl	25 mM
Glycine	190 mM
SDS	3.5 mM
pH	8.3

4x stacking gel buffer	
Tris-HCl	0.5 M
pH	6.8

4x separating gel buffer	
Tris-HCl	1.5 M
pH	8.8

Tris buffered saline with Tween® 20 (TBST)	
Tris-HCl	50 mM
NaCl	140 mM
Tween® 20	0.05% (v/w)
pH	7.4

Antibody diluting solution	
BSA	5% (w/v)
Skim milk powder	5% (w/v)
➔ in TBST	

Sodium dodecyl sulfate (SDS)-polyacrylamid gels:

Component	Separating gel (12%)	Separating gel (15%)	Stacking gel (4%)
40% Acrylamide/Bis-acrylamide (37.5%:1%)	3 mL	3.75 mL	0.3 mL
Separating gel buffer	2.5 mL	2.5 mL	-
Stacking gel buffer	-	-	0.75 mL
10% SDS	0.1 mL	0.1 mL	0.03 mL
ddH ₂ O	4.9 mL	3.85 mL	1.92 mL
TEMED	10 µL	10 µL	5 µL
10% APS	100 µL	100 µL	50 µL

Buffers and gel for IP/Chromatin Immunoprecipitation (ChIP):

IP-buffer		Dilution buffer	
Tris-HCl	50 mM	Tris-HCl	20 mM
NaCl	300 mM	SDS	0.01%
NP-40	1%	Triton™ X-100	1.1%
EDTA	5 mM	EDTA	1.1 mM
Glycerin	10%	NaCl	167 mM
NaF	1 mM	pH	8.0
Na ₃ VO ₄	1 mM		

Lysis buffer I (Cell buffer mix)		Elution buffer (EB)	
Tris-HCl	20 mM	NaHCO ₃	100 mM
KCl	85 mM	SDS	1%
NP-40	0.5%	→ add to 4 mL ddH ₂ O	
PI	2 µL/100 µL		
pH	8.0		

Lysis buffer II (Nuclear lysis buffer)		Tris-EDTA (TE)	
Tris-HCl	50 mM	Tris-HCl	10 mM
EDTA	10 mM	EDTA	1 mM

Lysis buffer II (Nuclear lysis buffer)		Reversion mix	
Tris-HCl	50 mM	Tris-HCl	304 µL
EDTA	10 mM	EDTA	152 µL
SDS	1%	NaCl	304 µL
PI	2 µL/100 µL	RNase A	190 µg
pH	8.0	Proteinase K	380 µg
		pH	6.8

Tris-acetate-EDTA (TAE) buffer		Agarose gel (1.2%)	
Tris-HCl	40 mM	TAE buffer	100 mL
Acetic acid	20 mM	Agarose	1.2 g
EDTA	1 mM	Ethidium bromide	0.5 µg/mL

Wash buffer	I	II	III
Tris-HCl	20 mM	20 mM	10 mM
NaCl	150 mM	500 mM	-
SDS	0.1%	0.1%	-
Triton™ X-100	1%	1%	-
EDTA	2%	2%	1%
LiCl	-	-	250 mM
NP-40	-	-	1%
Sodium deoxycholate	-	-	1%
pH	7.4	7.4	7.4

4.2.5 Stimuli and inhibitors

All stimuli and inhibitors used were diluted in Gibco™ RPMI 1640 Medium. Final concentrations are listed in Table 3.

Table 3. Stimuli and inhibitors

Stimuli/inhibitors	Dilution	Supplier
Murine IFN-γ	50 ng/mL	PeptoTech, Inc. (Rocky Hill, NJ, USA)
Ultra-pure LPS-EB	100 ng/mL	InvivoGen (San Diego, CA, USA)
Zymosan A	50 µg/mL	Sigma-Aldrich (St. Louis, MO, USA)
NS-398	1 µM	Cayman Chemical (Ann Arbor, MI, USA)

4.2.6 Antibodies

All antibodies used for Western blot analysis were diluted in 5% BSA or milk powder in TBST solution and listed in Table 4.

Table 4. Antibodies

Antibody	Dilution	Supplier
Anti-COX-2	1:1000	Cell Signaling Technology (Danvers, MA, USA)
Anti-mouse IgG	1:5000	GE Healthcare Europe GmbH (Freiburg)
Anti-mPGES-1	1:1000	Agrisera (Vännäs, Sweden)
Anti-phospho CREB (Ser133)	1:1000	Merck Millipore (Burlington, MA, USA)
Anti-phospho CREB (Ser133)	1:1000	Cell Signaling Technology (Danvers, MA, USA)
Anti-rabbit IgG	1:5000	GE Healthcare Europe GmbH (Freiburg)
Monoclonal Anti- β -Tubulin	1:3000	Sigma-Aldrich (St. Louis, MO, USA)

4.2.7 Kits

All commercially available kits used are listed in Table 5.

Table 5. Kits

Kit	Supplier
Agilent High Sensitivity DNA Kit	Agilent Technologies, Inc. (Santa Clara, CA, USA)
TG NextSeq [®] 500/550 High Output Kit v2 (75 cycles)	Illumina (San Diego, CA, USA)
KAPA Mouse Fast HotStart Genotyping Kit	Kapa Biosystems (Wilmington, MA, USA)
Maxima First Strand cDNA Synthesis Kit for qPCR	Thermo Fisher Scientific Inc. (Waltham, MA, USA)
NEBNext [®] Ultra [™] II DNA Library Prep Kit for Illumina [®]	New England Biolabs (Ipswich, MA, USA)
peqGOLD RNA Pure [™]	VWR International (Radnor, PA, USA)
QIAquick [®] PCR Purification Kit	QIAGEN (Hilden)

Qubit™ dsDNA BR Assay Kit	Thermo Fisher Scientific Inc. (Waltham, MA, USA)
RIPA Lysis Buffer	Santa Cruz Biotechnology, Inc. (Santa Cruz, CA, USA)
Standard DC™ Protein Assay Kit	Bio-Rad Laboratories, Inc. (Hercules, CA, USA)
SYBR™ Green Supermix	Bio-Rad Laboratories, Inc. (Hercules, CA, USA)

4.2.8 Consumables and instruments

All consumables are listed in Table 6.

Table 6. Consumables

Consumable	Supplier
6-Well Cell Culture Plate CELLSTAR®	Greiner Bio-One GmbH (Frickenhausen)
Amersham™ Protran® nitrocellulose membrane	GE Healthcare (Chicago, IL, USA)
BD Microlance™ 3 needles	Becton Dickinson (Franklin Lakes, NJ, USA)
Cell Scraper 2-Posit. Blade 25 cm	Sarstedt AG & Co. (Nümbrecht)
CELLSTAR® Cell Culture Flasks	Greiner Bio-One GmbH (Frickenhausen)
EASYstrainer™ Cell Sieves	Greiner Bio-One GmbH (Frickenhausen)
Falcon Tubes CELLSTAR® (15, 50 mL)	Greiner Bio-One GmbH (Frickenhausen)
Feather® Disposable Scalpel	FEATHER® Safety Razor Co. Ltd. (Osaka, Japan)
Glassware	Schott AG (Mainz)
Hard-Shell® Full Height 96-Well Semi-Skirted PCR Plates	Bio-Rad Laboratories, Inc. (Hercules, CA, USA)
Injekt® syringe	B. Braun Melsungen AG (Melsungen)
Microseal® 'B' PCR Plate Sealing Film	Bio-Rad Laboratories, Inc. (Hercules, CA, USA)
Pipettes CELLSTAR® (5, 10, 25 mL)	Greiner Bio-One GmbH (Frickenhausen)
Plastic material (cell culture)	Greiner Bio-One GmbH (Frickenhausen)
Reaction tubes (0.2, 0.5, 1.5, 2 mL)	Eppendorf AG (Hamburg)
TipOne® Filter Tips (10, 100, 1000 µL)	STARLAB International GmbH (Hamburg)
Whatman® paper GB 003	neoLab Migge GmbH (Heidelberg)

All instruments are listed in Table 7.

Table 7. Instruments

Instrument	Supplier
Agilent 2100 Bioanalyzer	Agilent Technologies, Inc. (Santa Clara, CA, USA)
Apollo-1 LB 911 photometer	Berthold Technologies GmbH & Co. KG (Bad Wildbad)
Autoclave HV 85	BPW GmbH (Süßen)
B250 Sonifier	Branson Ultrasonics (Danbury, USA)
Canon EOS 600D	Canon Deutschland GmbH (Krefeld)
Centrifuge 5415 R and 5810 R	Eppendorf GmbH (Hamburg)
CFX Connect™ Real-Time PCR Detection System	Bio-Rad Laboratories, Inc. (Hercules, CA, USA)
CKX31 inverted microscope	Olympus Life Science Research Europa GmbH (München)
Dell™Optiplex™ 7010 computer	Dell Inc. (Round Rock, TX, USA)
DynaMag™-2 Magnet	Thermo Fisher Scientific Inc. (Waltham, MA, USA)
Electrophoresis constant power supply ECPS 3000/150	Pharmacia (Peapack, NJ, USA)
Freezer Premium (-20°C)	Liebherr (Bulle FR, Switzerland)
Freezer VIP™ Series (-80°C)	Sanyo Fisher Sales GmbH (Munich)
GenoSmart2	VWR International (Radnor, PA, USA)
Hera safe (Lamina)	Thermo Fisher Scientific Inc. (Waltham, MA, USA)
Ice machine MF 30	Scotsman® (Vernon Hills, USA)
Incubator HERA cell 240	Thermo Fisher Scientific Inc. (Waltham, MA, USA)
Magnetic stirrer Combimag RCH	IKA Labortechnik GmbH & Co. KG (Staufen)
Mastercycler® nexus (Thermocycler)	Eppendorf GmbH (Hamburg)
Microwave NN-CF760M	Panasonic Marketing Europe GmbH (Wiesbaden)
Millipore Millipak 0.22 µM filter system	Merck Millipore (Burlington, MA, USA)
Mini-PROTEAN 3 System (SDS-PAGE)	Bio-Rad Laboratories, Inc. (Hercules, CA, USA)
MiniStar silverline	VWR International (Radnor, PA, USA)

NanoDrop™ 1000 spectrophotometer	Peqlab Biotechnologies GmbH (Erlangen)
Neubauer improved counting chamber	Labor Optik GmbH (Friedrichsdorf)
Odyssey infrared imaging system	Li-COR Biosciences GmbH (Bad Homburg)
PerfectBlue™ Gel System Mini L	Peqlab Biotechnologies GmbH (Erlangen)
ph meter CG 842	Schott AG (Mainz)
Pipettes (10, 100, 1000 µL)	Eppendorf GmbH (Hamburg)
Pipetus® pipetboy	Hirschmann Laborgeräte GmbH & Co.KG (Eberstadt)
Power Supply PowerPac™ HC	Bio-Rad Laboratories, Inc. (Hercules, CA, USA)
Refrigerator Premium (4°C)	Liebherr (Bulle FR, Switzerland)
Stuart® SRT9 Roller mixer	Bibby Scientific Ltd. (Staffordshire, UK)
Thermomixer 5436 compact	Eppendorf GmbH (Hamburg)
Vortexer	VWR international (Radnor, PA, USA)
Water bath TW20	JULABO GmbH (Seelbach)

4.2.9 Quantitative PCR oligonucleotides

Erlin1 (Catalog number: QT00156170) and Elovl5 (Catalog number: QT00117705) primers were purchased from Qiagen N.V. (Hilden). All other oligonucleotides used as forward and reverse primers for qPCR were purchased from Biomers.net (Ulm). The sequences are indicated in Table 8.

Table 8. Oligonucleotides for qPCR

Target	Forward Primer 5'→3'	Reverse Primer 5'→3'
Fos	TAC ACG CGG AAG GTC TAG GA	AAG CGC TGT GAA TGG ATG GA
Jun_1	ATC CAG CCT GAG CTC AAC AC	GAC GCA AGC CAA TGG GAA AG
Jun_2	CTT TCC CAT TGG CTT GCG TC	AGA AGG GCC CAA CTG TAG GA
Sp4_1	GCA TGG CTT TTC CTA AGG CG	GCC GTC AAA AAC TAC GAG GC
Sp4_2	GCC TCG TAG TTT TTG ACG GC	ATA GGC CCA GGC AAA CAA CA
RPS27a	GAC CCT TAC GGG GAA AAC CAT	AGA CAA AGT CCG GCC ATC TTC

4.2.10 Software

All software and used versions are listed in Table 9.

Table 9. Software

Software	Provider
Bio-Rad CFX Manager 3.1	Bio-Rad Laboratories, Inc. (Hercules, CA, USA)
Citavi v6.1	Swiss Academic Software GmbH (Wädenswil, Switzerland)
DNASTAR®	DNASTAR Inc. (Madison, WI, USA)
Image Studio™ Software	Li-COR Bioscience GmbH (Bad Homburg)
Microsoft Office 2016	Microsoft Deutschland GmbH (Unterschleißheim)
ND-1000 v3.2.1	Peqlab Biotechnologies GmbH (Erlangen)
Odyssey 2.1	Li-COR Bioscience GmbH (Bad Homburg)

4.3 Methods

4.3.1 Cell culture

4.3.1.1 Cell culture conditions

The cell culture work was performed under aseptic conditions using autoclaved solutions and consumables inside the laminar flow hood. For the work with living cells media and buffers were pre-warmed by placing them in a water bath set at 37°C. Primary cells as well as cell lines were cultivated in a cell culture incubator with a humidified atmosphere of 5% CO₂ and 37°C.

4.3.1.2 Isolation and culture of BMDMs

Murine BMDMs, i.e. primary macrophages cells were isolated from femur- and tibia-bone marrows from male and female C57Bl6/J mPGES-1 KO mice. For comparison reasons, male and female C57Bl6/J mice with different floxed alleles, but Cre-recombinase negative WT mice were used.

After euthanization each mouse was pinned to the dissection board and doused in 70% ethanol. Skin and muscle tissue from legs were removed, hip joint of each leg was exposed and cut above the joint. Subsequently, bones were cleaned of any remaining muscle and placed in 15 mL Falcon tubes containing ice-cold PBS and penicillin-streptomycin until further use.

Isolated bones were sterilized in 70% ethanol before opening them at their proximal and distal end under sterile conditions. Thereafter, bone marrow was flushed out (2.5 mL/bone) with penicillin-streptomycin-containing culture medium into a 50 mL Falcon tube by inserting a 18G needle attached to a 10 mL syringe until the bone cavity appeared white. The cell suspension of each mouse bone marrow was filtered through a 70 µm EASYstrainer™ Cell Sieve and was centrifuged for 10 min at 1,000 x g, room temperature. Meanwhile, pre-warmed culture medium with freshly added M-CSF (20 ng/mL) and GM-CSF (20 ng/mL) was prepared. The cell pellet was resuspended in

10 mL culture medium, 10 μ L of the cell suspension was used to determine cell numbers in a Neubauer chamber. The suspension with a final cell number of 4×10^6 cells/mL was seeded equally in 6 cm plates (8×10^6 cells/plate = 2 mL cell suspension + 3 mL culture medium) and in 6-Well Cell Culture Plates CELLSTAR[®] (4×10^6 cells/well = 1 mL cell suspension + 1 mL culture medium).

Plates were incubated for seven days allowing bone marrow monocyte/macrophage progenitors to differentiate. On day three and five cells were washed once with PBS and supplied with fresh culture medium containing M-CSF (20 ng/mL) and GM-CSF (20 ng/mL). At day seven cells were stimulated.

4.3.1.3 BMDM stimulation

Differentiated primary murine macrophages were treated with either 100 ng/mL LPS and 50 ng/mL IFN- γ or 50 μ g/mL zymosan in 5 mL (6 cm plates) or 2 mL (6-Well Cell Culture Plate CELLSTAR[®]) stimulation medium, respectively.⁶³ The stimulus was applied for the entire duration of the experiment. During stimulation, plates were kept at 37°C and 5% CO₂. Samples were taken at 2, 4, 8, 16, and 32 h post stimulation. Different sampling methods were performed, described in the following subchapters.

4.3.2 Protein analytics

4.3.2.1 Cell lysis

Cells were seeded in 6 cm plates and treated as indicated. Before sampling, cell culture supernatants were collected in 1.5 mL reaction tubes, centrifuged for 5 min at 16,000 x g and 4°C and stored at -80°C after snap-freezing in liquid nitrogen for later analysis.

Plates were washed twice with ice-cold PBS and kept on ice for sampling. For the cell lysis, RIPA lysis buffer system (composition of 1 x lysis buffer: 1 x TBS, 1% Nonidet P-40, 0.5% sodium deoxycholate, 0.1% SDS, 0.004% sodium azide) with freshly added PI (10 μ L/mL lysis buffer), PMSF (10 mM) and PhosSTOP[™] (1 tablet/10 mL lysis buffer) was used. 250 μ L RIPA lysis buffer was added per plate and incubated for 5 min, then the

cells were scraped off using a cell scraper. Cell debris was pelleted by centrifugation for 10 min at 16,000 x g and 4°C, then the supernatant was transferred to a new 1.5 mL reaction tube and stored at -20°C.

4.3.2.2 Protein quantification

The protein content of the cell lysates was determined using the Standard DC™ Protein Assay Kit, which is based on the Lowry method.⁶⁴ To accomplish that, BSA-standards were prepared in ddH₂O to cover the range of the assay (0, 0.25, 0.5, 1, 1.5, and 2 mg/mL). 5 µL of each standard as well as sample were added in duplicates to a clear flat-bottom 96-well microtiter plate. Subsequently, 25 µL reagent A, then 200 µL reagent B was added and incubated at room temperature on a shaker for a minimum of 15 min. The extinction was measured at 750 nm using the Apollo-1 LB 911 photometer.

4.3.2.3 SDS-polyacrylamide gel electrophoresis (PAGE) and Western blotting

For SDS-PAGE 12% and 15% SDS-polyacrylamid gels in handcasting frames were prepared according to protein molecular size. In the first step, a separating gel solution was prepared and filled into the frame. Then immediately, the solution was overlaid with isopropanol. While the gel was allowed to polymerize for at least 30 min the stacking gel was prepared. The overlay solution of the polymerized gel was poured off and the stacking gel solution was filled in. Immediately, the comb was placed into the assembled gel sandwich.

30 µg protein of each sample was denaturated at 95°C in 4 x SDS loading buffer for 5 min and loaded into the wells of the SDS-PAGE, along with the PageRuler™ Prestained Protein Ladder. After the gel was run for 15 min at 80 V, the voltage was increased to 120 V to finish the run in about 1 h. Proteins were transferred onto a nitrocellulose membrane by blotting the gel at a constant current of 0.25 A for 1.5 h. To ensure similar protein loadings on membranes, reversible staining with Ponceau S was used. Membranes were blocked with 5% TBST for 30 min at room temperature (RT) and incubated with the primary antibody in 5% BSA over night at 4°C. On the following day membranes were washed 3 x for 5 min with TBST and incubated with appropriate

secondary antibodies in light-protected Falcon tubes for 1 h at RT. After three more washing steps the membranes were visualized on an Odyssey infrared imaging system.

4.3.3 RNA analytics

4.3.3.1 Isolation

For RNA isolation, 1 mL peqGOLD RNA Pure™ was added per well. The cell suspension of each well was pipetted to 2 mL reaction tubes and 200 µL chloroform was added. After 15 s vortexing, incubation on ice for 10 min followed by centrifugation for 15 min at 16,000 x g and 4°C the upper aqueous phase of each sample was transferred to new reaction tubes and mixed with the same volume isopropanol. This was incubated at 4°C for 15 min and the precipitates were pelleted by centrifugation for 15 min at 16,000 x g and 4°C. Afterwards, supernatants were discarded and precipitates were washed twice with 500 µL 75% (v/v) ethanol. Between each washing step samples were centrifuged for 10 min at 16,000 x g and 4°C and reaction tubes were turned upside down for 10 min at RT. After pellets were dried for 5 min at 70°C, the remaining RNA was dissolved in 20 µL HPLC-water by shaking for 30 min at 60°C and 550 rpm. RNA content was quantified spectrometrically using a NanoDrop™ 1000 spectrophotometer.

4.3.3.2 Reverse transcription

To reverse transcribe the isolated RNA, as described in 4.3.3, into cDNA, a reverse transcription was performed according to the instructions of the Maxima First Strand cDNA Synthesis Kit. The components for each sample are listed in Table 10.

Table 10. Reverse transcription reaction components per sample

Component	Amount
RNA	500 – 1000 ng
5x reaction mix	4 µL
Maxima Enzyme Mix	1 µL
HPLC-water	add to 20 µL final reaction volume

The reaction was performed using the Eppendorf Mastercycler® nexus with program settings indicated in Table 11. The resulting cDNA samples were stored at -20°C until further analysis.

Table 11. Reverse transcription program settings

Step	Time [min]	Temperatur [C°]
1	10	25
2	15	50
3	5	85
4	∞	10

4.3.3.3 Quantitative PCR (qPCR)

The qPCR was performed using SYBR™ Green Supermix according to the manufacturer's protocol. Table 12 displays reaction components for each sample.

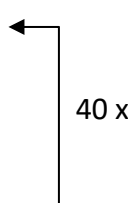
Table 12. qPCR reaction components per sample

Component	Volume [µL]	Concentration
Template cDNA	2	25 – 50 ng
Forward primer	0.25	5 pmol
Reverse primer	0.25	5 pmol
SYBR™ Green Supermix	5	-
ddH ₂ O	2.5	-

The listed components were loaded in duplicates in a Hard-Shell® Full Height 96-Well Semi-Skirted PCR Plate and sealed with Microseal® 'B' PCR Plate Sealing Film. The reaction was performed using the CFX Connect™ Real-Time PCR Detection System with program settings indicated in Table 13. The data were analyzed with the Bio-Rad CFX Manager 3.1.

Table 13. qPCR program settings

Step	Reaction	Time [min:s]	Temperatur [C°]
1	Activation of polymerase	2:00	50
2	Initial denaturation	3:00	95
3	Denaturation	0:15	95
4	Primer annealing	0:30	60
5	Elongation + plate read	0:30	72
6	Go to step 3	-	-
7	Final denaturation	0:30	95
8	Final renaturation	0:30	72
9	Melt curve + plate read	0:05	72 to 95, increment 0,5



4.3.4 Immunoprecipitation

To perform immunoprecipitations, two aliquots of well-mixed 90 μ L Dynabeads™ Protein G were transferred to a 1.5 mL reaction tube in a magnetic separation rack, respectively. Once the solution was clear, buffer was removed and 1 mL IP-buffer was added to wash the magnetic bead pellet. After a second washing step 180 μ L IP-buffer was pipetted to the beads. 90 μ L of the resuspension was incubated with 10 μ L anti-phospho CREB from either Cell Signaling Technology (CST) or Merck Millipore (Milli), respectively. Antibodies were coated to the beads for 2 h on a tube rotator at 4°C. Thereafter, coated Dynabeads™ Protein G were collected in the separation rack and washed twice with 1 mL IP-buffer. NIH/3T3 fibroblasts were cultured in 10 cm dishes and lysed with 400 μ L RIPA lysis buffer. Lysates were processed as described in 4.3.2. Subsequently, samples were diluted with IP-buffer to a final volume of 500 μ L containing a protein amount of 450 μ g. Each sample was incubated with either pCREB-coated or uncoated Dynabeads™ Protein G and incubated on a tube rotator over night at 4°C. On the following day, beads were collected and washed twice with IP-Buffer. 50 μ L 4 x SDS loading buffer was added to each sample and incubated for 5 min at 95°C.

Then, beads were collected and supernatants were transferred to fresh reaction tubes. Samples were loaded to a 12% SDS-PAGE and processed as indicated in 4.3.2.

4.3.5 pCREB-ChIP

For ChIP, BMDMs were isolated, cultured, and stimulated as described in subsection 4.3.1.

Fixation of cells:

Under the chemical fume hood, formaldehyde was added directly to the culture medium of each 6 cm dish to a final concentration of 1% and incubated for 10 min on an orbital shaker at RT. The reaction was stopped by adding glycine to a final concentration of 0.125 M and incubation on the orbital shaker for 5 min at RT.

Harvesting:

The fixed cells were washed twice with ice-cold PBS for 5 min and kept on ice for sampling, then the cells were scraped off using a cell scraper. The cells were collected in 15 mL Falcon tubes and pelleted by centrifugation for 5 min at 16,000 x g and 4°C, supernatant was discarded. Pellets were snap-frozen in liquid nitrogen and stored at -80°C until further use.

Lysis:

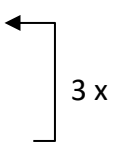
After thawing the pellets 2 mL lysis buffer I (freshly added PMSF + PI) was added and incubated on ice for 15 min. After centrifugation for 5 min at 16,000 x g and 4°C supernatants were aspirated, and the remaining nuclei were resuspended in 200 µL lysis buffer II. After 10 min of incubation on ice, suspensions were transferred to 1.5 mL reaction tubes.

Sonication:

Each sample tube was gently moved under the metal tip of the sonicator probe until the tip was immersed 60-80% in the liquid. During shearing the DNA to 300 – 500 bp fragments, lysates were cooled using an ice-ethanol bath. The sonication was performed on the B250 Sonifier (Branson Ultrasonics) using the following settings (Table 14).

Table 14. Program settings for sonication

Configuration	Set value
Duty cycle	0.5 s pulse ON / 1 s OFF
Amplitude	10%
Time	20 s with stop on ice in between



Lysates were then cleared by centrifugation for 5 min at 16,000 x g at 4°C. Supernatants were transferred to 2 mL reaction tubes and 1.8 mL dilution buffer was added to each sample.

Pre-clearing:

50 µL per IP of resuspended and blocked Protein A Sepharose® CL-4B was prepared for all samples and centrifuged at minimum possible speed for 1 min and 4°C. Supernatant was removed and replaced with the same volume of dilution buffer (with freshly added PI). 50 µL resuspended beads then were added to each sample and incubated for 45 min on the tube rotator at 4°C. Subsequently, samples were centrifuged at minimum possible speed for 1 min and 4°C and each supernatant was distributed to two new 1.5 mL reaction tubes (950 µL each). 2 µL IgG or 3 µL anti-pCREB (CST) was added to each aliquot and IP samples were incubated on the tube rotator over night at 4°C. Another aliquot (input) of 10 µL was stored for each sample at 4°C until further use.

Blocking of Protein A/G PLUS-Agarose beads:

50 µL resuspended beads per IP were pipetted to a 1.5 mL tube and washed twice with 1 mL dilution buffer, refilled with dilution buffer to a final volume of 50 µL to get 50% bead slurry. Thereafter, 1:20 of 10% BSA and 1:200 of sheared salmon sperm was added. Beads were blocked over night at 4°C.

Binding beads to complexes:

50 µL of resuspended blocked bead slurry was added to each IP antibody-incubation mix and rotated for 2 h at 4°C. Meanwhile, wash buffers were prepared with 20 µL PI/mL. After rotation, bead-complexes were centrifuged at minimum possible speed for 1 min and 4°C and supernatants were gently aspirated. Beads were washed with 1 mL wash

buffers I – III, and centrifuged at minimum possible speed for 1 min and 4°C, following by a last washing step with 1 mL room tempered TE.

Elution and reversion:

A sufficient volume BE was prepared and 100 µL of it was added to each bead-pellet. Beads were mixed at maximum speed (16,000 x g) at 55°C in the thermomixer. After centrifugation for 1 min at RT, supernatants were transferred to 0.5 mL tubes. The procedure was repeated and the supernatants were pooled. 200 µL of EB was added to the input samples and 42 µL reversion mix was pipetted to every sample. To reverse crosslinks, tubes were placed into the thermocycler over night at 65°C.

Purification of chromatin:

For DNA purification, the QIAquick® PCR Purification Kit was used according to the manufacturer's protocol. The precipitated chromatin was amplified by qPCR, using five primer sets against five different pCREB binding sites of the Fos-, Jun-, and Sp4-genes.

4.3.6 Next-Generation-Sequencing (NGS)

ChIP-seq libraries were prepared using the NEBNext® Ultra™ II DNA Library Prep Kit for Illumina®, according to the manufacturer's protocol. To optimize the fragment size distribution, DNA was purified by agarose gel electrophoresis and DNA bands between 300 and 500 bp along with the 100 bp DNA ladder were cut out and purified. The potential pCREB target DNA replicates were amplified by PCR to generate the final ChIP-seq libraries. Each library was assessed using Agilent 2100 Bioanalyzer as depicted in Figure 3. ChIP-seq libraries were sequenced on a NextSeq® 500 sequencer (Illumina®) according to the manufacturer's protocol using the TG NextSeq® 500/550 High Output Kit v2 (75 cycles). 24 samples in total were sequenced in two independent NGS runs with 12 samples in each run using 1.8 pM library for sequencing and 20% PhiX control. Sequence data were analyzed using DNASTAR®.

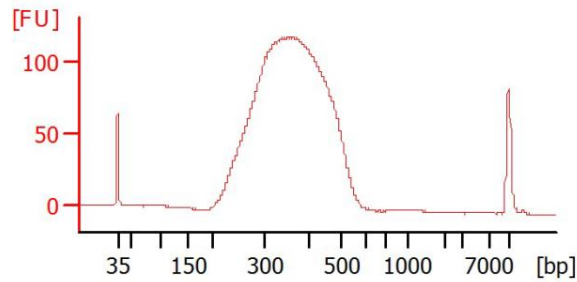


Figure 3. Representative size distribution of sequencing libraries.

1 μ L of a purified DNA library extracted from an agarose gel was applied to a DNA high sensitivity chip and analyzed on an Agilent 2100 Bioanalyzer according to the manufacturer’s protocol. Representative electropherogram with a maximum at approximately 300 base pairs (bps). FU = Fluorescence Units.

4.3.7 Genotyping

As in this project mPGES-1 KO mice were used and compared to WT mice in their biological functions, it was necessary to identify the genotype at every generation of all animals. To do so, earlobe or tail biopsies from mice were processed with the KAPA Mouse Fast HotStart Genotyping Kit according to the manufacturer’s protocol. To evaluate the integrity of DNA, a set of three primers (“a”, “b” and “c”) was used that allows for efficient genotyping by PCR reactions (Table 15):

Table 15. Oligonucleotides for genotyping-PCR

Label	Primer 5’→3’
“a”	CAG TAT TAC AGG AGT GAC CCA GAT GTG → primer specific for mPGES-1 gene
“b”	GGA AAA CCT CCC GGA CTT GGT TTT CAG → primer complementary for mPGES-1 gene downstream of targeting construct
“c”	ATC GCC TTC TAT CGC CTT CTT GAC GAG → primer specific for neomycin resistance gene

For detection of the WT allele, primers “a” and “b”; for the mutated allele, primers “b” and “c” were used. The samples were diluted 1:10 before reaction mixtures were prepared as shown in Table 16.

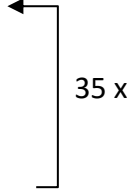
Table 16. Genotyping-PCR reaction components per sample

Component	Volume [μL]
Template DNA	3
Primer mix	1
Ready mix	6
ddH ₂ O	3

Each sample was analysed with both primer compositions. Final mixtures were loaded into 0.2 mL reaction tubes and amplified using the Mastercycler® nexus with program settings presented in Table 17.

Table 17. PCR program settings for genotyping

Step	Reaction	Time [min:sec]	Temperatur [C°]
1	Initiation	5:00	95
2	Denaturation	1:00	95
3	Primer annealing	0:30	62
4	Elongation	2:00	72
5	Go to step 2	-	-
6	Final elongation	2:00	72



Amplified PCR products were transferred to a 1.2% (w/v) agarose gel. DNA separation was performed by 130 V for 30 min and visualized using the UV transilluminator GenoSmart2. Both amplification products are about 1300 bp.

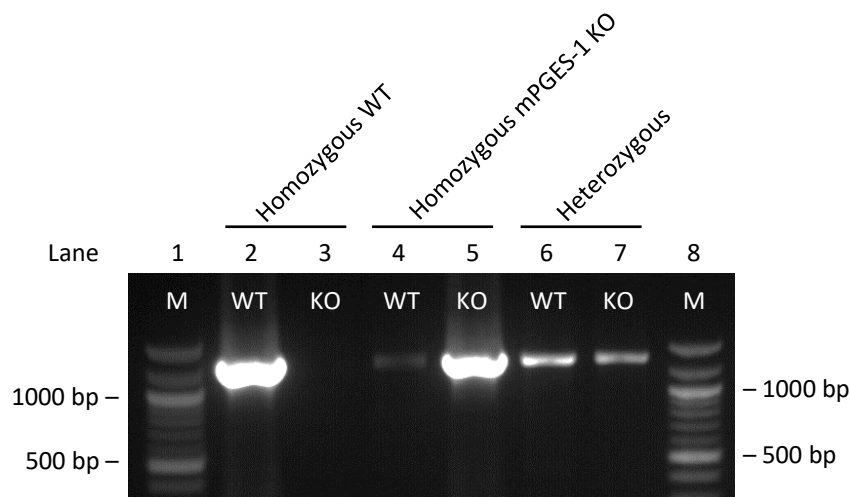


Figure 4. Genotyping results of WT and mPGES-1 KO mice.

Biopsy of earlobe or tail of WT and mPGES-1 KO mice was processed by KAPA Mouse Fast HotStart Genotyping Kit. Extracted DNA of each mouse was amplified by PCR reactions and products were separated by 1.2% agarose gel electrophoresis with ethidium bromide staining. Amplified products were both about 1300 base pairs (bp). Positive identification for mPGES-1 gene in lanes: 2 and 6. M = 100 bp DNA ladder. Left and right side labels indicate fragment length in bps.

4.3.8 Prostanoid quantification

The analysis of the prostanoids in the cell culture supernatants was carried out at the Institute of Clinical Pharmacology, University Clinics, Goethe University Frankfurt/M. For the determination of the concentrations liquid chromatography-mass spectrometry/mass spectrometry (LC-MS/MS) was used. 200 μ L sample volume each was spiked with isotopically labeled internal standards (PGE₂-d₄, PGD₂-d₄, TXB₂-d₄, PGF_{2 α} -d₄) and extracted using liquid-liquid-extraction with ethyl acetate. The LC-MS/MS analysis of all analytes was performed using an Agilent 1290 Infinity™ LC system (Agilent Technologies, Inc., Santa Clara, CA, USA) coupled to a hybrid triple quadrupole linear ion trap mass spectrometer QTRAP® 6500+ (AB Sciex, Darmstadt, Germany) equipped with a Turbo-V™-source operating in negative electrospray ionization (ESI) mode. The chromatographic separation of the prostanoids was carried out using a Synergi™ Hydro-RP column (150 \times 2 mm, 4 μ m particle size and 80 Ångström (Å) pore size; Phenomenex Ltd., Aschaffenburg, Germany) under gradient conditions with water and acetonitrile as

mobile phases, both containing 0.0025% formic acid. All analytes were evaluated by Analyst Software 1.6 and Multiquant Software 3.0.2 (both AB Sciex, Darmstadt, Germany) using the internal standard method (isotope-dilution mass spectrometry).

4.3.9 Statistical analysis

Each experiment was performed at least three times with different WT and mPGES-1 KO mice. The data graphs represented in this thesis showed arithmetic mean values \pm standard errors of the mean (SEM). Statistical analysis on significance levels was performed as indicated in the individual figure legends, by student's t-test with Microsoft Excel. The values were assumed to be significant if $p \leq 0.05$ (*), $p \leq 0.01$ (**) or $p \leq 0.001$ (***). Significance between normalized treated samples and control samples were analysed against the normalized control samples and determined as significant if $p \leq 0.05$ (#), $p \leq 0.01$ (##) or $p \leq 0.001$ (###). For Western blot analysis one representative blot for each condition is shown.

5 Results

5.1 Characterization of mPGES-1, pCREB and COX-2

To characterize the role of CREB in zymosan and LPS+IFN- γ -stimulated murine primary macrophages, activation of CREB in naïve and stimulated macrophages was evaluated. To achieve this, bone marrow-derived macrophages were stimulated with LPS+IFN- γ or zymosan for 2 – 32 h and CREB activation was analysed by Western blotting. Differences in CREB activation were compared in WT and mPGES-1 KO macrophages. Figure 5 shows the protein expression of mPGES-1, pCREB, and COX-2 after stimulation at the indicated time points. mPGES-1 protein expression was not detectable in mPGES-1 deficient macrophages confirming the KO status.

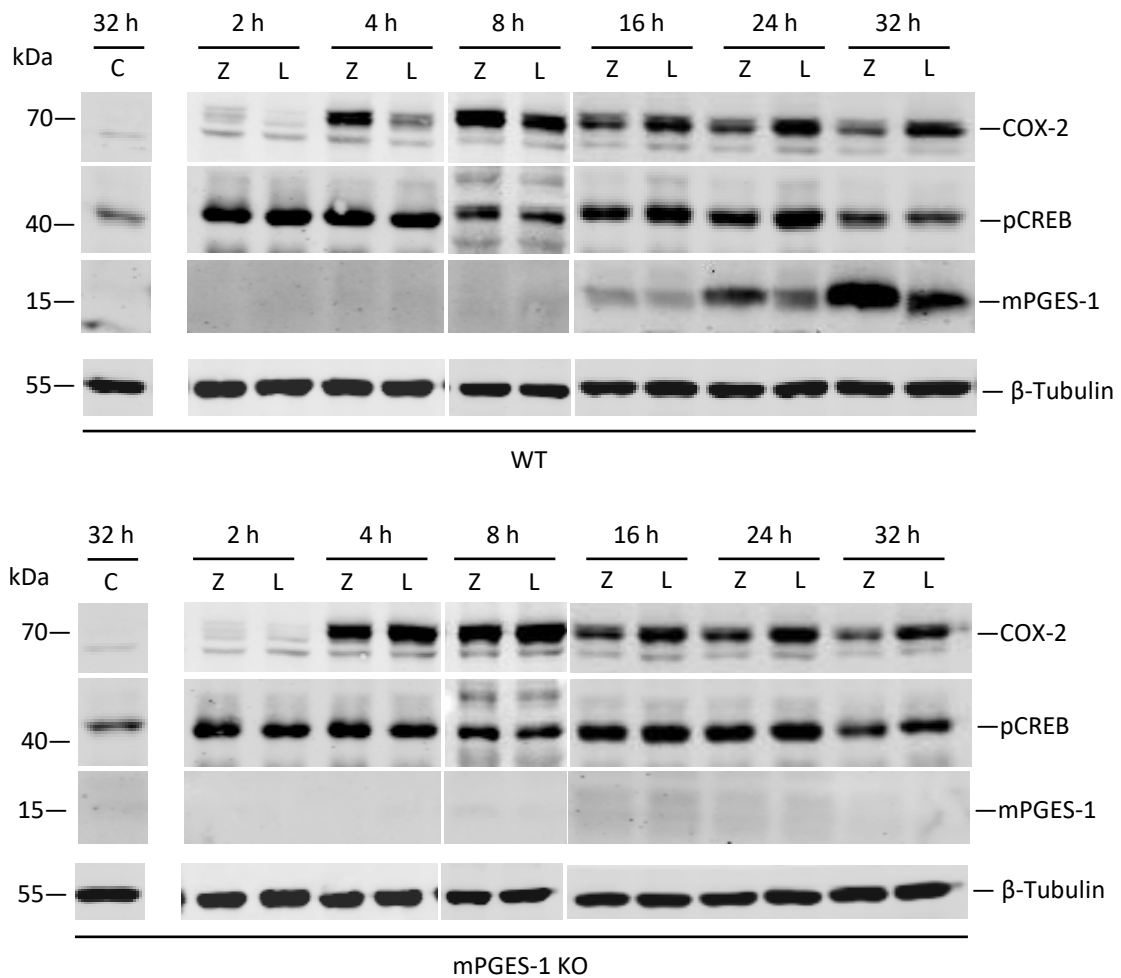


Figure 5. Detection of COX-2, pCREB, and mPGES-1 upon stimulation with LPS+IFN- γ and zymosan in WT and mPGES-1 KO BMDMs.

Isolated murine bone marrow was differentiated for 7 days in the presence of 20 ng/mL M-CSF and GM-CSF to bone marrow-derived macrophages (BMDMs) and stimulated with 50 μ g/mL zymosan (Z) or 100 ng/mL lipopolysaccharides (LPS, L) and 50 ng/mL interferon gamma (IFN- γ). Samples were taken at indicated time points and cyclooxygenase-2 (COX-2), phosphorylated cAMP response element-binding protein (pCREB), and microsomal prostaglandin E synthase-1 (mPGES-1) protein expression was detected by Western blot analysis. Controls (untreated samples) were generated at 4, 8, 16, 24, and 32 h. Protein loading in each experiment was normalized to β -tubulin. A representative blot is shown ($n = 2 - 6$). Control (C), kilodalton (kDa).

The quantitative analysis of the Western blots as shown in Figure 5 revealed that mPGES-1 was induced primarily at later time points in WT macrophages upon both LPS+IFN- γ and zymosan stimulation (Figure 6). Significant increases were observed in both after 8 and 24 h. Maximal mPGES-1 protein expression was detected after 32 h with a 8 ± 1.5 -fold induction in LPS+IFN- γ -treated WT macrophages and 44.3 ± 17.5 -fold induction in zymosan-treated WT macrophages, relative to control level. Quantification of mPGES-1 KO blots detected background noises only.

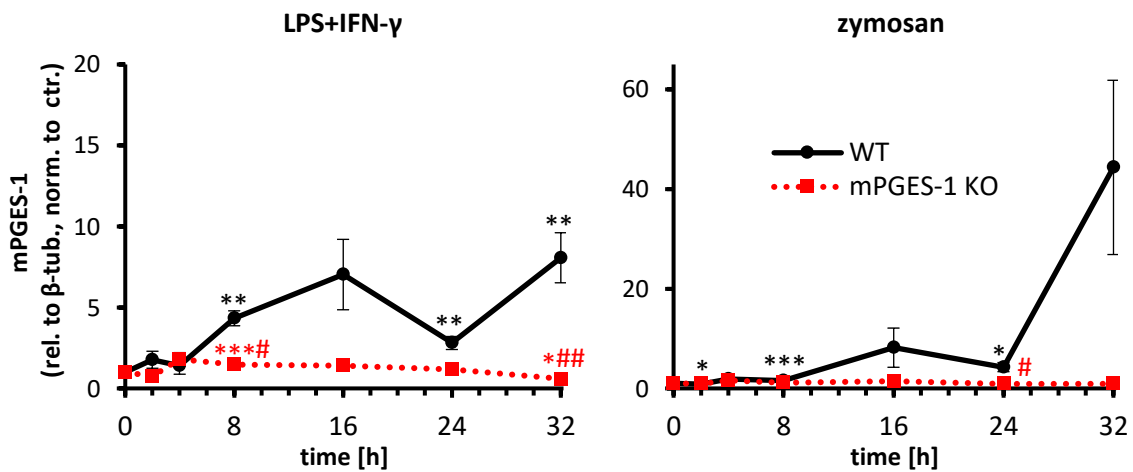


Figure 6. mPGES-1 protein expression in LPS+IFN- γ and zymosan-stimulated murine WT and mPGES-1 KO BMDMs.

Isolated murine bone marrow was differentiated for 7 days in the presence of 20 ng/mL M-CSF and GM-CSF to BMDMs and stimulated with 100 ng/mL LPS and 50 ng/mL IFN- γ or 50 μ g/mL zymosan. Samples were taken after 2, 4, 8, 16, 24, and 32 h and mPGES-1 protein expression relative to β -tubulin was detected by Western blot analysis. Data are normalized to untreated control and presented as means \pm SEM (n = 2 – 4). Statistical significance was determined relative to untreated control [$p \leq 0.05$ (*), $p \leq 0.01$ (**), or $p \leq 0.001$ (***)] and mPGES-1 KO to WT [$p \leq 0.05$ (#) or $p \leq 0.01$ (##)].

Thus, LPS+IFN- γ and zymosan induced mPGES-1 in WT but not in mPGES-1 KO macrophages.

Regarding pCREB activation, Figure 7 shows a fast induction of pCREB in WT macrophages upon stimulation with LPS+IFN- γ within the first 8 h with a maximum induction of 2.5 ± 0.5 relative to the control level. Significantly increased pCREB level

remained stable between 8 – 24 h and subsequently dropped to levels comparable to control after 32 h. In response to LPS+IFN- γ , mPGES-1 KO macrophages showed a delayed induction with maximum significant levels between 16 – 24 h (2.1 ± 0.3 -fold induction relative to control level). Induction declined after 24 h like in WT macrophages. Zymosan triggered a strong transient induction of pCREB in WT macrophages with a maximum after 8 h and subsequent stable reduction until 32 h. Compared to WT, mPGES-1 KO macrophages revealed a moderate increase up to a maximum after 24 h with a fold induction of 2.2 ± 0.3 relative to control level. Subsequently, pCREB level decreased in the mPGES-1 KO macrophages.

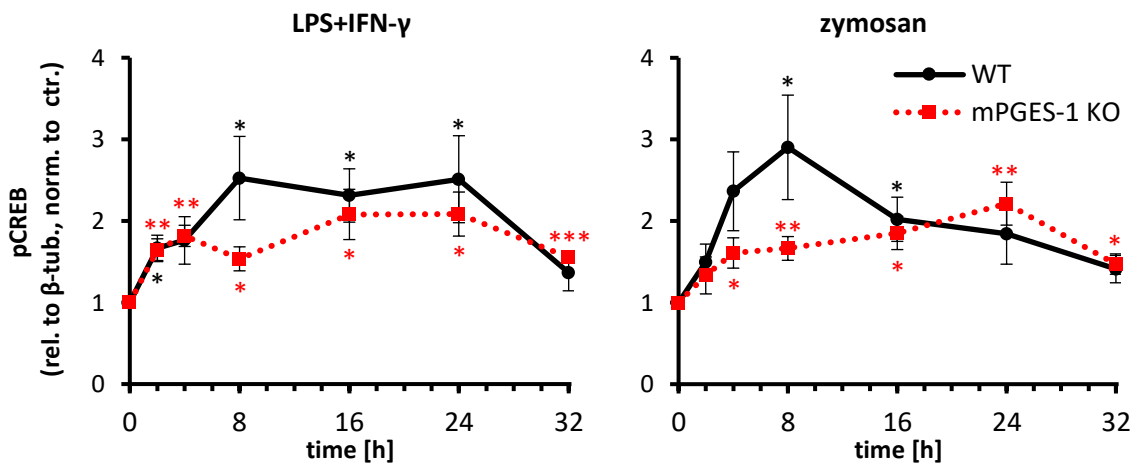


Figure 7. pCREB protein expression in LPS+IFN- γ and zymosan-stimulated murine WT and mPGES-1 KO BMDMs.

Isolated murine bone marrow was differentiated for 7 days in the presence of 20 ng/mL M-CSF and GM-CSF to BMDMs and stimulated with 100 ng/mL LPS and 50 ng/mL IFN- γ or 50 μ g/mL zymosan. Samples were taken after 2, 4, 8, 16, 24, and 32 h and pCREB protein expression relative to β -tubulin was detected by Western blot analysis. Data are normalized to untreated control and presented as means \pm SEM ($n = 4 - 6$). Statistical significance was determined relative to untreated control [$p \leq 0.05$ (*), $p \leq 0.01$ (**) or $p \leq 0.001$ (***)].

In conclusion, LPS+IFN- γ and zymosan induced a transient CREB activation in WT and a transient, however delayed activation in mPGES-1 KO macrophages.

As mPGES-1 is functionally coupled to COX-2, the expression profile of COX-2 was also determined by Western blot analysis. The quantification of COX-2 in WT LPS+IFN- γ -stimulated macrophages revealed a stable increase up to a significant maximum peak after 24 h with a 124 ± 10.8 -fold induction relative to control level, followed by a decrease to 81 ± 26.9 -fold induction relative to control level after 32 h (Figure 8). mPGES-1 KO macrophages showed an initial peak after 4 h (59 ± 29 -fold induction) and an overall stable induction to a plateau between 24 – 32 h and a maximum after 24 h with an 86.9 ± 26.2 -fold induction relative to control level. Zymosan leads to a rapid and strong induction of COX-2 to a significant initial peak after 4 h with a 57.4 ± 19.2 -fold induction in WT macrophages. COX-2 induction remained at stable levels between 4 – 24 h forming a plateau maximum after 24 h with a 77.7 ± 4.2 -fold induction relative to control. After 32 h COX-2 level declined to a 41.9 ± 13.6 -fold induction relative to control. The COX-2 profile in mPGES-1 KO macrophages showed very similar courses like in WT macrophages with an initial peak after 4 h with a 47.5 ± 20.1 -fold induction and a second peak after 24 h with a 67.7 ± 13.4 -fold induction relative to control.

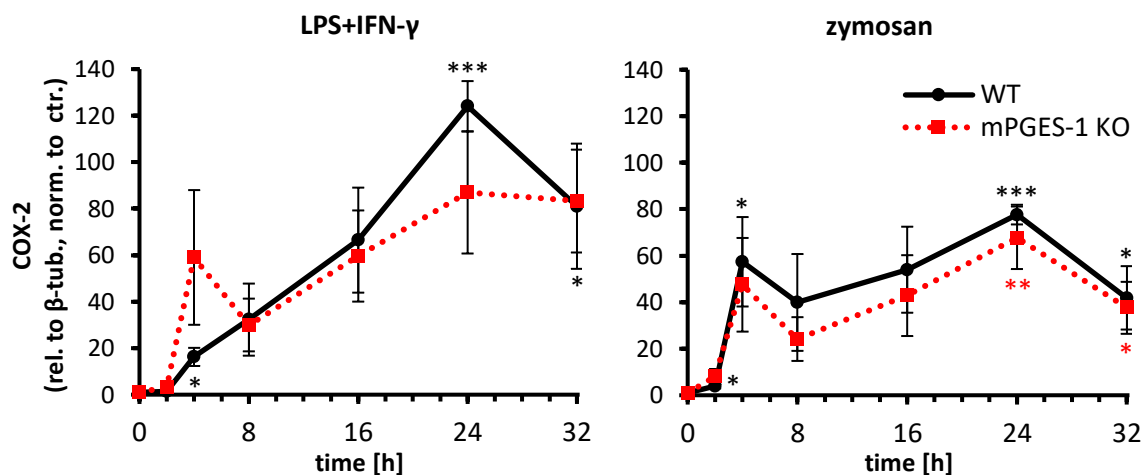


Figure 8. COX-2 protein expression in LPS+IFN- γ and zymosan-stimulated murine WT and mPGES-1 KO BMDMs.

Isolated murine bone marrow was differentiated for 7 days in the presence of 20 ng/mL M-CSF and GM-CSF to BMDMs and stimulated with 100 ng/mL LPS and 50 ng/mL IFN- γ or 50 μ g/mL zymosan. Samples were taken after 2, 4, 8, 16, 24, and 32 h and COX-2 protein expression relative to β -tubulin was detected by Western blot analysis. Data are normalized to untreated control and presented as means \pm SEM (n = 4 – 5). Statistical significance was determined relative to untreated control [$p \leq 0.05$ (*), $p \leq 0.01$ (**), or $p \leq 0.001$ (***)].

Taken together, LPS+IFN- γ and zymosan trigger a strong induction of COX-2 in both WT and mPGES-1 KO macrophages.

Based on the protein analytics, LPS+IFN- γ and zymosan appear as potent stimuli of inflammatory context-associated proteins in WT and mPGES-1 KO macrophages. Altered expression of COX-2 and mPGES-1 might result in altered prostanoid levels which the following subchapter deals with.

5.2 Prostanoid profiles

To get further insights into the effects of mPGES-1-derived PGE₂ on CREB activation upon stimulation with LPS+IFN- γ and zymosan, the kinetics of PGE₂ and other prostanoids were measured. Therefore, cell culture supernatants of the respective samples were collected and analyzed for their secreted prostanoid concentration by LC-MS/MS as described in subchapter 4.3.8.

LPS+IFN- γ triggered continuous increases in PGD₂ production to a significant maximum after 16 h with a 183.9 \pm 29.1-fold induction in WT and 244.4 \pm 30.3-fold induction in mPGES-1 KO macrophages (Figure 9). Subsequently, PGD₂ levels dropped slightly to 100.9 \pm 4.8-fold induction in WT and 152.8 \pm 22.1-fold induction in mPGES-1 KO macrophages after 32 h. Upon stimulation with zymosan PGD₂ level in WT macrophages increased strongly to a significant maximum 405.9 \pm 89.8-fold induction after 4 h and decreased slowly to levels comparable to control. The effect of zymosan on mPGES-1 KO macrophages is negligible and remained at levels comparable to control within 32 h.

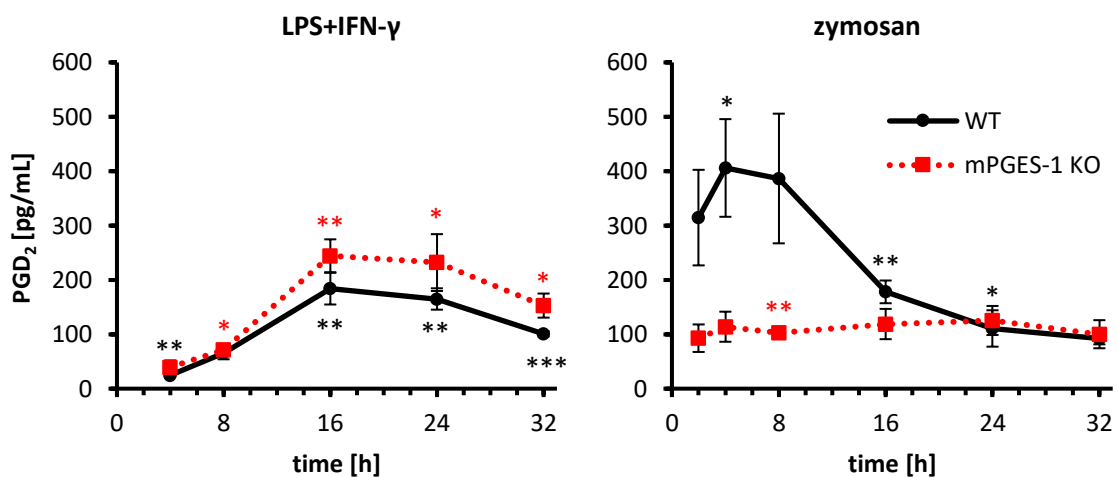


Figure 9. PGD₂ levels in LPS+IFN- γ and zymosan-stimulated murine WT and mPGES-1 KO BMDMs.

Isolated murine bone marrow was differentiated for 7 days in the presence of 20 ng/mL M-CSF and GM-CSF to BMDMs and stimulated with or without 100 ng/mL LPS and 50 ng/mL IFN- γ or 50 μ g/mL zymosan. Cell culture supernatants were taken and analyzed for PGD₂ levels via LC-MS/MS. Basal PGD₂ level: WT 38 \pm 1.7 pg/mL and mPGES-1 KO 9.2 \pm 9.2 pg/mL. Data are presented as mean values \pm SEM (n = 3). Statistical significance was determined relative to untreated control [p \leq 0.05 (*), p \leq 0.01 (**), or p \leq 0.001 (***)].

Thus, LPS+IFN- γ significantly increased PGD₂ levels in WT and mPGES-1 KO, whereas zymosan drives to strong transient secretion of PGD₂ in WT only.

Quantitative determination of TXB₂ levels revealed a continuous induction in both WT and mPGES-1 KO macrophages upon stimulation with LPS+IFN- γ up to a maximum 1379.5 \pm 406.5-fold induction and 1407.8 \pm 126.5-fold induction after 24 h, respectively (Figure 10). Zymosan induced significant alteration in TXB₂ production in WT slightly stronger compared to mPGES-1 KO macrophages. After 32 h TXB₂ reached a significant maximum level with a 1718.7 \pm 28.8-fold induction in WT and 1828.7 \pm 225.9-fold induction in mPGES-1 KO macrophages upon stimulation with zymosan.

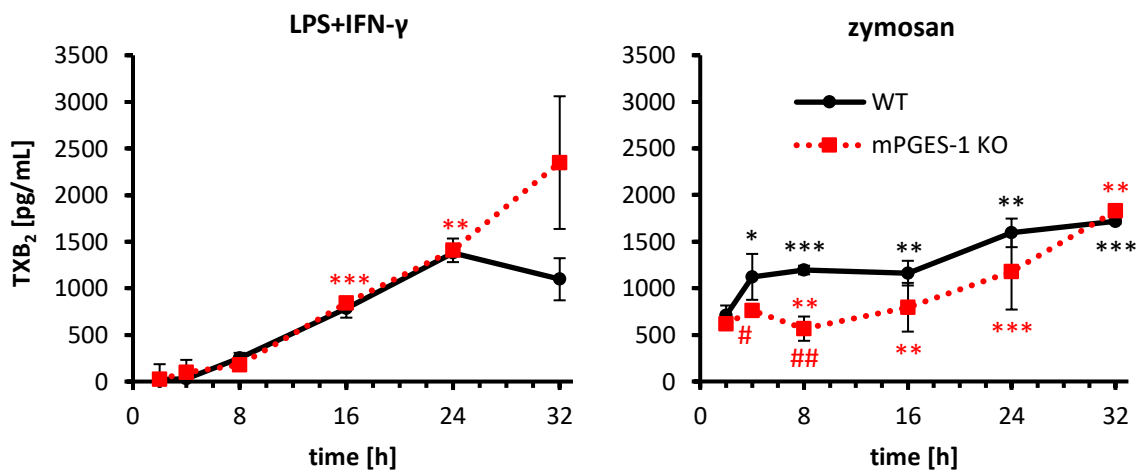


Figure 10. TXB₂ levels in LPS+IFN- γ and zymosan-stimulated murine WT and mPGES-1 KO BMDMs.

Isolated murine bone marrow was differentiated for 7 days in the presence of 20 ng/mL M-CSF and GM-CSF to BMDMs and stimulated with 100 ng/mL LPS and 50 ng/mL IFN- γ or 50 μ g/mL zymosan. Cell culture supernatants were taken and analyzed for TXB₂ levels via LC-MS/MS. Basal TXB₂ level: WT 119.5 \pm 26 pg/mL and mPGES-1 KO 111.6 \pm 36.2 pg/mL. Data are presented as mean values \pm SEM (n = 3). Statistical significance was determined relative to untreated control [$p \leq 0.05$ (*), $p \leq 0.01$ (**), or $p \leq 0.001$ (***)] and mPGES-1 KO to WT [$p \leq 0.05$ (#) or $p \leq 0.01$ (##)].

Consequently, both stimuli triggered strong increases in TXB₂ production with comparable kinetics in WT and mPGES-1 KO macrophages.

As presented in Figure 11, PGF_{2α} level started increasing after 8 h LPS+IFN-γ stimulation in both WT and mPGES-1 KO macrophages. After 32 h PGF_{2α} concentrations reached their maximum 130±15-fold induction in WT and 255.7±47.1-fold induction in mPGES-1 KO. PGF_{2α} profile showed a moderate increase in zymon-stimulated WT and mPGES-1 KO macrophages with maximal fold inductions of 102.6±3.4 and 137.3±17.9 after 32 h, respectively.

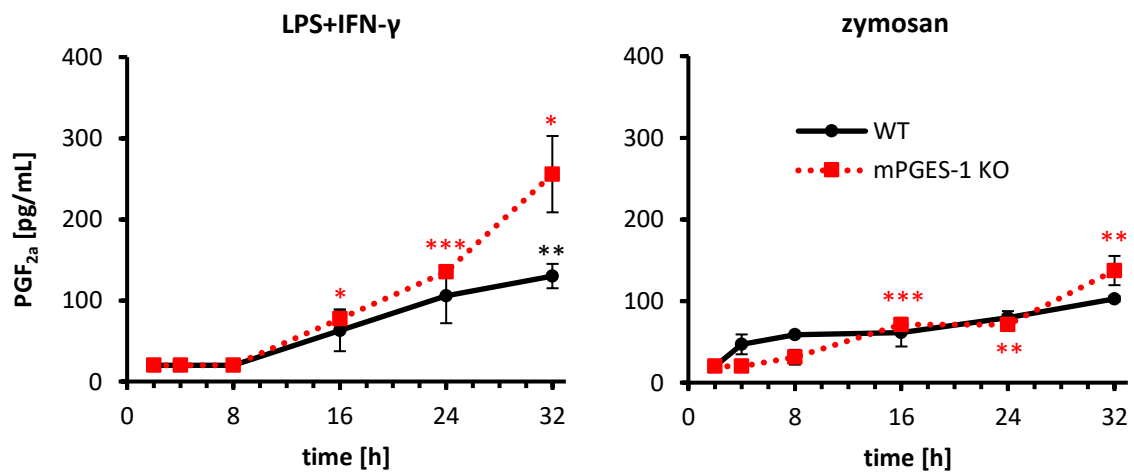


Figure 11. PGF_{2α} levels in LPS+IFN-γ and zymosan-stimulated murine WT and mPGES-1 KO BMDMs.

Isolated murine bone marrow was differentiated for 7 days in the presence of 20 ng/mL M-CSF and GM-CSF to BMDMs and stimulated with 100 ng/mL LPS and 50 ng/mL IFN-γ or 50 μg/mL zymosan. Cell culture supernatants were taken and analyzed for PGF_{2α} levels via LC-MS/MS. Basal PGF_{2α} level: WT and mPGES-1 KO <20 pg/mL (lower limit of quantification). Data are presented as mean values ± SEM (n = 3). Statistical significance was determined relative to untreated control [p ≤ 0.05 (*), p ≤ 0.01 (**), p ≤ 0.001 (***)].

In summary, both stimuli elevate PGF_{2α} level in WT and mPGES-1 KO macrophages.

As displayed in Figure 12, PGE₂ level in WT macrophages activated by LPS+IFN-γ showed a continuous increase to a significant maximum concentration of 610.1±35.6 pg/mL after 32 h meanwhile PGE₂ level in mPGES-1 KO macrophages changed in later time points and ended up with a concentration of 159.9±17.6 pg/mL after 32 h compared to control. Zymosan provoked similar effects with an initial stable induction of PGE₂ in WT up to 209.1±40.7 pg/mL after 16 h, followed by a plateau phase and another increase

after 24 h ending up with a concentration of 378.7 ± 52.4 pg/mL after 32 h. mPGES-1 KO macrophages indicate a delayed response to zymosan in early time points and a slight increase after 16 h up to a maximum concentration of 158.8 ± 44.8 pg/mL after 24 h in comparison to control and stable values between 24 – 32 h.

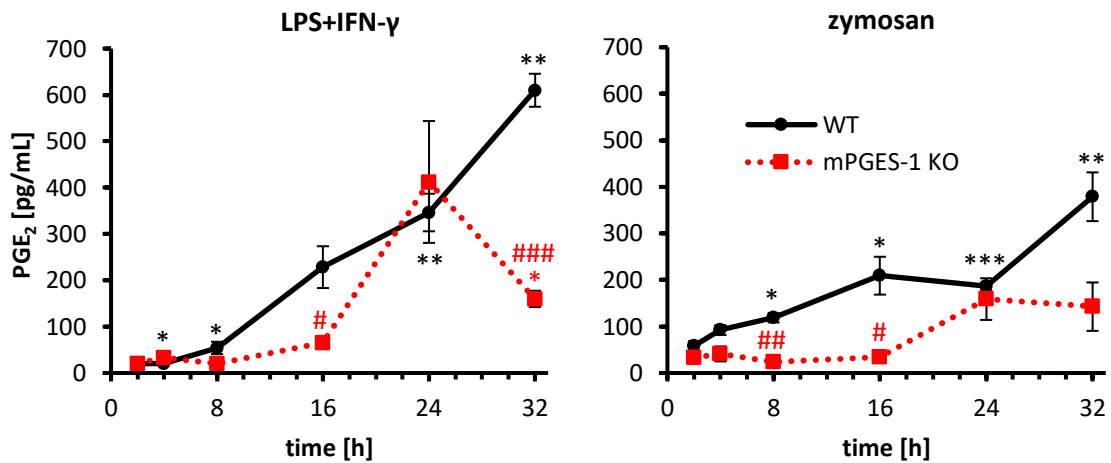


Figure 12. PGE₂ levels in LPS+IFN-γ and zymosan-stimulated murine WT and mPGES-1 KO BMDMs.

Isolated murine bone marrow was differentiated for 7 days in the presence of 20 ng/mL M-CSF and GM-CSF to BMDMs and stimulated with 100 ng/mL LPS and 50 ng/mL IFN-γ or 50 μg/mL zymosan. Cell culture supernatants were taken and analyzed for PGE₂ levels via LC-MS/MS. Basal PGE₂ level: WT 62.6 ± 7 pg/mL and mPGES-1 KO 45.6 ± 19.9 pg/mL. Data are presented as mean values \pm SEM (n = 3). Statistical significance was determined relative to untreated control [$p \leq 0.05$ (*), $p \leq 0.01$ (**), or $p \leq 0.001$ (***)] and mPGES-1 KO to WT [$p \leq 0.05$ (#), $p \leq 0.01$ (##) or $p \leq 0.001$ (###)].

In summary, PGE₂ production was delayed in mPGES-1 KO macrophages in response to LPS+IFN-γ and zymosan with significant differences to WT macrophages after 8, 16, and 32 h.

Taken together, both activation of CREB, as measured at protein level and the PGE₂ production support an activation of the COX-2/PGE₂ pathway in inflammatory settings both in WT as well as in mPGES-1 KO macrophages. Based on our determined PGE₂ profiles, 16 h incubations were chosen for the CHIP-seq experiment.

5.3 Establishing of the CHIP-protocol

Activated CREB acts as a transcription factor capable of binding DNA. To identify genomic binding sites, a CHIP assay was conducted as a suitable method to investigate interactions between proteins and DNA.

5.3.1 Validation of pCREB-Ab

For a CHIP, an appropriate pCREB antibody is required that is specific, sensitive and provides reproducible results. In order to assess pull-down efficiency, two commercially available rabbit polyclonal anti-pCREB antibodies purchased from Cell Signaling Technology, Inc. (CST) and Merck Millipore (Milli) were compared by immunoprecipitation.

Figure 13 demonstrates the detection of pCREB in NIH/3T3 fibroblast lysates. Whole cell lysate showed basal pCREB activity. Both antibodies were able to immunoprecipitate pCREB from cell lysate. pCREB immunoprecipitated by anti-pCREB (Milli) revealed stronger enrichment in line 2 compared to anti-pCREB (CST) in line 4.

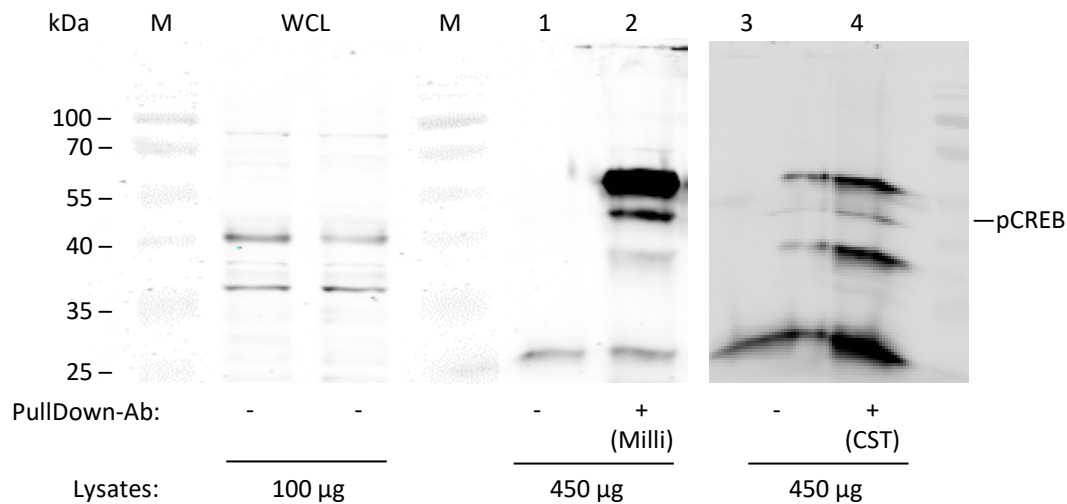


Figure 13. pCREB antibody validation by immunoprecipitation from NIH/3T3 fibroblast lysates.

NIH/3T3 fibroblasts were cultured in cell culture medium with 10% FCS and penicillin [100 U/mL]/streptomycin [100 µg/mL]. At 80–90% confluency fibroblasts were lysed and immunoprecipitated using anti-pCREB antibodies from Millipore (lane 2) or CST (lane 4) attached to Protein G Dynabeads®. Lane 1 and 3 are specificity controls of Protein G Dynabeads® with lysates in absence of anti-pCREB. Protein molecular weight markers (M) are shown on the left side and in center. Whole cell lysates (WCL), controls and immunoprecipitates were analyzed by SDS-PAGE with the respectively other anti-pCREB antibody.

As both commercially available anti-pCREB antibodies showed specificity in the detection of pCREB, yet, anti-pCREB antibody from CST is rigorously validated as a reliable antibody for ChIP, this antibody was chosen for further experiments.

5.3.2 Amplification of pCREB-ChIP

To investigate pCREB target genes differentially bound in WT and mPGES-1 KO macrophages upon stimulation with LPS+IFN- γ and zymosan, a pCREB-ChIP was performed as described in 4.3.5 and precipitated chromatin was amplified by PCR.

Validation of the five common pCREB binding sites: Fos (FBJ osteosarcoma oncogene), Jun (Jun proto-oncogene) and Sp4 (Trans-acting transcription factor 4) as indicated in Figure 14 showed, that all the selected targets were enriched in the pCREB-ChIP, as compared to the respective IgG control. For the above-mentioned targets, Fos was the target with the highest enrichment in both WT and mPGES-1 KO macrophages.

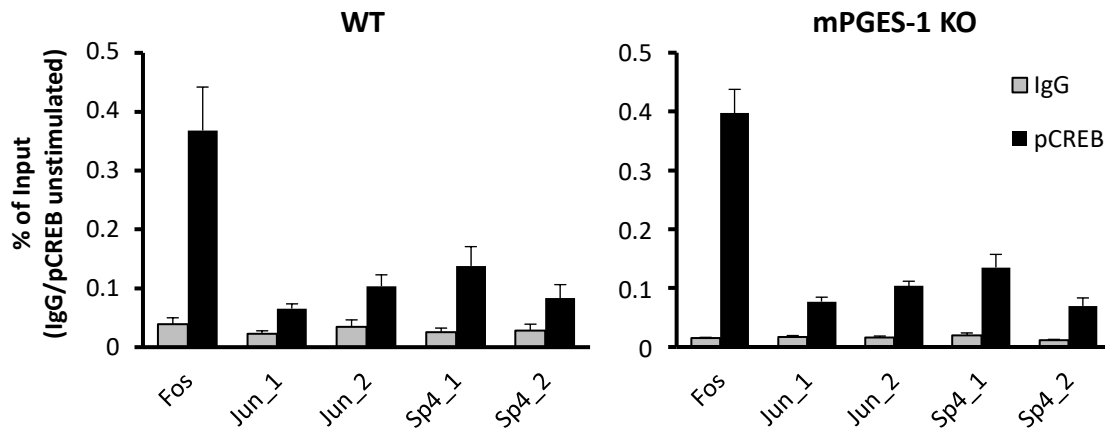


Figure 14. PCR amplification of pCREB-ChIP in untreated samples for WT and mPGES-1 KO BMDMs.

Isolated murine bone marrow was differentiated for 7 days in the presence of 20 ng/mL M-CSF and GM-CSF to BMDMs and samples were generated 16 h after changing the medium. ChIP was performed as described in chapter 4.3.5 with anti-pCREB versus control = IgG antibody. Enriched chromatin was amplified by PCR using primer sets against five pCREB binding sites within the indicated genes: Fos -242/-65 bp (chr:12), Jun_1 1938/2009 bp (chr:4), Jun_2 2009/2133 bp (chr:4), Sp4_1 513/665 bp(chr:12) and Sp4_2 665/850 bp (chr:12) relative to the transcription start site. Data shown as percentage of input DNA and presented as means \pm SEM (n = 4).

These findings suggest that the pCREB-ChIP is efficient to enrich pCREB binding sites in both WT and mPGES-1 KO macrophages.

Figure 15 shows the enrichment of the selected pCREB binding sites in WT and mPGES-1 KO macrophages upon stimulation with LPS+IFN- γ and zymosan. Compared to untreated macrophages both LPS+IFN- γ and zymosan-stimulated mPGES-1 KO macrophages revealed an enrichment in all selected pCREB binding sites, while enrichment of pCREB binding sites in WT macrophages was observed in Fos, Jun_1, Sp4_1 and Sp4_2 only. No enrichment was observed in Jun_2. Both stimuli had no effect on the IgG-ChIP.

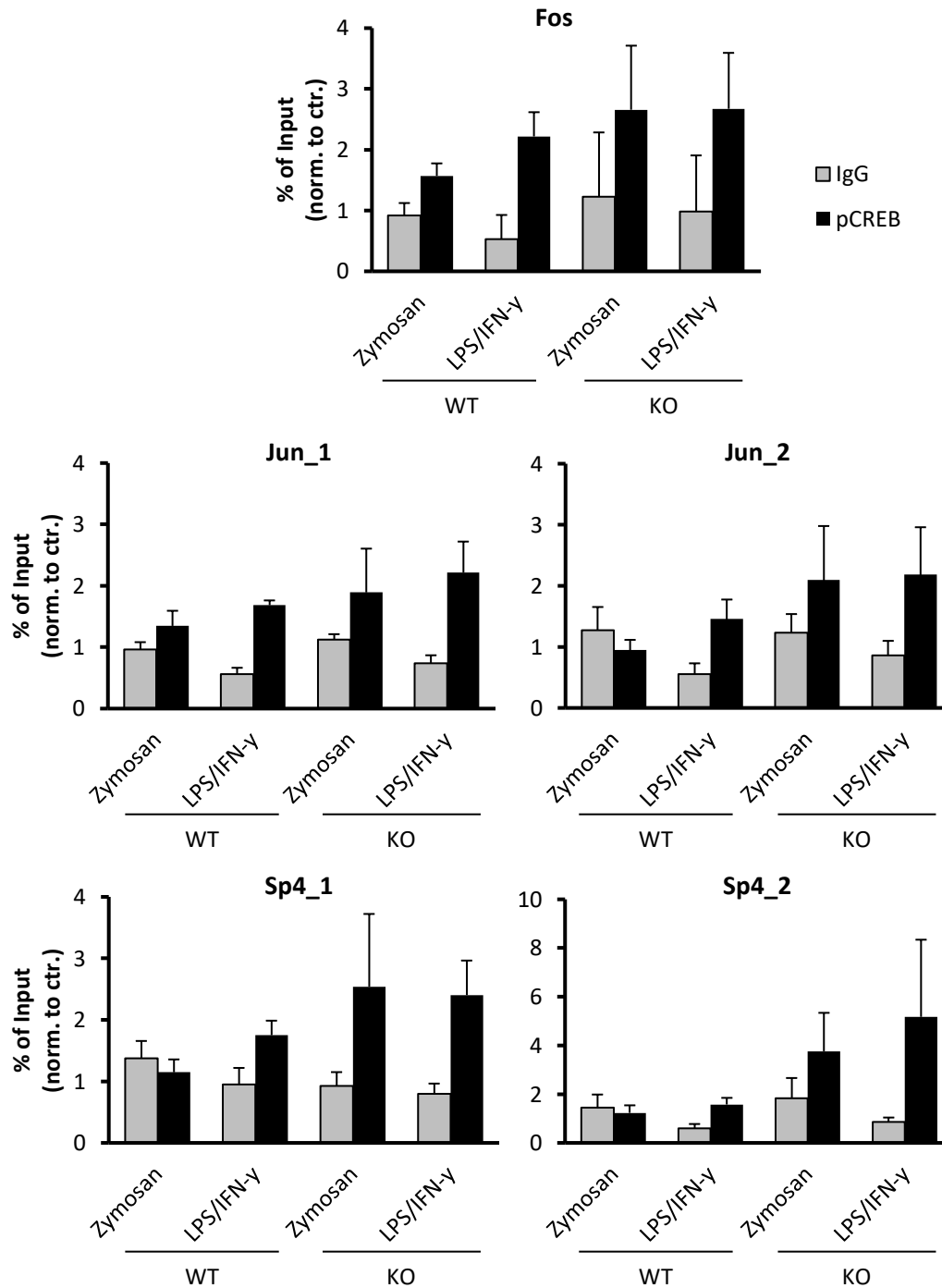


Figure 15. PCR amplification of pCREB-CHIP in LPS+IFN- γ and zymosan-treated murine WT and mPGES-1 KO BMDMs.

Isolated murine bone marrow was differentiated for 7 days in the presence of 20 ng/mL M-CSF and GM-CSF to BMDMs and stimulated with 100 ng/mL LPS and 50 ng/mL IFN- γ or 50 μ g/mL zymosan. Samples were taken after 16 h of stimulation and CHIP was performed as described in chapter 4.3.5 with anti-pCREB versus control = IgG antibody. Chromatin was amplified by PCR using primer sets against five pCREB binding sites within the indicated genes: Fos -242/-65 bp (chr:12), Jun_1 1938/2009 bp (chr:4), Jun_2 2009/2133 bp (chr:4), Sp4_1 513/665 bp (chr:12) and Sp4_2 665/850 bp (chr:12) relative to the transcription start site. Data shown as percentage of input DNA and presented as means \pm SEM (n = 4).

Thus, both stimuli appeared to enrich selected pCREB targets in WT and mPGES-1 KO macrophages. Meanwhile, the IgG controls indicate no alteration upon stimulation.

As a result, pCREB-ChIP enabled enrichment of selected pCREB targets with selected antibody in WT and mPGES-1 KO macrophages, compared to IgG control.

5.4 ChIP-seq

To identify novel pCREB targets, DNA fragments immunoprecipitated by pCREB were processed utilizing the NEBNext® Ultra™ II DNA Library Prep Kit for Illumina® and analyzed by Next-Generation-Sequencing (NGS). Analysis of the ChIP-seq data revealed that 46 – 61% of the pCREB immunoprecipitated control samples and 60 – 87% of the stimulated samples were aligned to the murine genome. DNASTAR® was used for annotation and identification of target genes as well as for peak calling. Across all 4 replicates, about 300 genes were found to be differentially bound in WT and mPGES-1 KO macrophages in response to LPS+IFN- γ at log₂-fold change >2 or <-2. 57 of these annotated pCREB-targeted genes were consistently identified for all four replicates and are presented in Figure 16.

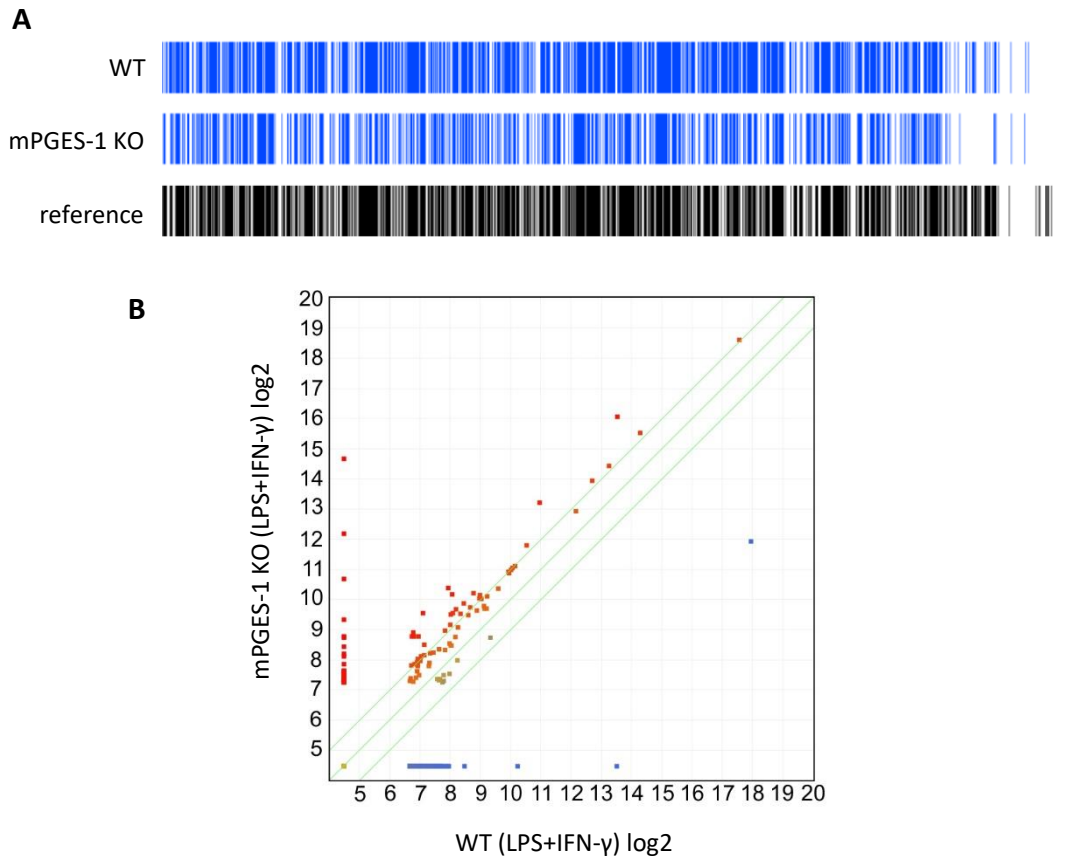


Figure 16. Comparison of pCREB binding sites differentially bound in WT vs. mPGES-1 KO BMDMs upon LPS+IFN- γ stimulation.

A. Heatmap of pCREB-ChIP-seq signals from 1 representative replicate in WT vs. mPGES-1 KO macrophages (blue) as compared to previously published whole-genome binding sites (black) **B.** Scatter Plot of pCREB target genes with consistent, differential binding in WT vs. mPGES-1 KO macrophages after 16 h stimulation with LPS+IFN- γ (log₂-fold change (WT vs. mPGES-1 KO) >2 (blue) or <-2 (red)). Each data point represents an individual gene. Middle green line corresponds to direct correlation (x=y line).

The selected target genes were grouped into different categories by Gene Ontology (GO) analysis to determine the biological significance. The GO database involves 3 hierarchies: biological process, cellular component, and molecular function. The significance threshold was determined by P-value <0.05 corrected by FDR (False Discovery Rate). Table 18 gives an overview of the GO category analysis.

The GO term analysis revealed that the genes, recognized by pCREB with significant P-value, were involved in the regulation of the fatty acid metabolic process and/or were associated with intracellular membrane-bounded organelles.

Table 18. GO category analysis of pCREB-targeted genes

Term	P-value	# of targets	Total
biological process			
regulation of fatty acid metabolic process	0.00277	5	82
cellular component			
intracellular membrane-bounded organelle	0.0121	30	9317

Top enriched GO terms (P-values <0.05). # = number. Total = Number of genes contained within the entire project for the term.

In conclusion, the sequencing data revealed that pCREB-targeted genes differentially bound in WT vs. mPGES-1 KO macrophages upon stimulation with LPS+IFN- γ . GO term analysis identified regulation of fatty acid metabolic process as a top enriched GO term.

In order to gain further insights, which distinct areas correspond to the protein-DNA binding sites, enriched regions were analysed through peak-calling algorithms. To implement this, QSeq Peak Finder based on ERANGE 3.1 algorithm for ChIP-seq and RNA-seq analysis (Mortazavi *et al.*, 2008), provided by DNASTAR[®], was used. Out of the top enriched GO term (regulation of fatty acid metabolic processes), Erlin1 (Endoplasmic reticulum lipid raft-associated protein 1) and Elovl5 (Elongation of very long chain fatty acids protein 5) appeared to be promising candidates for validation.

As displayed in Figure 17, peak calling identified 3 overlapping peaks for pCREB binding sites in the Erlin1 as well as in the Elovl5 gene. In the case of Erlin1, all predicted peaks were gathered within the gene and were overlapping 1 exon. ChIP-seq enrichment peak call identified P1 +32,000 nt, P2 +31,684 nt and P3 32,159 nt relative to the transcription start site (TSS). On the contrary, all the predicted peaks of Elovl5 are overlapping the TSS. P1 is located -427 nt, P2 -1016 nt and P3 -322 nt relative to the TSS.

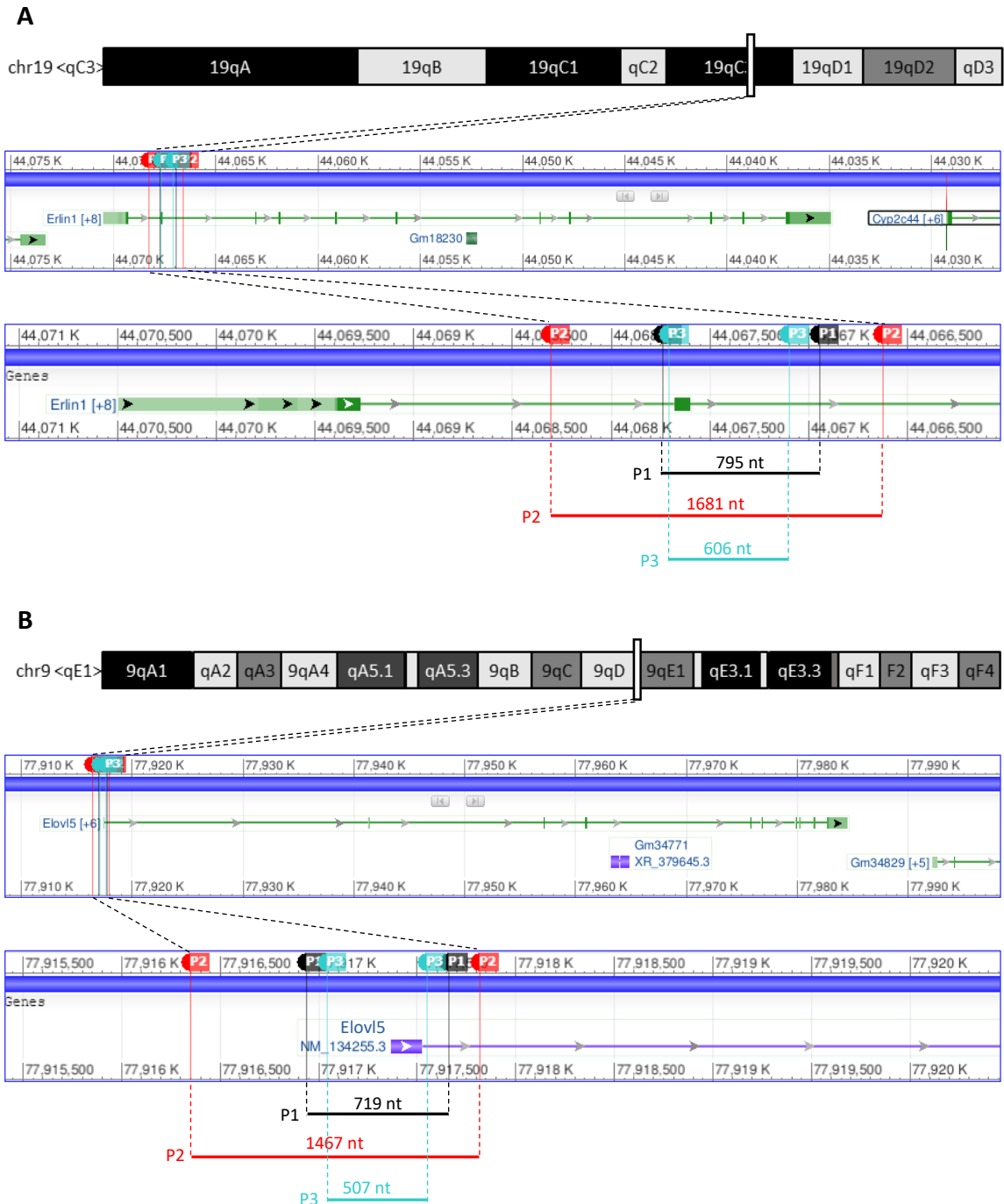


Figure 17. pCREB-CHIP-seq peaks of Erlin1 and Elov5.

Differential peak calling identified 3 peaks in both Erlin1 and Elov5 (P1 – P3) visualized in the UCSC (University of California, Santa Cruz) genome browser. Predicted peak regions are labeled P1 – P3 **A**. Schematic of distribution of peaks on the pCREB target Erlin1 gene. Erlin1 is located on chr. 19: 44,034,943 – 44,070,494 bp. Peaks identified: P1: 44,066,945 – 44,067,740 nt (Δ_{P1} =795 nt); P2: 44,066,627 – 44,068,308 nt (Δ_{P2} =1681 nt); P3: 44,067,102 – 44,067,708 nt (Δ_{P3} =606 nt). **B**. Schematic of distribution of peaks on the pCREB target Elov5 gene. Elov5 is located on chr. 9: 77,917,365 – 77,984,519 bp. Peaks identified: P1: 77,916,938 – 77,917,657 nt (Δ_{P1} =719 nt); P2: 77,916,349 – 77,917,816 nt (Δ_{P2} =1467 nt); P3: 77,917,043 – 77,917,550 nt (Δ_{P3} =507 nt).

Taken together, peak calling facilitated the localization of pCREB binding sites in Erlin1 and Elovl5 gene.

pCREB-ChIP-seq showed differently bound pCREB binding sites in WT and mPGES-1 KO macrophages upon stimulation. Erlin1 and Elovl5, associated in the regulation of fatty acid metabolic process, appeared to be promising targets for further analysis.

5.5 Validation of pCREB-ChIP-seq

For quality control and functional validation of the pCREB-ChIP, the expression of Erlin1 and Elovl5 was validated by qPCR analysis. To realize this, macrophages were obtained as described in subchapter 4.3.1. The cells were further preincubated with 1 μ M NS-398 (COX-2-selective inhibitor) 30 min prior to the stimulation with LPS+IFN- γ , in WT and mPGES-1 KO macrophages.

Untreated macrophages showed a basal expression of Erlin1 in WT and mPGES-1 KO macrophages. Figure 18 revealed a significant 4.3 ± 0.2 -fold induction of Erlin1 in LPS+IFN- γ -stimulated WT macrophages. The induction of Erlin1 in mPGES-1 KO macrophage was significantly reduced with a 3.2 ± 0.2 -fold induction after 16 h compared to WT macrophages. Stimulated WT macrophages that were preincubated with NS-398 followed by stimulation showed a significant but reduced induction of Erlin1, compared to WT control macrophages. Meanwhile, Erlin1 was not induced in mPGES-1 KO macrophages upon treatment with NS-398 and LPS+IFN- γ . Elovl5 expression in WT and mPGES-1 KO macrophages was neither affected upon treatment with LPS+IFN- γ , nor by the COX-2-inhibitor.

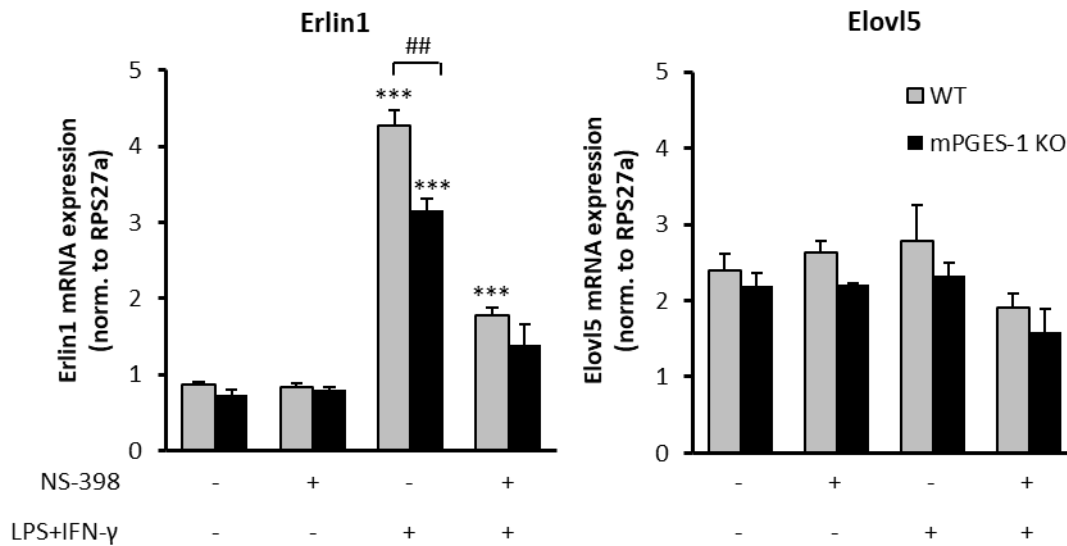


Figure 18. Erlin1 and Elovl5 ChIP-seq validation by qPCR.

Isolated murine bone marrow was differentiated for 7 days in the presence of 20 ng/mL M-CSF and GM-CSF to BMDMs and stimulated with or without 100 ng/mL LPS, 50 ng/mL IFN- γ and 1 μ M NS-398 (COX-2-selective inhibitor) as indicated. Samples were taken after 16 h of incubation. mRNA expression was normalized to 40S ribosomal protein S27a (RPS27a). Data are presented as mean values \pm SEM (n = 4). Statistical significance was determined relative to untreated control [$p \leq 0.001$ (***)] and mPGES-1 KO to WT [$p \leq 0.01$ (##)].

Thus, stimulation led to a significantly stronger induction of Erlin1 in WT macrophages. Further COX-2 inhibition slows down Erlin1 induction in both WT and mPGES-1 KO. Elovl5 showed no response to stimuli.

In summary, the *in vitro* model system presented an activation of CREB in WT and mPGES-1 KO macrophages upon stimulation with LPS+IFN- γ and zymosan. At protein level, there appeared to be no relevant differences in CREB-activation between WT and mPGES KO macrophages although further characterization of CREB binding sites revealed different targetome profiles. Validation of ChIP-seq further revealed a PGE₂ dependency of the Erlin1 expression.

6 Discussion

With this study, I wanted to investigate transcriptional changes induced by mPGES-1-derived PGE₂ in macrophages mediated via the transcription factor CREB in an inflammatory context. To achieve this, I determined the protein expression profiles of the relevant PGE₂-synthesizing enzymes, i.e. COX-2 and mPGES-1, as well as of the activation, i.e. phosphorylation, of the downstream transcription factor pCREB. The enzyme activity was simultaneously analysed via assessment of the prostanoid kinetics. Subsequently, potential CREB-regulated targets were identified in macrophages upon inflammatory stimuli after 16 h. The validation revealed a strong enrichment of the CREB-targeted genes in the regulation of the fatty acid metabolism. Among them, Erlin1 seemed to be not only mPGES-1-dependently, but PGE₂-dependently regulated. Figure 19 provides a schematic overview of the PGE₂/cAMP signaling axis in macrophages during inflammation.

The inducible mPGES-1 enzyme, one of the most important terminal synthases, facilitates the conversion of the COX-derived PGH₂ to the biologically active mediator PGE₂, the most abundant PG in the human body and major PG in inflammation. The inducible mPGES-1 synthase expression level can be markedly increase upon stimulation by pro-inflammatory stimuli *in vivo* as well *in vitro*. In our study, LPS+IFN- γ and zymosan show comparable effects on mPGES-1 induction in WT macrophages. In line with previous publications, the expression kinetics of COX-2 upon both stimuli in WT macrophages is characterized by a significant induction in the early phase (\geq 2-16 h), whereas the main protein induction of mPGES-1 appeared in the late phase (\geq 16-32 h).⁶⁵⁻⁶⁷ This cooperates with previous findings from Inada and co-workers, who analyzed the effects of LPS on the mRNA expression level in cultured mouse osteoblasts, i.e. bone-resident macrophages. They revealed a peak-induction on mRNA level of COX-2 and mPGES-1 slightly prior to the protein expression, meaning after 3 h and 12 h, respectively. *In vivo* studies of Stichtenoth *et al.* also confirmed these findings in synovial cells from patients suffering from RA. In accordance with our protein expression data, the mRNA level of mPGES-1 was induced in synovial cells to maximum levels after 24 h, and the COX-2 mRNA was evident by 4-8 h and dropped after 24 h.⁶⁶

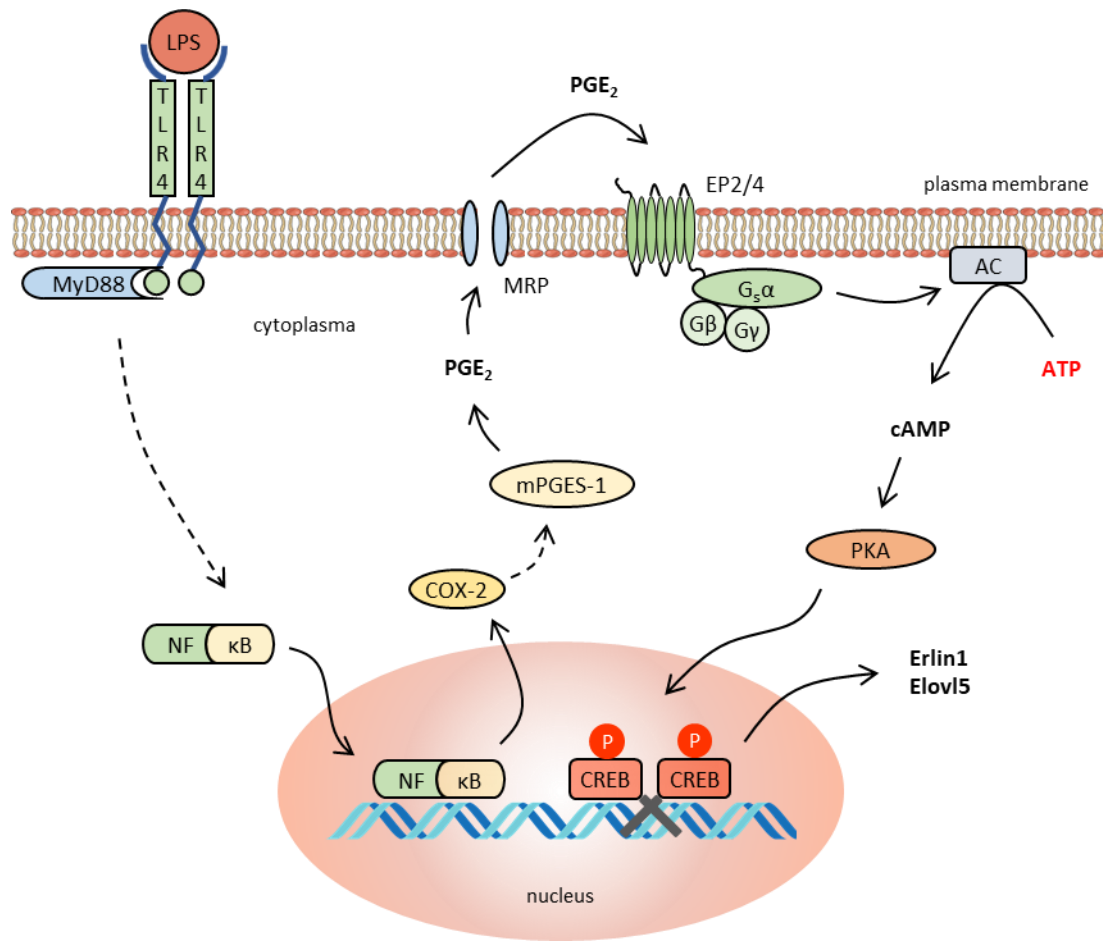


Figure 19. Schematic overview of the PGE₂/cAMP signaling axis in macrophages during inflammation.

Lipopolysaccharides (LPS) builds a complex with LPS-binding protein (LBP) and is recognized via toll-like receptor 4 (TLR4), which is expressed on macrophages. This activates a intracellular kinase cascade, which ultimately leads to the activation of the transcription factor nuclear factor 'κ-light-chain-enhancer' of activated B cells (NF-κB). This induces the transcription of the cyclooxygenase-2 (COX-2) and microsomal prostaglandin E synthase-1 (mPGES-1). mPGES-1-derived prostaglandin E₂ (PGE₂) acts in an autocrine or paracrine manner and activates PG receptors for prostaglandin E₂ (EP2/4) on macrophages. Following increasing cyclic adenosine monophosphate (cAMP) level through activation of adenylyl cyclase (AC) leads to the cAMP-dependent cAMP response element-binding protein (CREB) activation, which induces the transcription of various genes, such as endoplasmic reticulum lipid raft-associated protein 1 (Erlin1) and elongation of very long chain fatty acids protein 5 (Elov15). Myeloid differentiation primary response 88 (MyD88), multidrug resistance protein (MRP), protein kinase A (PKA).

The delayed response of mPGES-1 relative to COX-2 upon pro-inflammatory stimuli is not restricted to macrophages, it is rather a generally observed phenotype that extends to other cell types.⁶⁸ The largely stable increase in PGE₂ secretion upon stimulation with LPS+IFN-γ and zymosan in macrophages can be logically explained by the difference in synthase expression levels. Because mPGES-1 is the final step for PGE₂ formation, the

enhanced induction of its synthase results in an increased PGE₂ secretion. At the same time, this leads to the question of whether the increasing PGE₂ production is also triggered by altered enzyme activities of mPGES-1 or COX-2 at the given time. Xiao *et al.* examined the activity of both enzymes using equal amounts of immunoprecipitated COX-2 or mPGES-1 protein at 8 h and 16 h after LPS stimulation and concluded that the altered PGE₂ levels were not caused by altered COX-2 or mPGES-1 enzyme activities.⁶⁷ This indicates that the correlation of PGE₂ production is largely determined by the available protein amount, therefore our kinetics for the protein should also result in functional consequences. The mPGES-1 selective inhibitor CAY10526 and mPGES-1-specific siRNA attenuated LPS-induced secretion of PGE₂ only in the late phase, underlining the crucial role of mPGES-1 protein for the major induction of PGE₂ production.⁶⁷ In addition, consideration should be given to further factors that might modulate the PGE₂ profile, e.g. AA availability as controlled by the releasing enzyme PLA2. Yet, there are no data currently available towards the potential mechanism of regulation. Generally speaking, the early phase of PGE₂ production in LPS-stimulated macrophages is mainly coordinated by the COX-2 protein amount, whereas the boost of PGE₂ synthesis during the late phase is basically promoted by the increased expression of mPGES-1. Thus, it will be interesting to see how this differential regulation comes about, such as the regulation of transcriptional activation, knowing there are shared transcription factors for both, inducing different expression profiles.

To gain further insights into the contribution of CREB-mediated transcriptional changes induced by mPGES-1-derived PGE₂, we compared WT to mPGES-1 KO macrophages. Whereas mPGES-1 KO mice are phenotypically not distinguishable from WT mice, our data revealed a delayed, but still remarkable increase in the PGE₂ production in response to both LPS+IFN- γ and zymosan in mPGES-1 KO macrophages, in contrary to our expectations. This is controversially discussed in literature. Most of the publications state the inducible mPGES-1 is critically important for the PGE₂ burst in inflammatory settings, meaning mPGES-1 deficient macrophages exhibit no LPS-induced augmentation of PGE₂ production.^{48,69} Just as with mPGES-1-deficient mice, heterozygous mice show higher levels of PGE₂ upon LPS stimulation relative to mPGES-1 KO and lower levels than in WT macrophages.⁷⁰ Our findings go in line with a

study of Monrad and colleagues, describing a much smaller increase in PGE₂ production but still significant increase in response to LPS treatment.⁷¹ What these studies all have in common towards this issue is, that the isoforms cPGES and mPGES-2 play a less decisive role in the inflammatory context, meaning mPGES-1 is the primary source of inflammatory PGE₂. Reasons for the non-mPGES-1 triggered PGE₂ response upon pro-inflammatory stimuli remain speculative. Boulet and co-workers assume residual PGE₂ emergence upon LPS in mPGES-1 KO due to the fact that COX-2-derived PGH₂ can non-enzymatically degrade to PGE₂ and PGD₂.⁷² Consequently, the increasing COX-2 expression upon pro-inflammatory stimuli increases the production of PGH₂, which in turn, spontaneously is degraded to PGE₂. While this is an individual study and just has been shown *in vitro*, this concept must be critically reviewed and has to be further validated *in vitro* and *in vivo*. Another explanation is provided by Monrad and colleagues, reporting that PGES isoforms, primarily the previously discovered mPGES-2, may contribute to the PGE₂ production by coupling with either COX-1 or COX-2, depending on the exact situation. Nevertheless, these concepts provide insufficient explanations and it remains to be shown how exactly PGE₂ levels increase in our model. The introduction of COX inhibitors or selective inhibitors for mPGES-2 and cPGES to investigate alterations in the PGE₂ production might be promising approaches in this context.

Whereas our findings with regard to the PGE₂ profile in mPGES-1 KO macrophages were unexpected, i.e. macrophages rely on mPGES-1 activity as an inflammatory response, we observed a tendency of slightly increased PGD₂ amounts upon LPS treatment at the timepoints when PGE₂ levels were reduced in mPGES-1 KO macrophages compared to WTs. This may indicate a shunting of the prostanoid biosynthesis in mPGES-1 KO from PGE₂ to PGD₂. In our study, the other prostanoid levels, i.e. TXB₂ and PGF_{2α}, seem to be unaffected regarding this. The diversion of the prostanoid production profile in the absence of mPGES-1 is a common but not consistent phenomenon described previously. However, the presence of metabolic shunting is a variable concept depending mainly on the cell type/function and *in vitro* conditions. Kapoor *et al.* demonstrated a shunting in LPS-stimulated mPGES-1 KO peritoneal macrophages with a significant shunting from PGE₂ production to other prostanoids in the order of

TXB₂ > 6-keto PGF_{1α} > PGF_{2α} > PGD₂ > PGE₂. As a side note, higher levels of 6-keto PGF_{1α} are an indicator of increased prostaglandin I₂ (PGI₂) levels, better known as prostacyclin.⁷³ PGI₂, the precursor of 6-keto PGF_{1α}, also has a putative role in inflammation, especially known for its cAMP-mediated vasodilatory effect as well as the inhibition of platelet aggregation. The diversion of prostanoid production can be observed in different cell types and tissues. While mPGES-1 KO thioglycollate-elicited macrophages, for instance, are characterized by increased PGF_{2α} levels upon stimuli, the PGF_{2α} levels in resident macrophages are not altered. This goes in line with the fact that in some tissues, such as the spleen, of mPGES-1 KO mice no changes in prostanoid levels were observed at all.⁷⁰ My project was performed on the inbred mouse strain C57Bl6/J, whereas the studies of Kapoor *et al.* and Boulet and co-workers were performed on an inbred DBA1 lac/J and C3H/HeJ genetic background, respectively.^{73,74} As a side note, supporting the strain-specific PGE₂ production, macrophages from BALB/c mice, an albino, laboratory-bred strain of the house mouse have been known to produce one of the highest PGE₂ amounts upon stimulation with LPS, compared to other mouse strains, including C57Bl6/J. This goes in line with previous publications, showing that the same genetic deletion in different genetic backgrounds may result in very different phenotypes.⁷⁵ The strain-dependent divergence in the prostanoid secretion, especially in the PGE₂ profile in macrophages, might explain some of the differences observed in these studies. Further, Karim and co-workers proposed that the PGH₂ redirection can occur both intracellularly and extracellularly in multicellular systems. For instance, they observed a transcellular PGH₂ metabolism between endothelial and platelet cells.⁷⁶ It can be speculated that in our case, this phenomenon might also contribute to the differential PGE₂ levels observed. Hence, the redirection of prostanoids is a complex phenomenon with various factors contributing to the phenotype of the shunting pattern, that may vary from tissue to tissue. The prostanoid pattern we observed, thus cannot be clearly evaluated regarding the redirection of prostanoids in the absence of mPGES-1. Besides the redirection of PGH₂ to other terminal synthases, other factors may modulate the prostanoid composition in macrophages, as described in the previous paragraphs. To further examine the prostanoid shunting in the absence of mPGES-1 in macrophages, radiolabeling studies might be an interesting approach using

tritium (³H)-labeled [³H]AA. This could make it possible to track the passage of the radiolabeled AA through their metabolic pathway in a time-dependent manner.

Considering the diverse effects of PGE₂ at health and disease states, the overwhelming majority of scientists agree that potent drugs targeting the mPGES-1-derived PGE₂ production may be a promising therapeutic alternative. Most NSAIDs, like Aspirin[®] or Ibuprofen[®], act as nonselective inhibitors of both COX-1 and COX-2, causing potentially harmful side effects, e.g. gastric ulceration and renal problems. Also selective COX-2 inhibitors, known as coxibs, indicate an increased risk of myocardial infarction.⁷⁷ However, these compounds suppress the production of all prostanoids. Thus, it appears rational to speculate that mPGES-1 might be a promising novel therapeutic target with improved selectivity and safety profile for the treatment of symptoms mediated by increased PGE₂ production, as already described in chapter 3.3. Several compounds have already been found that potently inhibit mPGES-1 *in vitro*, such as compound III, but these structures are not widely available and often have a loss of efficacy when used *in vivo*, presumably due to their strong protein-binding properties.^{78,79} As a result, mPGES-1 KO mice were generated to characterize the physiological effects of mPGES-1. Nevertheless, it is necessary to evaluate if the mPGES-1 inhibitors can recapitulate the results observed in mPGES-1 KO mice.

Mechanistically, CREB is a well-characterized phosphorylation-dependent transcription factors. Intracellular PKA phosphorylates CREB at Ser-133 in response to elevated cAMP levels, which, in turn, is sufficient to induce the transcription of target genes equipped with CREs. In my study, the stimuli LPS+IFN- γ and zymosan led to an increased activation of CREB in both WT and mPGES-1 KO macrophages. We suggest, that the applied stimuli operate via the mainly PGE₂-dependent increase of the intracellular cAMP level. In contrast, despite prominent differences in the PGE₂ production in WT and mPGES-1 KO macrophages, our data showed an equal activation of CREB. Moreover, both stimuli appear as similarly potent activators of CREB. While LPS and IFN- γ are recognized by TLR4 and the interferon-gamma receptor (IFNGR), respectively, zymosan is recognized via the TLR2 receptor.^{80,81} As already mentioned in chapter 3.2, all TLRs elicit their effects through the MyD88-dependent pathway, but it is necessary to add that the noncanonical MyD88-independent pathway is additionally used by TLR4 and TLR3,

exclusively.⁸² Therefore, these receptors possess an intracellular TRIF adaptor. MyD88 leads to the induction of inflammatory cytokines via the transcription factors NF- κ B and AP-1. Concurrently, the TRIF adaptor drives the activation of the interferon regulatory factor 3 (IRF-3), which induces IFN- β . In turn, IFN- β is important for the activation of the signal transducer and activator of transcription 1 (STAT1), which again leads to the expression of LPS-inducible genes, such as interferon gamma-induced protein 10 (IP-10) and iNOS.⁸³ This shows that TIR domain-containing adaptors, like MyD88 and TRIF, are essential to allow for cellular signal discrimination. Attention must be paid to the fact, that the CREB phosphorylation pattern in the inflammatory context was not significantly altered between WT and mPGES-1 KO macrophages. As indicated in the previous paragraphs, indeed, the PGE₂ levels are significantly decreased between WT and mPGES-1 KO macrophages in some of the determined time points. This points to the fact that CREB activity may also be triggered through additional signal transduction pathways in addition to the PGE₂/cAMP signaling axis.

The CREB proteins contribute to various cellular effects, e.g. cell survival, proliferation, differentiation, and immune responses.⁸⁴ The significance of CREB was first investigated in the synaptic plasticity associated with long-term memory.⁸⁵ Once discovered, emerging evidence over the past decades revealed its essential role in almost every cell type in a context-dependent manner. This is further strengthened by the fact that CREB-deficient mice suffer from perinatal lethality, whereas in contrast ATF1, which is also a CREB-related protein, appears to be much less important as it does not exhibit any developmental deficits.⁸⁶ As CREB appears to be involved in innumerable processes in different cell types, the question needs to be asked, whether there are further mechanisms, in addition to its regulation by phosphorylation, to differentially respond to various cellular signals. Previous publications provide evidence that stimulation-specific selection of pCREB-targeted genes differentially bound in WT vs. mPGES-1 KO macrophages might be multifactorial regulated. As stated in chapter 3.3, CREs are high-affinity eight-base-pair palindromic CREB-binding site motifs, however, there are CREs that exist in a five-base-pair palindromic motif (5'-CGTCA-3') as well. pCREB binds with a lower affinity to the five-base-pair motif, in comparison to the full CRE palindrome. Most of the known CREs usually reside within about 170 bps of the transcription start

site of the targeted gene and promote their activity in a distance-dependent manner.⁸⁷ Nevertheless, the presence of CREs in genomic DNA are often not accessible to CREB. Rather different epigenetic modifications, such as DNA methylation and nucleosome positioning are responsible to determine the accessibility of CREs to regulatory proteins, following differences in cellular gene expression. A possible mechanism in which CRE/CREB interaction can be modulated, is the 5'-cytosine-phosphate-guanine-3' (CpG) methylation within the CRE site. Robertson *et al.*, for example, pointed out that CpG methylation is crucial to maintain viral latency of a persistent infection with Epstein-Barr virus (EBV) and human immunodeficiency virus (HIV)-associated Burkitt's lymphoma.⁸⁸ The location of the CRE on the promoter and the CpG methylation might explain some of the multifaceted patterns of gene expression in different cell types, but it remains to be shown if other mechanisms contribute as well. Besides reversible Ser-133 phosphorylation of CREB, transcriptional coactivators, including CBP and p300, are necessary to augment the transactivation potential.⁸⁹ Specifically, these coactivators are responsible for recruiting the basal transcriptional machinery. Their intrinsic histone acetyltransferase (HAT) activity enhances cAMP-induced CRE/CREB-directed transcription by acetylating specific lysine residues on histones to relax the chromatin structure at the gene promoter site.⁹⁰ The interaction between CREB and its coactivators is elicited via their kinase-inducible domain (KID) and the KID-interacting domain (KIX), respectively. Both KID and KIX are necessary for complex formation of activated CREB. Emerging evidence over the past years has demonstrated their putative role in signal discrimination through CREB. For instance, in transfection studies, Sun and colleagues observed that calcium/calmodulin-dependent protein kinases (CaMK), i.e. CaMKIV and CaMKII, also may phosphorylate CREB at Ser-133. CaMKII further phosphorylates CREB at another site, Ser-142. Additional phosphorylation at Ser-142 within the KID blocks the CREB/CBP formation and consequently inhibits CREB-dependent gene transcription, despite the fact that CREB is phosphorylated at Ser-133.⁹¹ Another possibility is the presence of a third cofactor acting by binding to the KID or KIX domain, which can activate or inactivate the complex formation with pCREB, as postulated by Ernst *et al.*⁹² Moreover, it should be noted, that CREB is a substrate for further, even non-cAMP dependent, cellular kinases, which are essential for various signaling pathways and well characterized in different cell types such as PKC, phosphoinositide 3-kinase (PI3K)/AKT

(also known as PKB), mitogen- and stress-activated protein kinase 1 (MSK-1) and phospho-90 kDa ribosomal S6 kinase (p-p90RSK).^{93,94} However, this brief account on how the activation of CREB is modulated, indicates that this is a very complex regulatory mechanism, whereas the potential roles in different systems on signal discrimination achieved by CREB is only partially understood. The following figure gives an overview of different signal transduction pathways and epigenetic modifications that might modulate CREB expression and activity (Figure 20).

We found that Erlin1 was differentially bound by pCREB in WT vs. mPGES-1 KO macrophages upon stimulation with LPS+IFN- γ . Erlin1, an endoplasmic reticulum (ER) resided integral membrane protein, was also described as SPFH1, because of the common stomatin, prohibitin, flotillin, and Hflk/C containing protein domains.^{95,96} SPFH proteins show sequence similarities by an about 250-amino acid motif and are usually found in lipid raft membrane microdomains, e.g. plasma membrane, mitochondria, and the ER.⁹⁶ Its wide distribution in membrane microdomains in various subcellular localizations indicates its relevance in the regulation of cellular membrane processes, such as ion channel regulation as well as vesicle and protein trafficking.⁹⁷ In interaction with its homolog Erlin2 (SPFH2), Erlin1 forms a heteromeric about 2 MDa complex, mediating the endoplasmic reticulum-associated degradation (ERAD) of inositol 1,4,5-trisphosphate (InsP3) receptors (InsP3Rs).⁹⁶ InsP3Rs are mainly localized within the membrane of the ER and act as Ca²⁺ release channels, activated by InsP3. They play a fundamental role in physiological processes, such as gene expression, muscle contraction, apoptosis, learning, and memory.⁹⁸ Erlin1 is also involved in the regulation of the cellular cholesterol homeostasis by regulation of the sterol regulatory element binding protein (SREBP) signaling pathway.⁹⁹

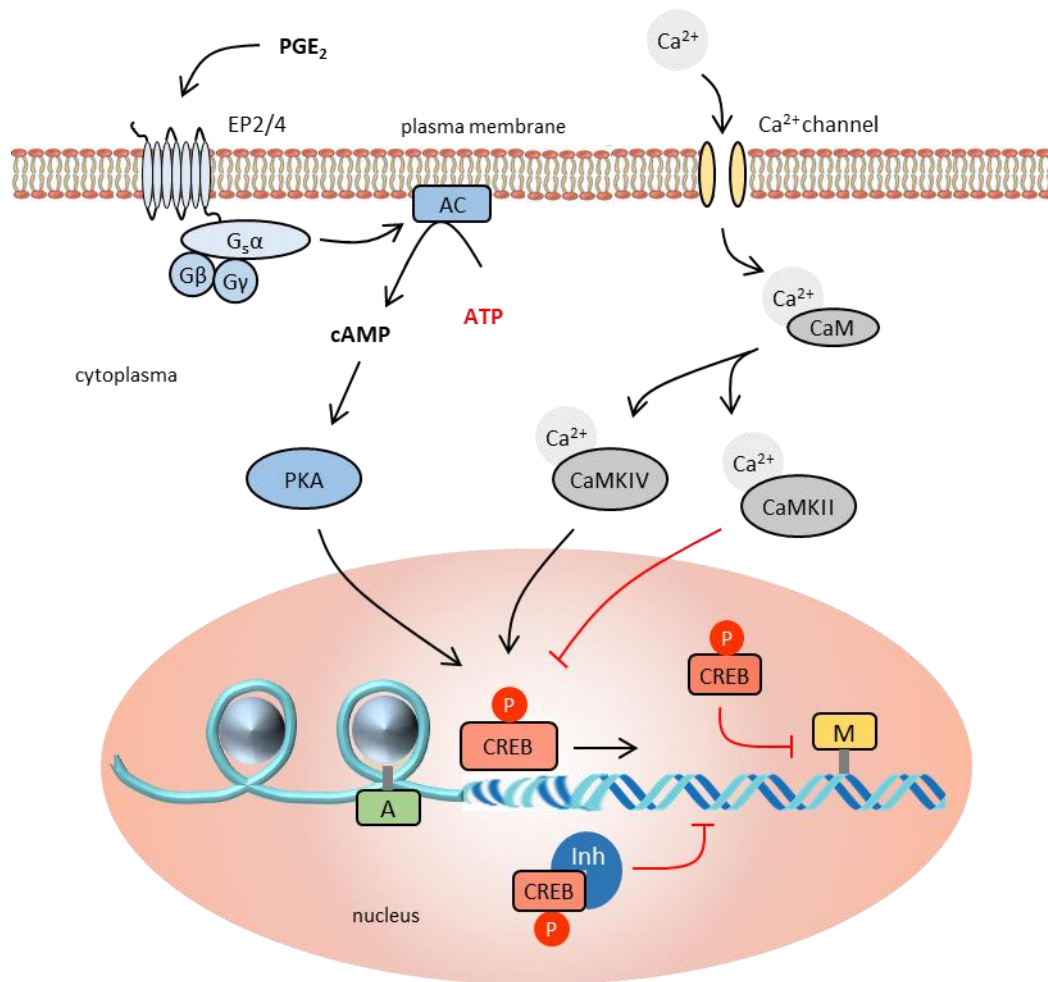


Figure 20. Enhancer and silencer of the transactivation potential of activated CREB.

Prostaglandin E₂ (PGE₂) activates PG receptors for PGE₂ (EP2/4) on macrophages. The activated G_sα subunit activates adenylyl cyclase (AC), which in turn, catalyzes the conversion of ATP into cyclic adenosine monophosphate (cAMP). Increased levels of cAMP drive the phosphorylation of cAMP-dependent cAMP response element-binding protein (CREB), which induces the transcription of selected targets. In contrast, calcium/calmodulin-dependent protein kinase (CaMK)IV phosphorylates CREB at Serine (Ser)-133 only, which, like cAMP, induces the transactivation potential of CREB, whereas CaMKII in addition to Ser-133 phosphorylates CREB at Ser-142, thereby blocking the Ser-133 phosphorylation dependent activation. Epigenetic modifications, such as histone acetylation (A), increases gene transcription, whereas CpG methylation (M) typically acts to repress gene transcription. Target-gene activation can also be disrupted by an inhibitor (Inh) that binds to the KID or KIX domains of CREB. Calcium (Ca²⁺), Protein kinase A (PKA).

In summary, the transcription factor CREB plays an ambiguous role in the inflammatory context in macrophages. On one hand, CREB drives inflammation processes, on the other hand, it promotes anti-inflammatory immune responses. In the present project, I was interested in characterizing pCREB-dependent transcriptional changes brought about by mPGES-1-derived PGE₂. Interestingly, despite prominent changes in the PGE₂ production in WT and mPGES-1 KO macrophages, we observed an equal activation of CREB. Yet, despite equal phosphorylation of CREB we identified DNA binding sites differently bound by pCREB in WT and mPGES-1 KO macrophages in inflammatory conditions. Herein, mPGES-1-deficient macrophages showed a markedly reduced binding of activated CREB to fatty acid metabolic processes-associated targets. Of note, we also unexpectedly observed an induction of the PGE₂ production at longer incubation times in mPGES-1 KO macrophages. Thus, it would be interesting characterize the activation of CREB in more detail to identify additional signal cascades contributing to the CREB activation in this context to provide possibilities of therapeutic interventions.

7 References

1. Hunter P. The inflammation theory of disease: The growing realization that chronic inflammation is crucial in many diseases opens new avenues for treatment. *EMBO Reports*. 2012;13(11):968-970. doi:10.1038/embor.2012.142.
2. Libby P. Inflammation in atherosclerosis. *Nature*. 2002;420(6917):868-874. doi:10.1038/nature01323.
3. Barnes PJ, Karin M. Nuclear factor-kappaB: a pivotal transcription factor in chronic inflammatory diseases. *The New England journal of medicine*. 1997;336(15):1066-1071. doi:10.1056/NEJM199704103361506.
4. Medzhitov R. Inflammation 2010: new adventures of an old flame. *Cell*. 2010;140(6):771-776. doi:10.1016/j.cell.2010.03.006.
5. Ryan GB, Majno G. Acute inflammation. A review. *The American Journal of Pathology*. 1977;86(1):183-276.
6. Xing Z, Gauldie J, Cox G, Baumann H, Jordana M, Lei XF, Achong MK. IL-6 is an antiinflammatory cytokine required for controlling local or systemic acute inflammatory responses. *Journal of Clinical Investigation*. 1998;101(2):311-320. doi:10.1172/JCI1368.
7. Herold G. *Innere Medizin 2019: Eine vorlesungsorientierte Darstellung: unter Berücksichtigung des Gegenstandskataloges für die Ärztliche Prüfung: mit ICD 10-Schlüssel im Text und Stichwortverzeichnis*. Köln: Herold Gerd; 2018.
8. Chaplin DD. Overview of the immune response. *The Journal of allergy and clinical immunology*. 2010;125(2 Suppl 2):S3-23. doi:10.1016/j.jaci.2009.12.980.
9. Bauer M, Weis S, Netea MG, Wetzker R. Remembering Pathogen Dose: Long-Term Adaptation in Innate Immunity. *Trends in Immunology*. 2018;39(6):438-445. doi:10.1016/j.it.2018.04.001.
10. Brodsky I, Medzhitov R. Two modes of ligand recognition by TLRs. *Cell*. 2007;130(6):979-981. doi:10.1016/j.cell.2007.09.009.
11. Jounai N, Kobiyama K, Takeshita F, Ishii KJ. Recognition of damage-associated molecular patterns related to nucleic acids during inflammation and vaccination. *Frontiers in cellular and infection microbiology*. 2012;2:168. doi:10.3389/fcimb.2012.00168.

12. Liang MD, Bagchi A, Warren HS, Tehan MM, Trigilio JA, Beasley-Topliffe LK, Tesini BL, Lazzaroni J-C, Fenton MJ, Hellman J. Bacterial peptidoglycan-associated lipoprotein: a naturally occurring toll-like receptor 2 agonist that is shed into serum and has synergy with lipopolysaccharide. *The Journal of infectious diseases*. 2005;191(6):939-948. doi:10.1086/427815.
13. Abdulkhaleq LA, Assi MA, Abdullah R, Zamri-Saad M, Taufiq-Yap YH, Hezmee MNM. The crucial roles of inflammatory mediators in inflammation: A review. *Veterinary world*. 2018;11(5):627-635. doi:10.14202/vetworld.2018.627-635.
14. Bourigault M-L, Segueni N, Rose S, Court N, Vacher R, Vasseur V, Erard F, Le Bert M, Garcia I, Iwakura Y, Jacobs M, Ryffel B, Quesniaux VFJ. Relative contribution of IL-1 α , IL-1 β and TNF to the host response to Mycobacterium tuberculosis and attenuated M. bovis BCG. *Immunity, inflammation and disease*. 2013;1(1):47-62. doi:10.1002/iid3.9.
15. Forrester SJ, Kikuchi DS, Hernandez MS, Xu Q, Griendling KK. Reactive Oxygen Species in Metabolic and Inflammatory Signaling. *Circulation research*. 2018;122(6):877-902. doi:10.1161/CIRCRESAHA.117.311401.
16. Nesargikar PN, Spiller B, Chavez R. The complement system: history, pathways, cascade and inhibitors. *European journal of microbiology & immunology*. 2012;2(2):103-111. doi:10.1556/EuJMI.2.2012.2.2.
17. Herr N, Bode C, Duerschmied D. The Effects of Serotonin in Immune Cells. *Frontiers in cardiovascular medicine*. 2017;4:48. doi:10.3389/fcvm.2017.00048.
18. Fullerton JN, Gilroy DW. Resolution of inflammation: a new therapeutic frontier. *Nature Reviews Drug Discovery*. 2016;15:551 EP -. doi:10.1038/nrd.2016.39.
19. Ueha S, Shand FHW, Matsushima K. Cellular and molecular mechanisms of chronic inflammation-associated organ fibrosis. *Frontiers in Immunology*. 2012;3:71. doi:10.3389/fimmu.2012.00071.
20. Drewry AM, Hotchkiss RS. Sepsis: Revising definitions of sepsis. *Nature reviews. Nephrology*. 2015;11(6):326-328. doi:10.1038/nrneph.2015.66.
21. Smith T, Hewson AK, Quarrie L, Leonard JP, Cuzner ML. Hypothalamic PGE2 and cAMP production and adrenocortical activation following intraperitoneal endotoxin injection: in vivo microdialysis studies in Lewis and Fischer rats. *Neuroendocrinology*. 1994;59(4):396-405. doi:10.1159/000126683.
22. Tak T, Drylewicz J, Conemans L, Boer RJ de, Koenderman L, Borghans JAM, Tesselaar K. Circulatory and maturation kinetics of human monocyte subsets in vivo. *Blood*. 2017;130(12):1474-1477. doi:10.1182/blood-2017-03-771261.

23. Favus MJ, Karnauskas AJ, Parks JH, Coe FL. Peripheral blood monocyte vitamin D receptor levels are elevated in patients with idiopathic hypercalciuria. *The Journal of clinical endocrinology and metabolism*. 2004;89(10):4937-4943. doi:10.1210/jc.2004-0412.
24. Epelman S, Lavine KJ, Randolph GJ. Origin and functions of tissue macrophages. *Immunity*. 2014;41(1):21-35. doi:10.1016/j.immuni.2014.06.013.
25. Witsell AL, Schook LB. Macrophage heterogeneity occurs through a developmental mechanism. *Proceedings of the National Academy of Sciences of the United States of America*. 1991;88(5):1963-1967. doi:10.1073/pnas.88.5.1963.
26. Mosser DM, Edwards JP. Exploring the full spectrum of macrophage activation. *Nature reviews. Immunology*. 2008;8(12):958-969. doi:10.1038/nri2448.
27. Munder M. Arginase: an emerging key player in the mammalian immune system. *British journal of pharmacology*. 2009;158(3):638-651. doi:10.1111/j.1476-5381.2009.00291.x.
28. Martinez FO, Gordon S, Locati M, Mantovani A. Transcriptional Profiling of the Human Monocyte-to-Macrophage Differentiation and Polarization: New Molecules and Patterns of Gene Expression. *The Journal of Immunology*. 2006;177(10):7303-7311. doi:10.4049/jimmunol.177.10.7303.
29. Xue J, Schmidt SV, Sander J, Draffehn A, Krebs W, Quester I, Nardo D de, Gohel TD, Emde M, Schmidleithner L, Ganesan H, Nino-Castro A, Mallmann MR, Labzin L, Theis H, Kraut M, Beyer M, Latz E, Freeman TC, Ulas T, Schultze JL. Transcriptome-based network analysis reveals a spectrum model of human macrophage activation. *Immunity*. 2014;40(2):274-288. doi:10.1016/j.immuni.2014.01.006.
30. Murray PJ, Allen JE, Biswas SK, Fisher EA, Gilroy DW, Goerdt S, Gordon S, Hamilton JA, Ivashkiv LB, Lawrence T, Locati M, Mantovani A, Martinez FO, Mege J-L, Mosser DM, Natoli G, Saeij JP, Schultze JL, Shirey KA, Sica A, Suttles J, Udalova I, van Ginderachter JA, Vogel SN, Wynn TA. Macrophage activation and polarization: nomenclature and experimental guidelines. *Immunity*. 2014;41(1):14-20. doi:10.1016/j.immuni.2014.06.008.
31. Jaguin M, Houlbert N, Fardel O, Lecreur V. Polarization profiles of human M-CSF-generated macrophages and comparison of M1-markers in classically activated macrophages from GM-CSF and M-CSF origin. *Cellular immunology*. 2013;281(1):51-61. doi:10.1016/j.cellimm.2013.01.010.
32. Kawasaki T, Kawai T. Toll-Like Receptor Signaling Pathways. *Frontiers in Immunology*. 2014;5. doi:10.3389/fimmu.2014.00461.
33. Kawai T, Akira S. The role of pattern-recognition receptors in innate immunity: update on Toll-like receptors. *Nature Immunology*. 2010;11(5):373. doi:10.1038/ni.1863.

34. Berg JM, Tymoczko JL, Stryer L. *Biochemistry*. 6th ed. New York: W.H. Freeman; 2007.
35. Kajino T, Ren H, Iemura S-i, Natsume T, Stefansson B, Brautigan DL, Matsumoto K, Ninomiya-Tsuji J. Protein Phosphatase 6 Down-regulates TAK1 Kinase Activation in the IL-1 Signaling Pathway. *Journal of Biological Chemistry*. 2006;281(52):39891-39896. doi:10.1074/jbc.M608155200.
36. Ullah MO, Sweet MJ, Mansell A, Kellie S, Kobe B. TRIF-dependent TLR signaling, its functions in host defense and inflammation, and its potential as a therapeutic target. *Journal of leukocyte biology*. 2016;100(1):27-45. doi:10.1189/jlb.2RI1115-531R.
37. Harizi H, Corcuff J-B, Gualde N. Arachidonic-acid-derived eicosanoids: roles in biology and immunopathology. *Trends in molecular medicine*. 2008;14(10):461-469. doi:10.1016/j.molmed.2008.08.005.
38. Meek IL, van de Laar MAFJ, E Vonkeman H. Non-Steroidal Anti-Inflammatory Drugs: An Overview of Cardiovascular Risks. *Pharmaceuticals (Basel, Switzerland)*. 2010;3(7):2146-2162. doi:10.3390/ph3072146.
39. Sostres C, Gargallo CJ, Arroyo MT, Lanas A. Adverse effects of non-steroidal anti-inflammatory drugs (NSAIDs, aspirin and coxibs) on upper gastrointestinal tract. *Best practice & research. Clinical gastroenterology*. 2010;24(2):121-132. doi:10.1016/j.bpg.2009.11.005.
40. Smith JB, Willis AL. Aspirin selectively inhibits prostaglandin production in human platelets. *Nature: New biology*. 1971;231(25):235-237.
41. Fu JY, Masferrer JL, Seibert K, Raz A, Needleman P. The induction and suppression of prostaglandin H₂ synthase (cyclooxygenase) in human monocytes. *The Journal of biological chemistry*. 1990;265(28):16737-16740.
42. Vane JR, Mitchell JA, Appleton I, Tomlinson A, Bishop-Bailey D, Croxtall J, Willoughby DA. Inducible isoforms of cyclooxygenase and nitric-oxide synthase in inflammation. *Proceedings of the National Academy of Sciences of the United States of America*. 1994;91(6):2046-2050.
43. Nakanishi M, Rosenberg DW. Multifaceted roles of PGE₂ in inflammation and cancer. *Seminars in immunopathology*. 2013;35(2):123-137. doi:10.1007/s00281-012-0342-8.
44. Tanioka T, Nakatani Y, Semmyo N, Murakami M, Kudo I. Molecular identification of cytosolic prostaglandin E₂ synthase that is functionally coupled with cyclooxygenase-1 in immediate prostaglandin E₂ biosynthesis. *The Journal of biological chemistry*. 2000;275(42):32775-32782. doi:10.1074/jbc.M003504200.

45. Hara S, Kamei D, Sasaki Y, Tanemoto A, Nakatani Y, Murakami M. Prostaglandin E synthases: Understanding their pathophysiological roles through mouse genetic models. *Biochimie*. 2010;92(6):651-659. doi:10.1016/j.biochi.2010.02.007.
46. Murakami M, Naraba H, Tanioka T, Semmyo N, Nakatani Y, Kojima F, Ikeda T, Fueki M, Ueno A, Oh S, Kudo I. Regulation of prostaglandin E2 biosynthesis by inducible membrane-associated prostaglandin E2 synthase that acts in concert with cyclooxygenase-2. *The Journal of biological chemistry*. 2000;275(42):32783-32792. doi:10.1074/jbc.M003505200.
47. Stahn C, Buttgerit F. Genomic and nongenomic effects of glucocorticoids. *Nature clinical practice. Rheumatology*. 2008;4(10):525-533. doi:10.1038/ncprheum0898.
48. Trebino CE, Stock JL, Gibbons CP, Naiman BM, Wachtmann TS, Umland JP, Pandher K, Lapointe J-M, Saha S, Roach ML, Carter D, Thomas NA, Durtschi BA, McNeish JD, Hambor JE, Jakobsson P-J, Carty TJ, Perez JR, Audoly LP. Impaired inflammatory and pain responses in mice lacking an inducible prostaglandin E synthase. *Proceedings of the National Academy of Sciences of the United States of America*. 2003;100(15):9044-9049. doi:10.1073/pnas.1332766100.
49. Reid G, Wielinga P, Zelcer N, van der Heijden I, Kuil A, Haas M de, Wijnholds J, Borst P. The human multidrug resistance protein MRP4 functions as a prostaglandin efflux transporter and is inhibited by nonsteroidal antiinflammatory drugs. *Proceedings of the National Academy of Sciences of the United States of America*. 2003;100(16):9244-9249. doi:10.1073/pnas.1033060100.
50. Díaz-Muñoz MD, Osma-García IC, Fresno M, Iñiguez MA. Involvement of PGE2 and the cAMP signalling pathway in the up-regulation of COX-2 and mPGES-1 expression in LPS-activated macrophages. *The Biochemical journal*. 2012;443(2):451-461. doi:10.1042/BJ20111052.
51. Leyme A, Marivin A, Maziarz M, DiGiacomo V, Papakonstantinou MP, Patel PP, Blanco-Canosa JB, Walawalkar IA, Rodriguez-Davila G, Dominguez I, Garcia-Marcos M. Specific inhibition of GPCR-independent G protein signaling by a rationally engineered protein. *Proceedings of the National Academy of Sciences of the United States of America*. 2017;114(48):E10319-E10328. doi:10.1073/pnas.1707992114.
52. Ricciotti E, FitzGerald GA. Prostaglandins and Inflammation. *Arteriosclerosis, thrombosis, and vascular biology*. 2011;31(5):986-1000. doi:10.1161/ATVBAHA.110.207449.
53. Moon E-Y, Lee Y-S, Choi WS, Lee M-H. Toll-like receptor 4-mediated cAMP production up-regulates B-cell activating factor expression in Raw264.7 macrophages. *Experimental cell research*. 2011;317(17):2447-2455. doi:10.1016/j.yexcr.2011.07.003.

54. Dash PK, Hochner B, Kandel ER. Injection of the cAMP-responsive element into the nucleus of Aplysia sensory neurons blocks long-term facilitation. *Nature*. 1990;345(6277):718-721. doi:10.1038/345718a0.
55. Casadio A, Martin KC, Giustetto M, Zhu H, Chen M, Bartsch D, Bailey CH, Kandel ER. A transient, neuron-wide form of CREB-mediated long-term facilitation can be stabilized at specific synapses by local protein synthesis. *Cell*. 1999;99(2):221-237.
56. Kandel ER. The molecular biology of memory: cAMP, PKA, CRE, CREB-1, CREB-2, and CPEB. *Molecular brain*. 2012;5:14. doi:10.1186/1756-6606-5-14.
57. Bartsch D, Casadio A, Karl KA, Serodio P, Kandel ER. CREB1 Encodes a Nuclear Activator, a Repressor, and a Cytoplasmic Modulator that Form a Regulatory Unit Critical for Long-Term Facilitation. *Cell*. 1998;95(2):211-223. doi:10.1016/S0092-8674(00)81752-3.
58. Barco A, Bailey CH, Kandel ER. Common molecular mechanisms in explicit and implicit memory. *Journal of neurochemistry*. 2006;97(6):1520-1533. doi:10.1111/j.1471-4159.2006.03870.x.
59. Mayr B, Montminy M. Transcriptional regulation by the phosphorylation-dependent factor CREB. *Nature reviews. Molecular cell biology*. 2001;2(8):599-609. doi:10.1038/35085068.
60. Boulpaep EL. *Medical Physiology*. 3. Aufl. s.l.: Elsevier Health Care - Lehrbücher; 2017. <https://institut.elsevierelibrary.de/product/medical-physiology78616>.
61. Uematsu S, Matsumoto M, Takeda K, Akira S. Lipopolysaccharide-dependent prostaglandin E(2) production is regulated by the glutathione-dependent prostaglandin E(2) synthase gene induced by the Toll-like receptor 4/MyD88/NF-IL6 pathway. *Journal of immunology (Baltimore, Md. : 1950)*. 2002;168(11):5811-5816. doi:10.4049/jimmunol.168.11.5811.
62. Todaro GJ, Green H. Quantitative studies of the growth of mouse embryo cells in culture and their development into established lines. *The Journal of Cell Biology*. 1963;17(2):299-313. doi:10.1083/jcb.17.2.299.
63. Ying W, Cheruku PS, Bazer FW, Safe SH, Zhou B. Investigation of macrophage polarization using bone marrow derived macrophages. *Journal of visualized experiments: JoVE*. 2013;(76). doi:10.3791/50323.
64. LOWRY OH, ROSEBROUGH NJ, FARR AL, RANDALL RJ. Protein measurement with the Folin phenol reagent. *The Journal of biological chemistry*. 1951;193(1):265-275.

65. Inada M, Matsumoto C, Uematsu S, Akira S, Miyaura C. Membrane-Bound Prostaglandin E Synthase-1-Mediated Prostaglandin E2 Production by Osteoblast Plays a Critical Role in Lipopolysaccharide-Induced Bone Loss Associated with Inflammation. *The Journal of Immunology*. 2006;177(3):1879-1885. doi:10.4049/jimmunol.177.3.1879.
66. Stichtenoth DO, Thoren S, Bian H, Peters-Golden M, Jakobsson P-J, Crofford LJ. Microsomal Prostaglandin E Synthase Is Regulated by Proinflammatory Cytokines and Glucocorticoids in Primary Rheumatoid Synovial Cells. *The Journal of Immunology*. 2001;167(1):469-474. doi:10.4049/jimmunol.167.1.469.
67. Xiao L, Ornatowska M, Zhao G, Cao H, Yu R, Deng J, Li Y, Zhao Q, Sadikot RT, Christman JW. Lipopolysaccharide-induced expression of microsomal prostaglandin E synthase-1 mediates late-phase PGE2 production in bone marrow derived macrophages. *PLoS one*. 2012;7(11):e50244. doi:10.1371/journal.pone.0050244.
68. Díaz-Muñoz MD, Osma-García IC, Cacheiro-Llaguno C, Fresno M, Iñiguez MA. Coordinated up-regulation of cyclooxygenase-2 and microsomal prostaglandin E synthase 1 transcription by nuclear factor kappa B and early growth response-1 in macrophages. *Cellular signalling*. 2010;22(10):1427-1436. doi:10.1016/j.cellsig.2010.05.011.
69. Uematsu S, Matsumoto M, Takeda K, Akira S. Lipopolysaccharide-Dependent Prostaglandin E2 Production Is Regulated by the Glutathione-Dependent Prostaglandin E2 Synthase Gene Induced by the Toll-Like Receptor 4/MyD88/NF-IL6 Pathway. *The Journal of Immunology*. 2002;168(11):5811-5816. doi:10.4049/jimmunol.168.11.5811.
70. Boulet L, Ouellet M, Bateman KP, Ethier D, Percival MD, Riendeau D, Mancini JA, Méthot N. Deletion of microsomal prostaglandin E2 (PGE2) synthase-1 reduces inducible and basal PGE2 production and alters the gastric prostanoid profile. *The Journal of biological chemistry*. 2004;279(22):23229-23237. doi:10.1074/jbc.M400443200.
71. Monrad SU, Kojima F, Kapoor M, Kuan EL, Sarkar S, Randolph GJ, Crofford LJ. Genetic deletion of mPGES-1 abolishes PGE2 production in murine dendritic cells and alters the cytokine profile, but does not affect maturation or migration. *Prostaglandins, leukotrienes, and essential fatty acids*. 2011;84(3-4):113-121. doi:10.1016/j.plefa.2010.10.003.
72. Nugteren DH, Christ-Hazelhof E. Chemical and enzymic conversions of the prostaglandin endoperoxide PGH2. *Advances in prostaglandin and thromboxane research*. 1980;6:129-137.

73. Kapoor M, Kojima F, Qian M, Yang L, Crofford LJ. Shunting of prostanoid biosynthesis in microsomal prostaglandin E synthase-1 null embryo fibroblasts: regulatory effects on inducible nitric oxide synthase expression and nitrite synthesis. *FASEB journal: official publication of the Federation of American Societies for Experimental Biology*. 2006;20(13):2387-2389. doi:10.1096/fj.06-6366fje.
74. Hoshino K, Takeuchi O, Kawai T, Sanjo H, Ogawa T, Takeda Y, Takeda K, Akira S. Pillars Article: Cutting Edge: Toll-Like Receptor 4 (TLR4)-Deficient Mice Are Hyporesponsive to Lipopolysaccharide: Evidence for TLR4 as the Lps Gene Product. *J. Immunol.* 1999. 162: 3749-3752. *Journal of immunology (Baltimore, Md. : 1950)*. 2016;197(7):2563-2566.
75. Murakami M, Kambe T, Shimbara S, Kudo I. Functional Coupling Between Various Phospholipase A 2 s and Cyclooxygenases in Immediate and Delayed Prostanoid Biosynthetic Pathways. *Journal of Biological Chemistry*. 1999;274(5):3103-3115. doi:10.1074/jbc.274.5.3103.
76. Karim S, Habib A, Lévy-Toledano S, Maclouf J. Cyclooxygenases-1 and -2 of Endothelial Cells Utilize Exogenous or Endogenous Arachidonic Acid for Transcellular Production of Thromboxane. *Journal of Biological Chemistry*. 1996;271(20):12042-12048. doi:10.1074/jbc.271.20.12042.
77. Caldwell B, Aldington S, Weatherall M, Shirtcliffe P, Beasley R. Risk of cardiovascular events and celecoxib: a systematic review and meta-analysis. *Journal of the Royal Society of Medicine*. 2006;99(3):132-140.
78. Leclerc P, Idborg H, Spahiu L, Larsson C, Nekhotiaeva N, Wannberg J, Stenberg P, Korotkova M, Jakobsson P-J. Characterization of a human and murine mPGES-1 inhibitor and comparison to mPGES-1 genetic deletion in mouse models of inflammation. *Prostaglandins & other lipid mediators*. 2013;107:26-34. doi:10.1016/j.prostaglandins.2013.09.001.
79. Koeberle A, Werz O. Inhibitors of the microsomal prostaglandin E(2) synthase-1 as alternative to non steroidal anti-inflammatory drugs (NSAIDs)--a critical review. *Current medicinal chemistry*. 2009;16(32):4274-4296.
80. Lu Y-C, Yeh W-C, Ohashi PS. LPS/TLR4 signal transduction pathway. *Cytokine*. 2008;42(2):145-151. doi:10.1016/j.cyto.2008.01.006.
81. Sato M, Sano H, Iwaki D, Kudo K, Konishi M, Takahashi H, Takahashi T, Imaizumi H, Asai Y, Kuroki Y. Direct binding of Toll-like receptor 2 to zymosan, and zymosan-induced NF-kappa B activation and TNF-alpha secretion are down-regulated by lung collectin surfactant protein A. *Journal of immunology (Baltimore, Md. : 1950)*. 2003;171(1):417-425.
82. Takeda K, Akira S. TLR signaling pathways. *Seminars in Immunology*. 2004;16(1):3-9. doi:10.1016/j.smim.2003.10.003.

83. Toshchakov V, Jones BW, Perera P-Y, Thomas K, Cody MJ, Zhang S, Williams BRG, Major J, Hamilton TA, Fenton MJ, Vogel SN. TLR4, but not TLR2, mediates IFN-beta-induced STAT1alpha/beta-dependent gene expression in macrophages. *Nature Immunology*. 2002;3(4):392-398. doi:10.1038/ni774.
84. Wen AY, Sakamoto KM, Miller LS. The role of the transcription factor CREB in immune function. *Journal of immunology (Baltimore, Md. : 1950)*. 2010;185(11):6413-6419. doi:10.4049/jimmunol.1001829.
85. Shaywitz AJ, Greenberg ME. CREB: a stimulus-induced transcription factor activated by a diverse array of extracellular signals. *Annual review of biochemistry*. 1999;68:821-861. doi:10.1146/annurev.biochem.68.1.821.
86. Bleckmann SC, Blendy JA, Rudolph, Monaghan AP, Schmid W, Schutz G. Activating Transcription Factor 1 and CREB Are Important for Cell Survival during Early Mouse Development. *Molecular and Cellular Biology*. 2002;22(6):1919-1925. doi:10.1128/MCB.22.6.1919-1925.2002.
87. Tinti C, Yang C, Seo H, Conti B, Kim C, Joh TH, Kim K-S. Structure/Function Relationship of the cAMP Response Element in Tyrosine Hydroxylase Gene Transcription. *Journal of Biological Chemistry*. 1997;272(31):19158-19164. doi:10.1074/jbc.272.31.19158.
88. Robertson KD, Manns A, Swinnen LJ, Zong JC, Gulley ML, Ambinder RF. CpG methylation of the major Epstein-Barr virus latency promoter in Burkitt's lymphoma and Hodgkin's disease. *Blood*. 1996;88(8):3129-3136.
89. Karamouzis MV, Konstantinopoulos PA, Papavassiliou AG. Roles of CREB-binding protein (CBP)/p300 in respiratory epithelium tumorigenesis. *Cell research*. 2007;17(4):324-332. doi:10.1038/cr.2007.10.
90. Fauquier L, Azzag K, Parra MAM, Quillien A, Boulet M, Diouf S, Carnac G, Waltzer L, Gronemeyer H, Vandel L. CBP and P300 regulate distinct gene networks required for human primary myoblast differentiation and muscle integrity. *Scientific reports*. 2018;8(1):12629. doi:10.1038/s41598-018-31102-4.
91. Sun P, Enslin H, Myung PS, Maurer RA. Differential activation of CREB by Ca²⁺/calmodulin-dependent protein kinases type II and type IV involves phosphorylation of a site that negatively regulates activity. *Genes & development*. 1994;8(21):2527-2539.
92. Ernst P, Wang J, Huang M, Goodman RH, Korsmeyer SJ. MLL and CREB bind cooperatively to the nuclear coactivator CREB-binding protein. *Molecular and Cellular Biology*. 2001;21(7):2249-2258. doi:10.1128/MCB.21.7.2249-2258.2001.
93. Deak M, Clifton AD, Lucocq LM, Alessi DR. Mitogen- and stress-activated protein kinase-1 (MSK1) is directly activated by MAPK and SAPK2/p38, and may mediate activation of CREB. *The EMBO journal*. 1998;17(15):4426-4441. doi:10.1093/emboj/17.15.4426.

94. Xing J, Ginty DD, Greenberg ME. Coupling of the RAS-MAPK pathway to gene activation by RSK2, a growth factor-regulated CREB kinase. *Science (New York, N.Y.)*. 1996;273(5277):959-963.
95. Tavernarakis N, Driscoll M, Kyrpides NC. The SPFH domain: implicated in regulating targeted protein turnover in stomatins and other membrane-associated proteins. *Trends in Biochemical Sciences*. 1999;24(11):425-427. doi:10.1016/S0968-0004(99)01467-X.
96. Pearce MMP, Wormer DB, Wilkens S, Wojcikiewicz RJH. An endoplasmic reticulum (ER) membrane complex composed of SPFH1 and SPFH2 mediates the ER-associated degradation of inositol 1,4,5-trisphosphate receptors. *The Journal of biological chemistry*. 2009;284(16):10433-10445. doi:10.1074/jbc.M809801200.
97. Browman DT, Hoegg MB, Robbins SM. The SPFH domain-containing proteins: more than lipid raft markers. *Trends in cell biology*. 2007;17(8):394-402. doi:10.1016/j.tcb.2007.06.005.
98. Foskett JK, White C, Cheung K-H, Mak D-OD. Inositol trisphosphate receptor Ca²⁺ release channels. *Physiological reviews*. 2007;87(2):593-658. doi:10.1152/physrev.00035.2006.
99. Huber MD, Vesely PW, Datta K, Gerace L. Erlins restrict SREBP activation in the ER and regulate cellular cholesterol homeostasis. *The Journal of Cell Biology*. 2013;203(3):427-436. doi:10.1083/jcb.201305076.

8 Danksagung

An dieser Stelle möchte ich mich herzlichst bei allen Personen bedanken, die diese Arbeit ermöglicht und zu ihrem Gelingen beigetragen haben. Mein besonderer Dank gilt:

Meinem Doktorvater **Prof. Bernhard Brüne** für die Bereitstellung des Themas und die Möglichkeit meine Arbeit in seinem Institut durchführen zu können.

Ganz besonders danken möchte ich meinem Betreuer **PD Dr. Tobias Schmid** für die geduldige und selbstlose Unterstützung, den wertvollen Diskussionen und das in meine Arbeit und mich gesetzte Vertrauen. Seine hervorragende Betreuung hat maßgeblich zum Gelingen dieser Arbeit beigetragen.

Auch danke ich besonders **Dr. Shahzad Nawaz Syed** für die zahlreichen wissenschaftlichen Diskussionen und seine praktische Unterstützung, die mich in jeglicher Hinsicht vorangebracht haben.

Mein Dank richtet sich auch an meine Laborkollegen **Anica, Arnaud, Sofia** und insbesondere **Peter**, für seine verantwortungsvolle Unterstützung, angefangen bei der Einarbeitung im Labor bis hin zur Fertigstellung meiner Arbeit hat er mir jederzeit mit Rat und Tat zur Seite gestanden.

Ich danke **allen Mitarbeitern des Instituts für Biochemie I** für die freundliche Hilfsbereitschaft und die angenehme Zusammenarbeit. Außerdem danke ich dem **Institut für Klinische Pharmakologie**, insbesondere **Dr. Dominique Thomas**, für die massenspektrometrischen Analysen meiner Proben.

Ebenso gilt mein Dank **Leonie** und **Victor** für das gewissenhafte Korrekturlesen dieser Arbeit.

Zu guter Letzt geht mein außerordentlicher Dank an meine **Familie** und meine **Freunde** für ihre moralische Begleitung und dass sie in dieser Zeit immer an mich geglaubt haben.

9 Lebenslauf

10 Schriftliche Erklärung

Ich erkläre ehrenwörtlich, dass ich die dem Fachbereich Medizin der Johann Wolfgang Goethe-Universität Frankfurt am Main zur Promotionsprüfung eingereichte Dissertation mit dem Titel

**The PGE₂/cAMP signaling axis in macrophages
during inflammation**

in dem Institut für Biochemie I – Pathobiochemie unter Betreuung und Anleitung von Prof. Dr. Bernhard Brüne mit Unterstützung durch PD Dr. Tobias Schmid und Dr. Shahzad Nawaz Syed ohne sonstige Hilfe selbst durchgeführt und bei der Abfassung der Arbeit keine anderen als die in der Dissertation angeführten Hilfsmittel benutzt habe. Darüber hinaus versichere ich, nicht die Hilfe einer kommerziellen Promotionsvermittlung in Anspruch genommen zu haben.

Ich habe bisher an keiner in- oder ausländischen Universität ein Gesuch um Zulassung zur Promotion eingereicht. Die vorliegende Arbeit wurde bisher nicht als Dissertation eingereicht.

Frankfurt am Main, den _____

(Bernd Patrick Maul)